Small-Angle X-Ray (SAXS) A Brief Overview

Prof. Greg Beaucage
Department of Chemical and Materials Engineering
University of Cincinnati
Cincinnati OH 45221-0012
gbeaucage@gmail.com; 513 556-3063

23,300 full time undergraduate students
5,560 full-time graduate
7,100 part-time undergraduate students
3,690 part-time graduate
40,000 students

83.9 percent residents of Ohio

$378 million External Grants (2009)
3,000 full time faculty

5 SAXS Cameras APS, HFIR, SNS ~ 6 hrs.
Roe, Schaefer, Beaucage, Jim Mark etc.

Small-Angle X-Ray (SAXS) A Brief Overview

Prof. Greg Beaucage
Department of Chemical and Materials Engineering
University of Cincinnati
gbeaucage@gmail.com; 513 556-3063

Why use small-angle x-ray scattering?

•Compliment microscopy, diffraction, NMR, spectroscopy techniques.

•Statistical description of structure is needed, mean particle size.

•In situ measurements are needed. Especially for biological and chemical systems, stop-flow or flow through experiments, processing studies, deformation studies etc.

•Disordered structures and transitions between disorder and order, i.e. folding processes, aggregation, polymer chain structure.

•Quantification of polydispersity.

•Measure thermodynamics, interaction parameter, critical phenomena.

•Quantify nanoscale orientation.

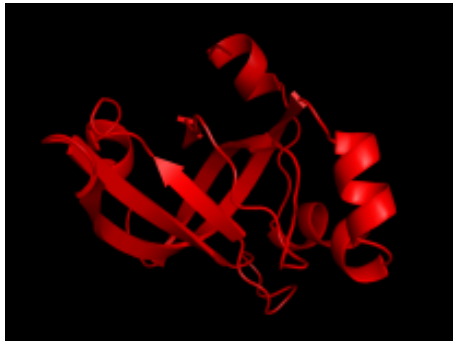

“Typical” SAXS Problems

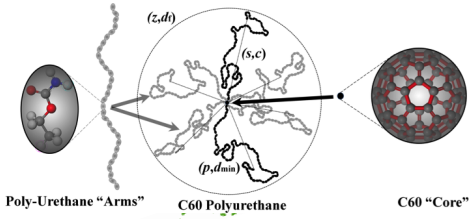

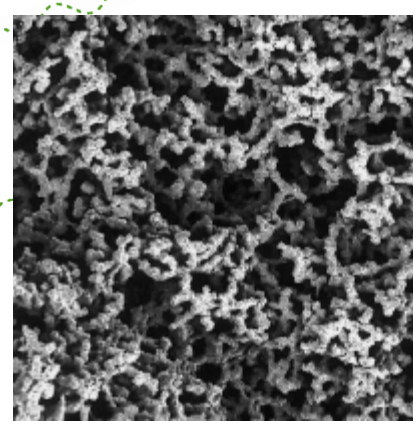

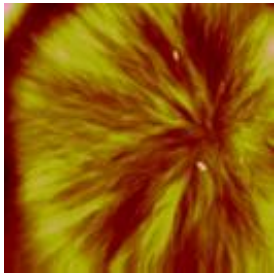

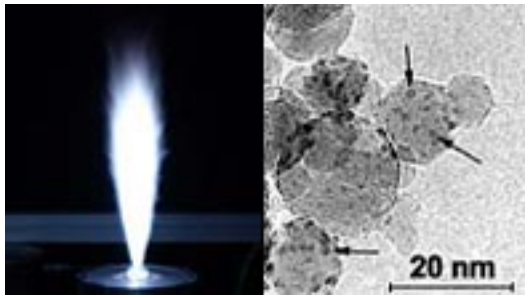

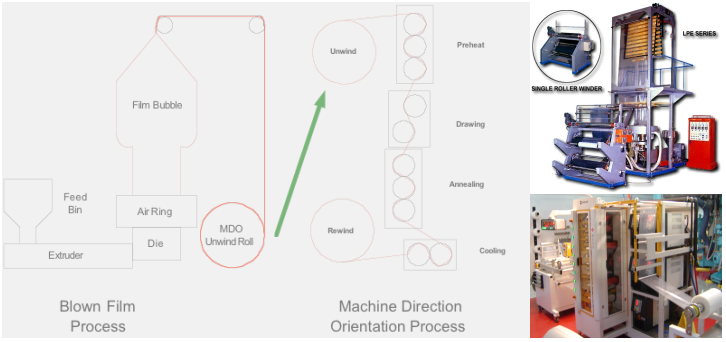

Outline:

1) Experimental Instrumentation
2) Specific Scattering Laws
3) General Scattering Laws
   Guinier's Law
   Porod's Law
   Unified Scattering Function
   Fractals
   Branching
4) Polydispersity
5) Summary

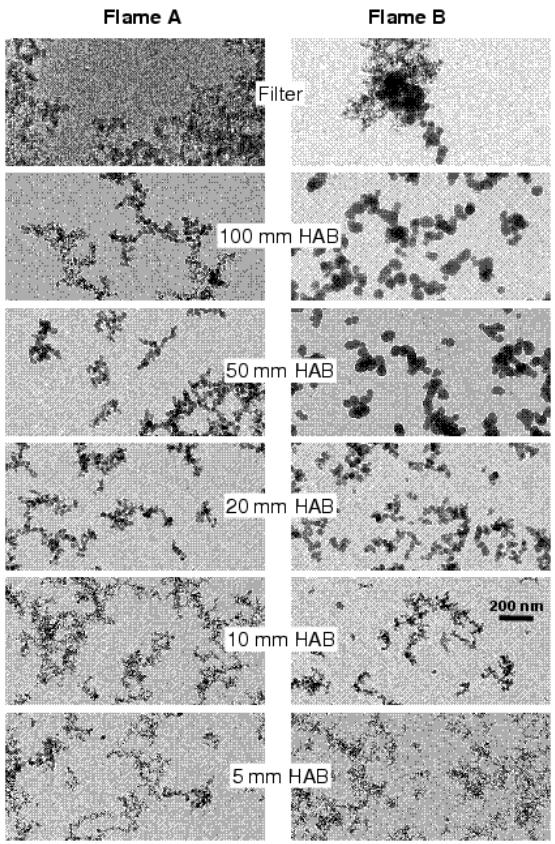

Kammler HK, Beaucage G, Kohls DJ, Agashe N. Ilavsky J
J Appl. Phys. **97**(2005) (Article 054309).

Small- and Wide-Angle X-ray Scattering Measurements

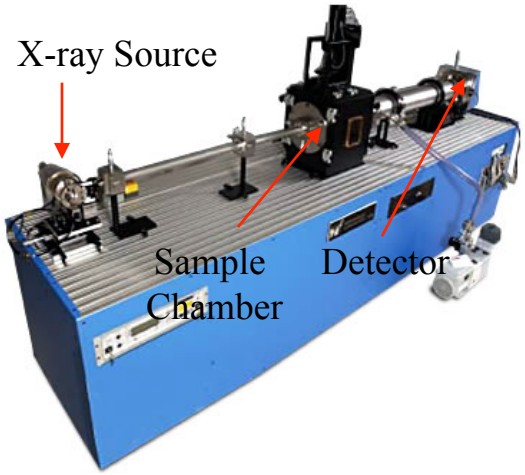

SAXS : pinhole camera : 2-d detector at 1m from the sample

WAXS : pinhole geometry camera : image plate detector at 5cm from the sample

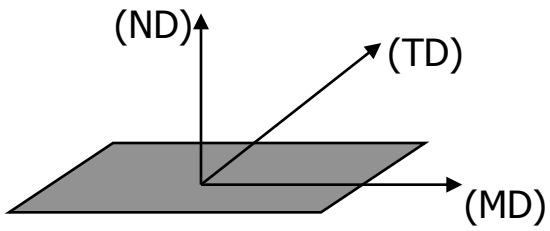

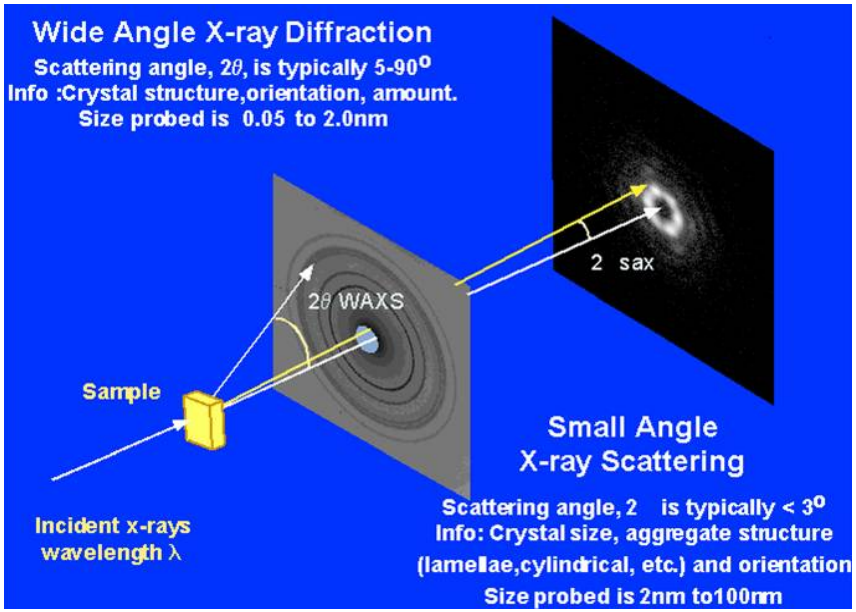

- 2D measurements are useful in determining both size and relative orientation of various structural components

The SAXS Experiment

Source Collimination Sample Detector

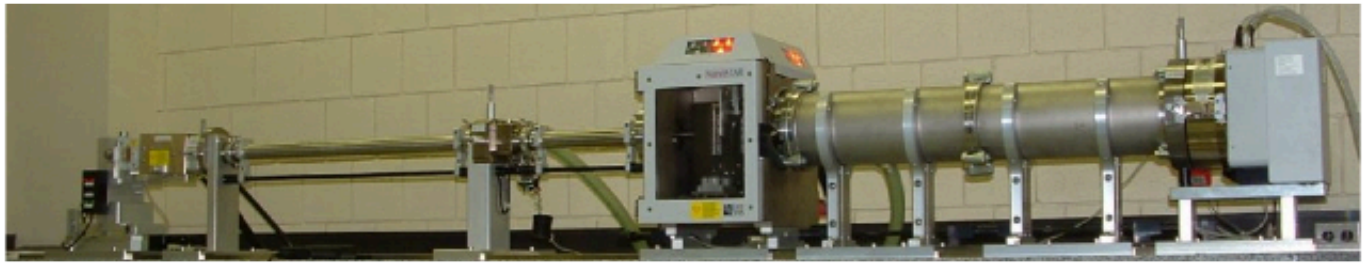

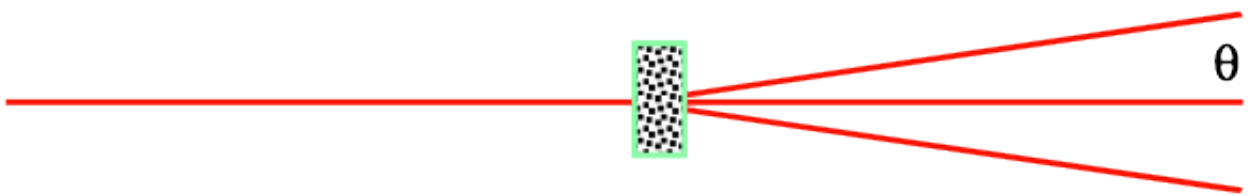

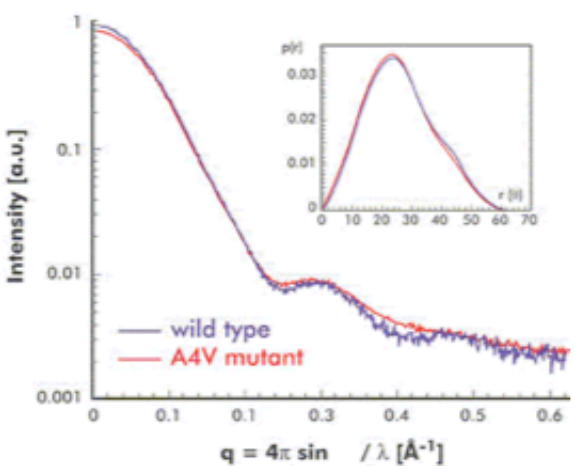

$$q = \frac{4\pi}{\lambda}\sin\left(\frac{\theta}{2}\right) = \frac{2\pi}{d}$$

$$I(q) = Nn_e^2 = A^2(q)$$

Collimation for Small-Angles is a Technical Hurdle

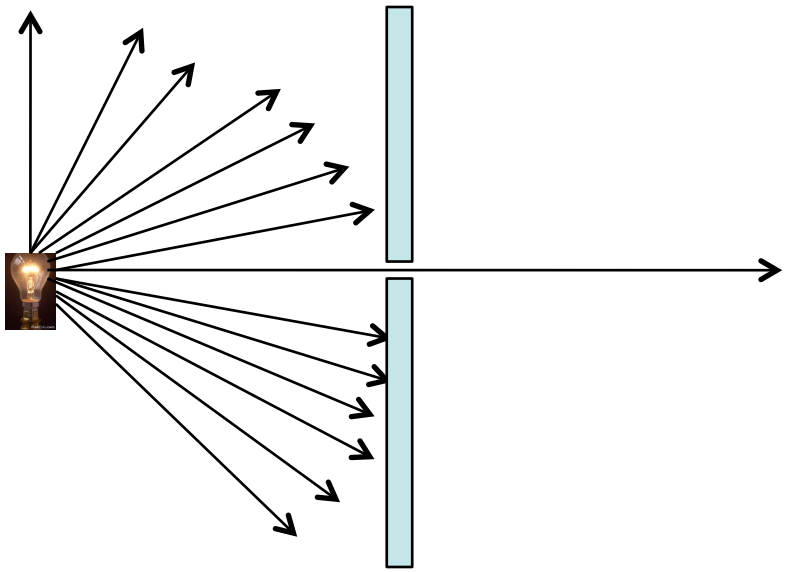

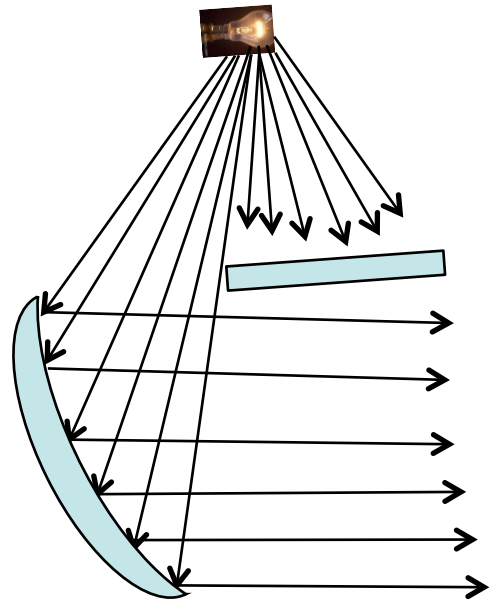

Use Goebel Mirrors
or Fresnel Zone Plate
Optics (diffraction based)

Two Alternative Camera Geometries Offer Improvement in Flux or Improvement in Angular Resolution with Smearing of Scattering Pattern

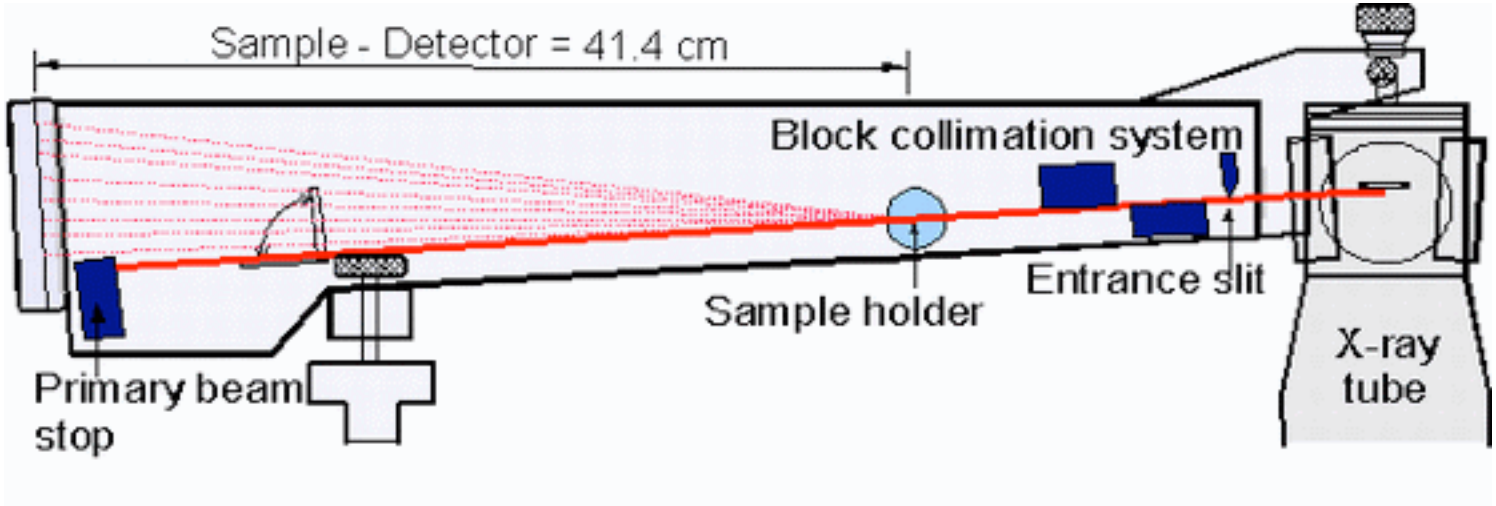

www.chemie.uni-bayreuth.de/pci/de/forschung/22427/saxs1.gif

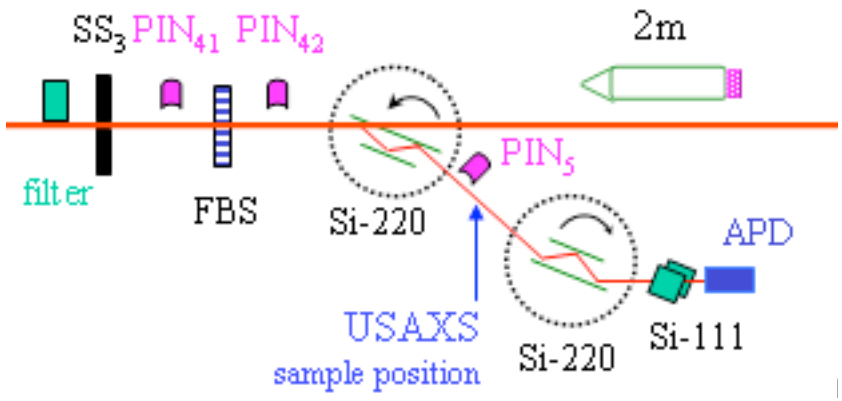

www.esrf.eu/UsersAndScience/Experiments/SoftMatter/ID02/BeamlineLayout/EH1

Nanostructure from Small Angle X-ray Scattering

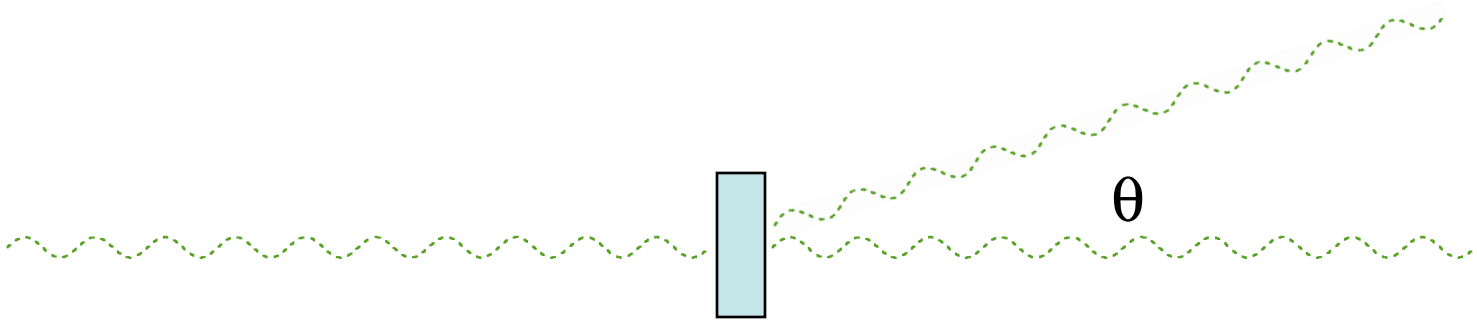

3-Techinques are similar
SALS/LS, SANS, SAXS

λ = 0.5 μm
For light

λ = 0.1 - 0.5 nm
For x-ray/neutron

Contrast: index of refraction, electron density, neutron cross section

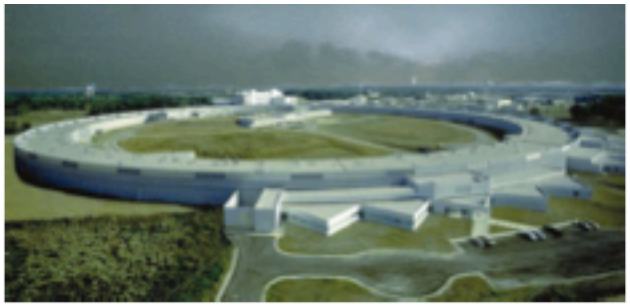

1-meter

SAXS

30-meter

SANS

Small-Angle X-ray Scattering, (SAXS)

We Get Intensity as
A Function of Angle
(or radial position)

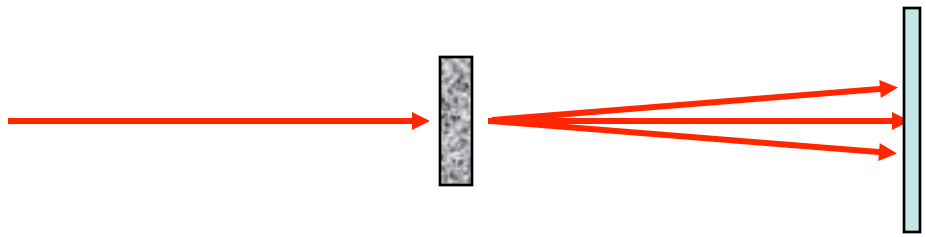

-Collimated Beam
-Monochromatic Beam
-Coherent Beam
-Focusing Optics Perhaps

-Longer Distance for Lower Angle (Pinhole)
-Large Dynamic Range Detector
-Evacuated Flight Path
-Extend Angle Range with Multiple SDD's

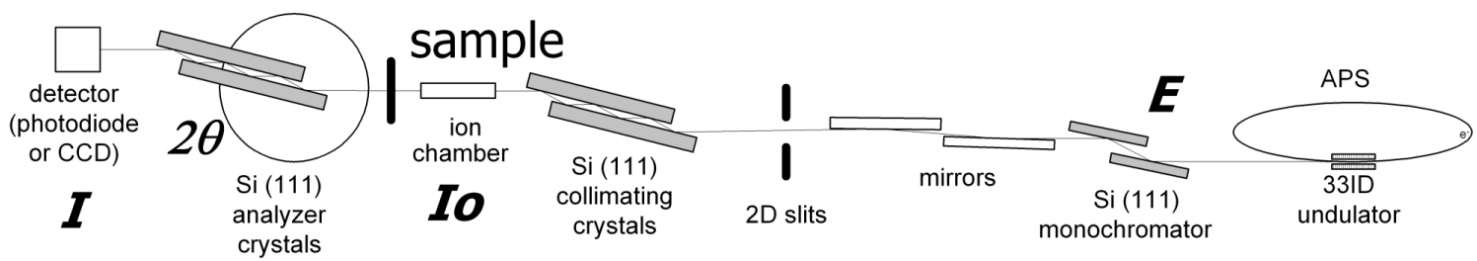

Small-Angle X-ray Scattering at Synchrotrons

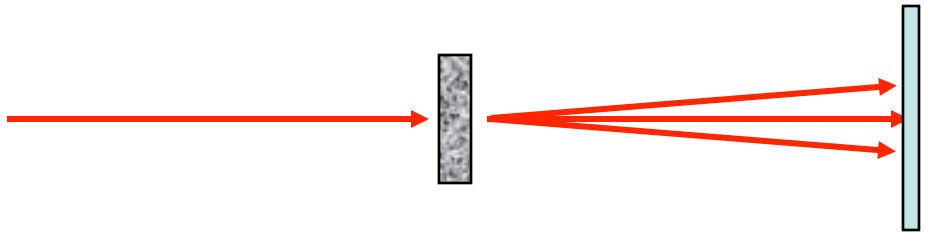

ESRF we use ID2 with T. Naryanan, APS 32-ID with Jan Ilavsky
(9 other SAXS instruments at APS, Chicago)

Much easier to get time on smaller synchrotrons
We use SSRL (Stanford); CHESS (Cornell), CAMD (LSU)

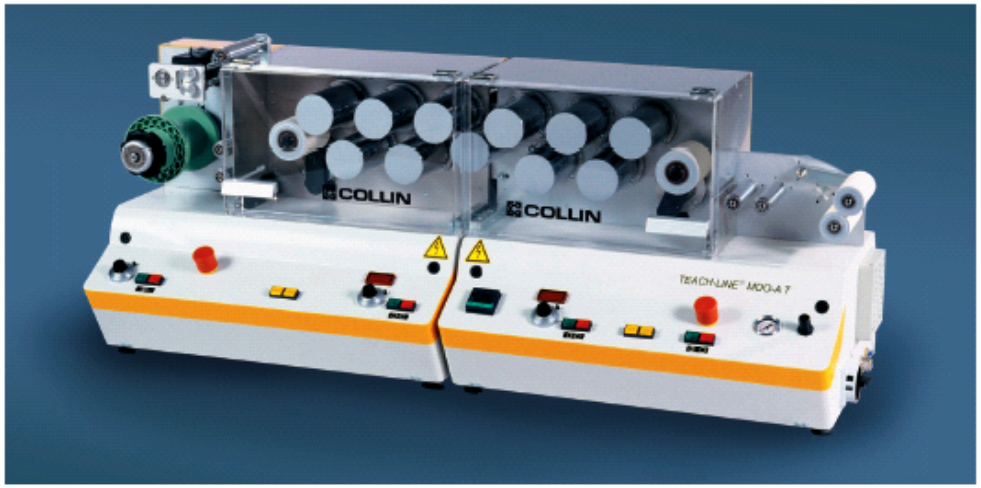

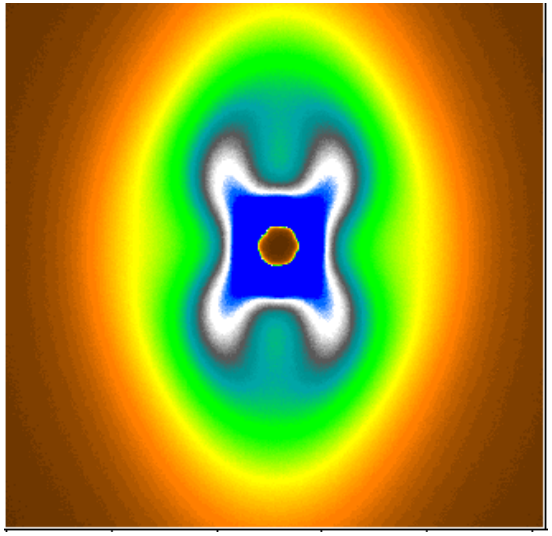

The 2-d pattern can be analyzed for orientation (azimuthal angle ψ) or for structure I(q) (radial angle θ).

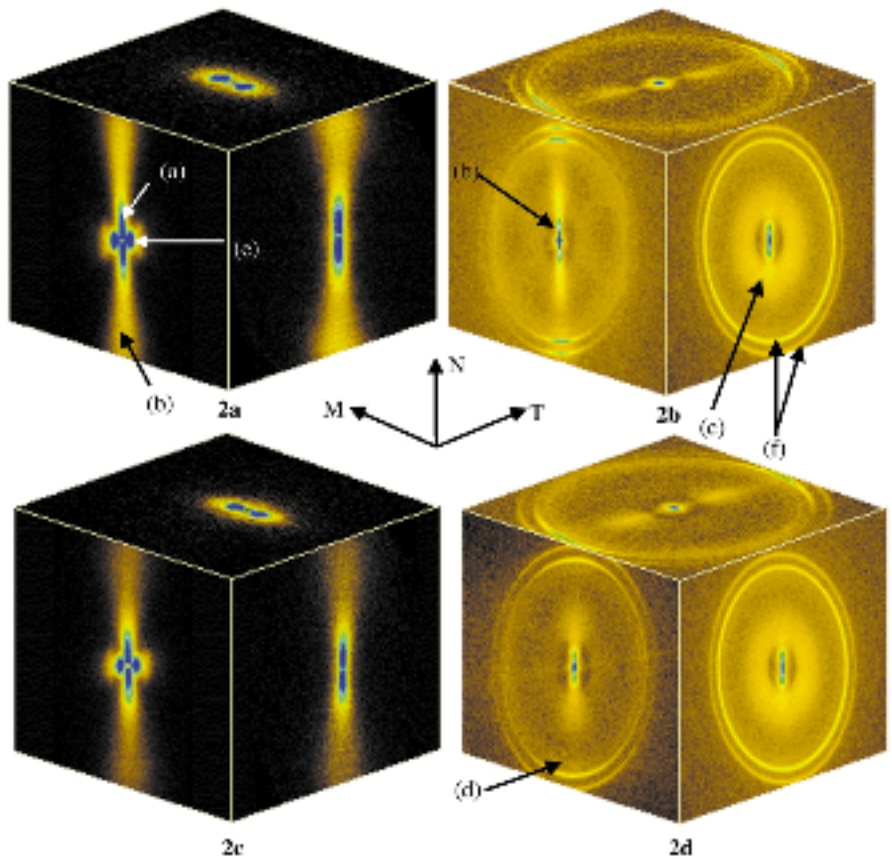

Fig. 2. 2-D SAXS ((a) and (c)) and WAXS ((b) and (d)) patterns for orientation MN (left face), NT (right face) and MT (top face) of films HD603 ((a) and (b)) and HD612 ((c) and (d)). The numbers in the parenthesis represent the reflections from the following: (a) clay tactoids, (b) modified/intercalated clay (002) plane, (c) unmodified clay (002) plane, (d) clay (110) and (020) plane, (e) polymer crystalline lamellar, (f) polymer unit cell (110) plane (inner ring) and (200) plane (outer ring).

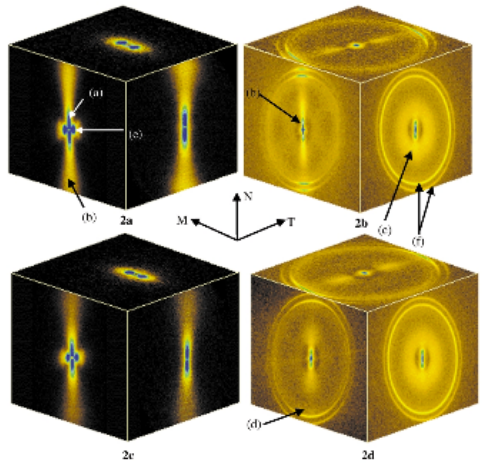

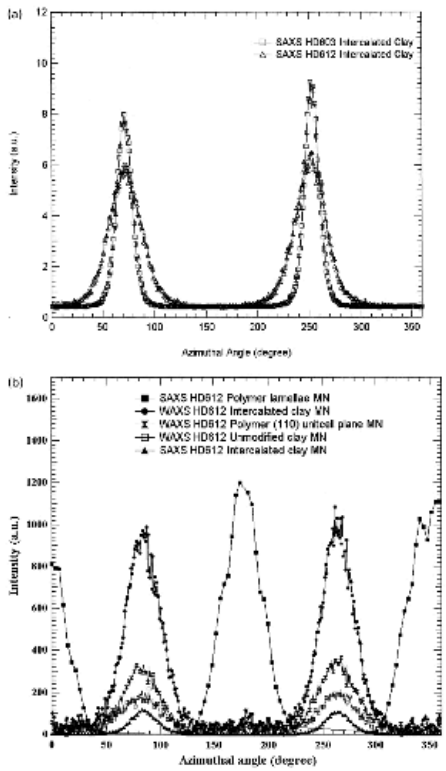

Fig. 4. (a) Azimuthal plot showing the orientation of intercalated clay platelets in HD603 and HD612 in film MN orientation (data averaged from $q = 0.15$–$0.30\ \text{Å}^{-1}$). (b) Azimuthal plot showing orientation of unmodified clay, intercalated clay, polymer lamellae and polymer unit cell (110) plane in HD612. The polymer lamellae curve has been truncated owing to the bright anisotropic streak associated with tactoids at 90 and 270° (Fig. 2) as discussed in the text.

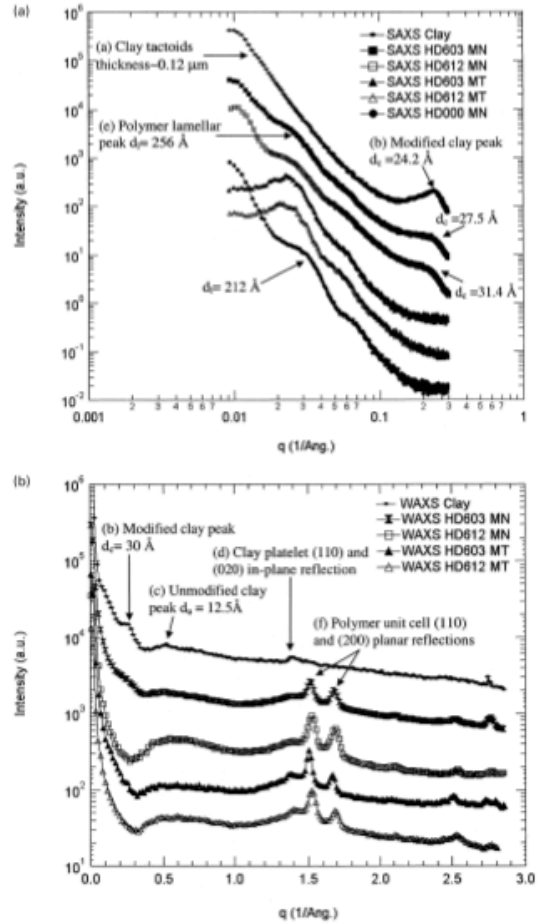

Fig. 3. (a) SAXS log–log radial plots for clay and HD603, HD612 and HD000 in orientation MN and MT. Here d_c represents the d-spacing of the intercalated/modified clay while d_l represents the d-spacing of the polymer lamellar structures in the nanocomposite. (b) WAXS log–linear radial plots for clay and the two films in orientation MT and MN. Here d_u represents the d-spacing of the unmodified clay in the nanocomposite.

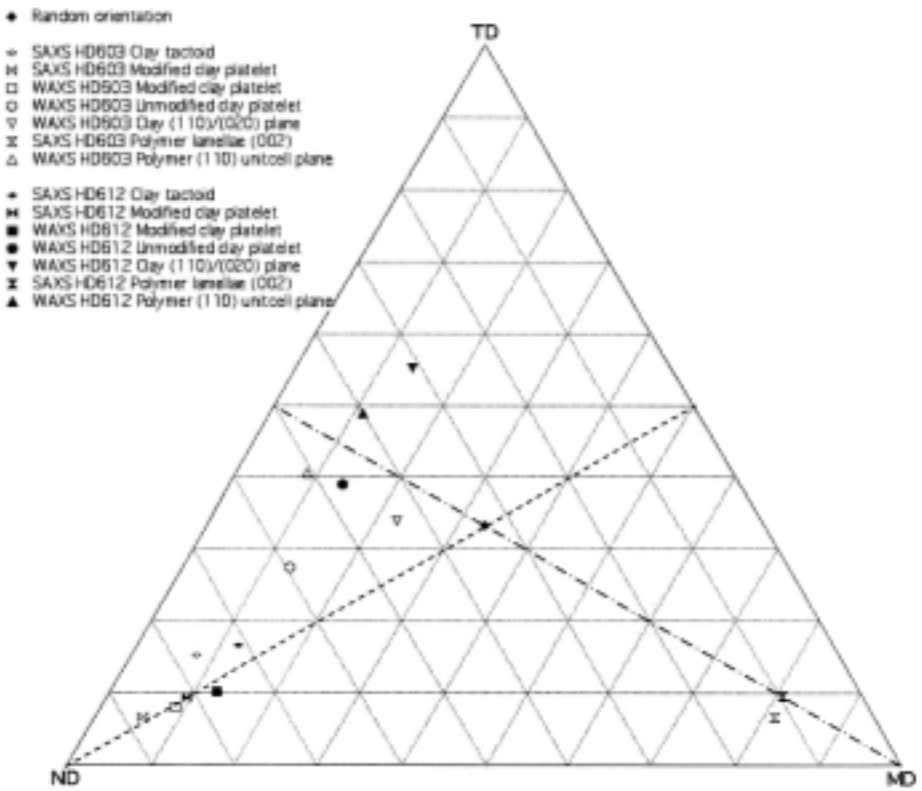

Fig. 6. Wilchinsky triangle [29–32] for average normal orientation of clay tactoids, unmodified clay platelets, intercalated clay platelets, clay (110)/(020) plane, polymer lamellae (001) and polymer (110) unit cell plane of HD603 and HD612 examined here. For a completely random oriented sample a point in the center results. (- - -) Points on this line have their normals randomly arranged in a MT projection. Proximity to ND reflects coplanarity with the MT plane. (—·—·—) Points on this line have their normals randomly arranged in the NT projection. Proximity to MD reflects coplanarity with the NT plane.

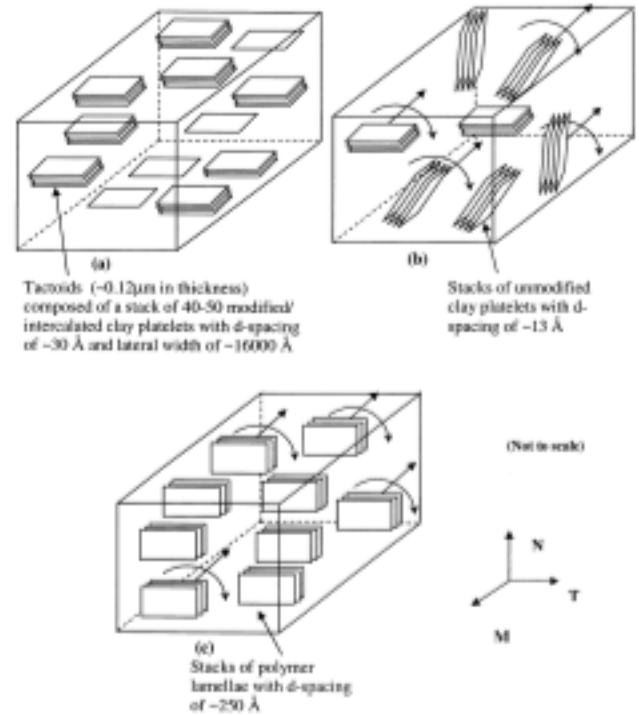

Fig. 7. Schematic of the orientation of (a) tactoids of modified/intercalated clay platelets, (b) unmodified clay platelets, and (c) polymer crystalline lamellae in the nanocomposite films.

Time Resolution at APS/ESRF

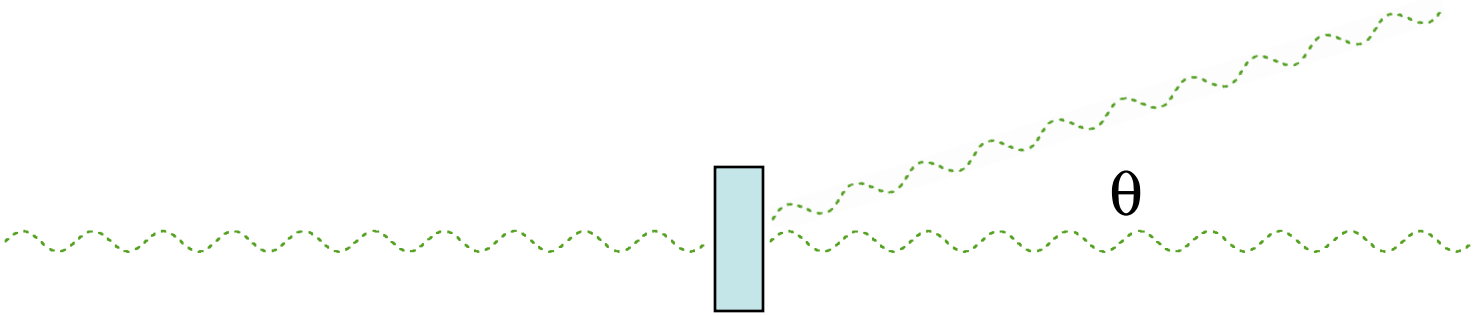

Time Resolution 10 ms (Synchrotron Facility)

For Flow Through Experiment (Flame/Liquid/ Gas Flow) can be 10 μs

Size Resolution 1 Å to 1 μm

Nano-particles are unstable and form far from equilibrium.

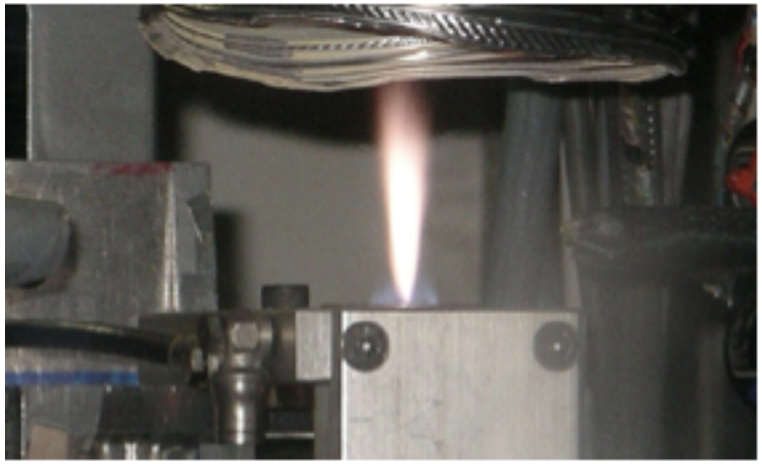

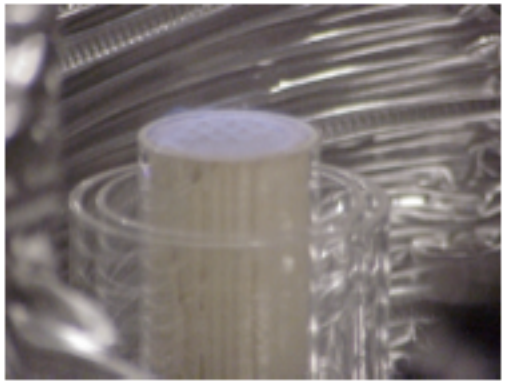

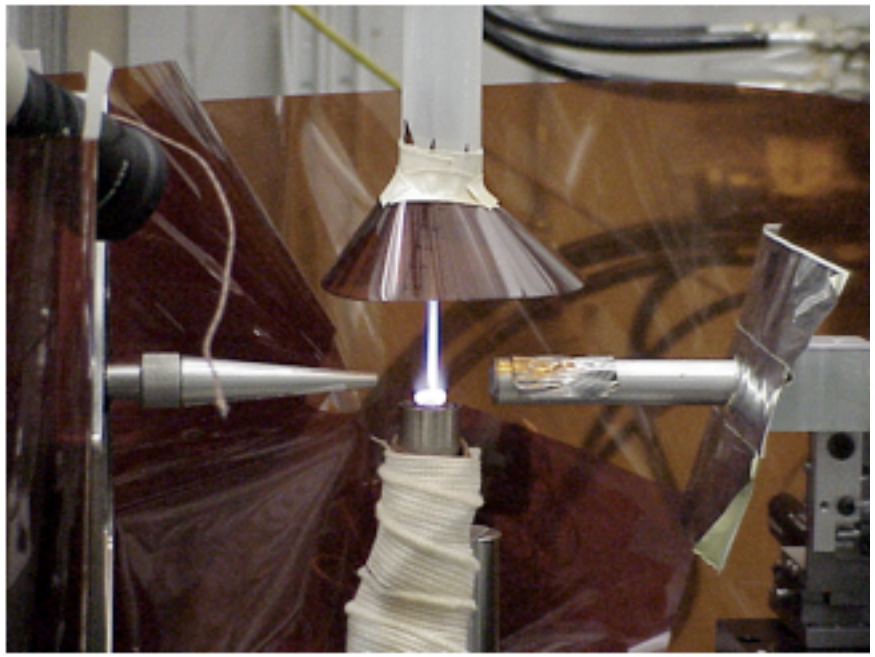

$T \sim 2500°K$

Time ~ 100 ms

$\phi_s \sim 1 \times 10^{-6}$

$d_p \sim 5$ to 50 nm

2-Closely related Techniques:

ASAXS- Anomalous x-ray scattering, vary wavelength leads to change in contrast due to the complex absorption spectra, requires synchrotron source.

GISAXS- Promise of high resolution spectra for surface structures but there are technical issues with data interpretation.

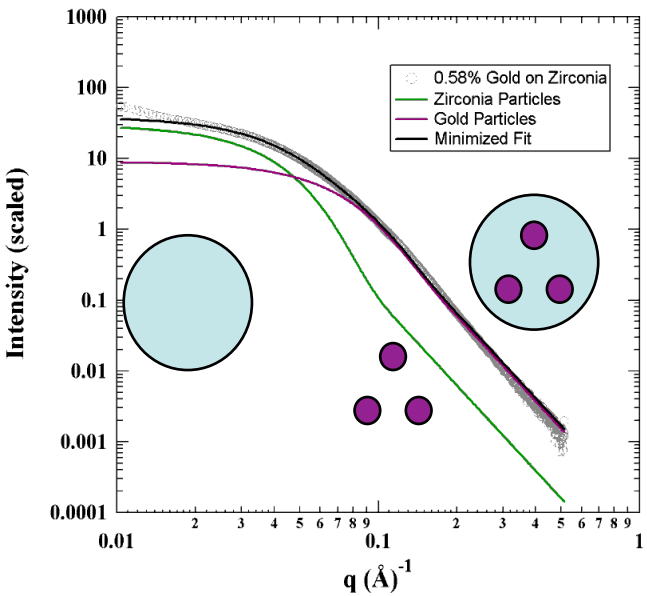

Chopra S, Beaucage G, in preparation

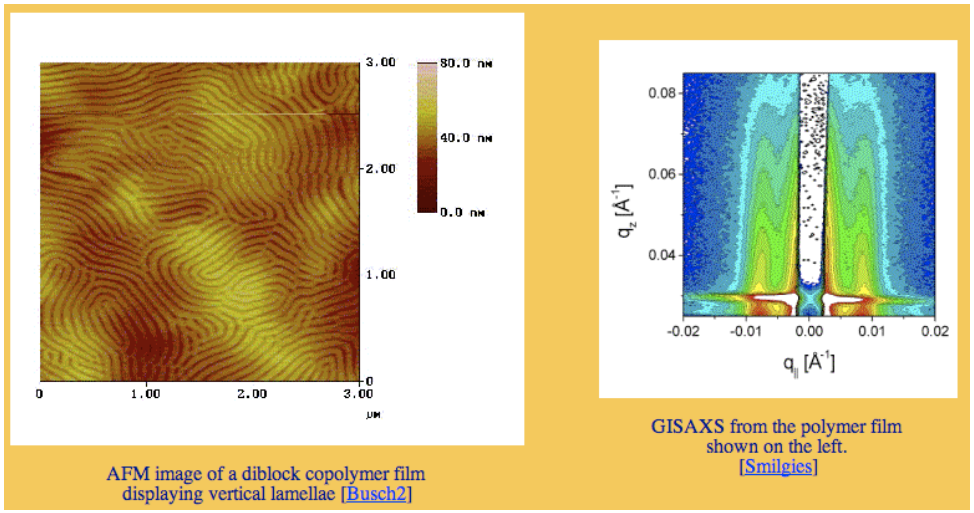

http://staff.chess.cornell.edu/~smilgies/gisaxs/GISAXS.php

Outline:

1) Experimental Instrumentation
2) Specific Scattering Laws
3) General Scattering Laws
   Guinier's Law
   Porod's Law
   Unified Scattering Function
   Fractals
   Branching
4) Polydispersity
5) Summary

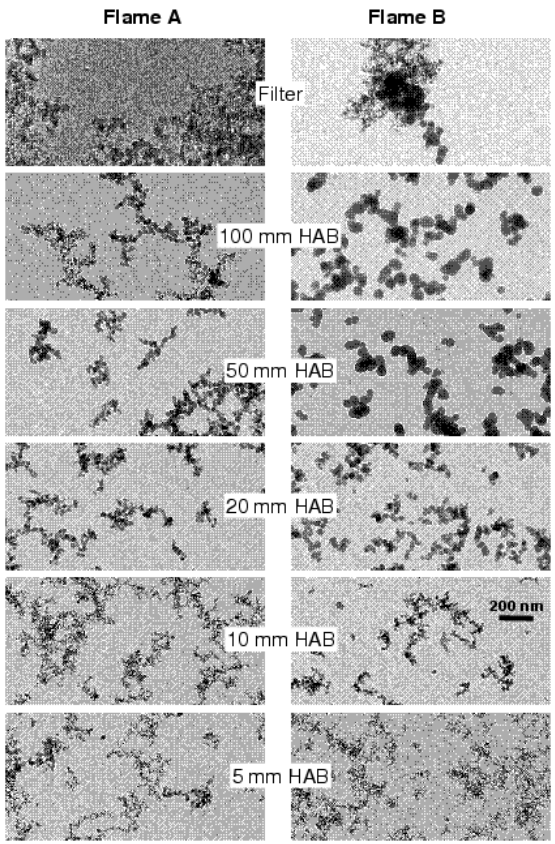

Kammler HK, Beaucage G, Kohls DJ, Agashe N. Ilavsky J
J Appl. Phys. **97**(2005) (Article 054309).

SAXS Modeling

Assumption: Binary interference pattern.

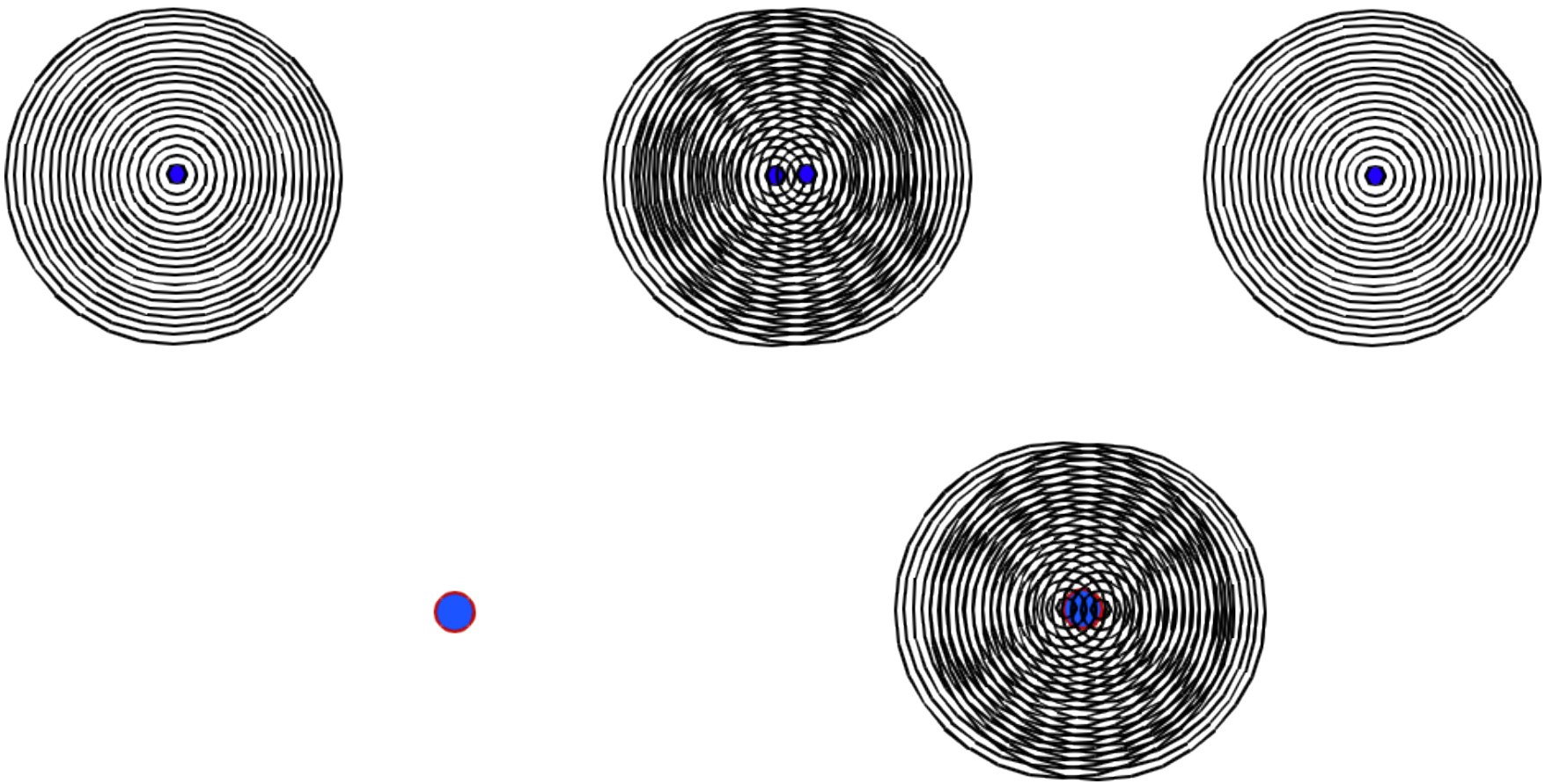

SAXS Modeling

Assumption: Binary interference pattern.

Structure Factor, S(q)

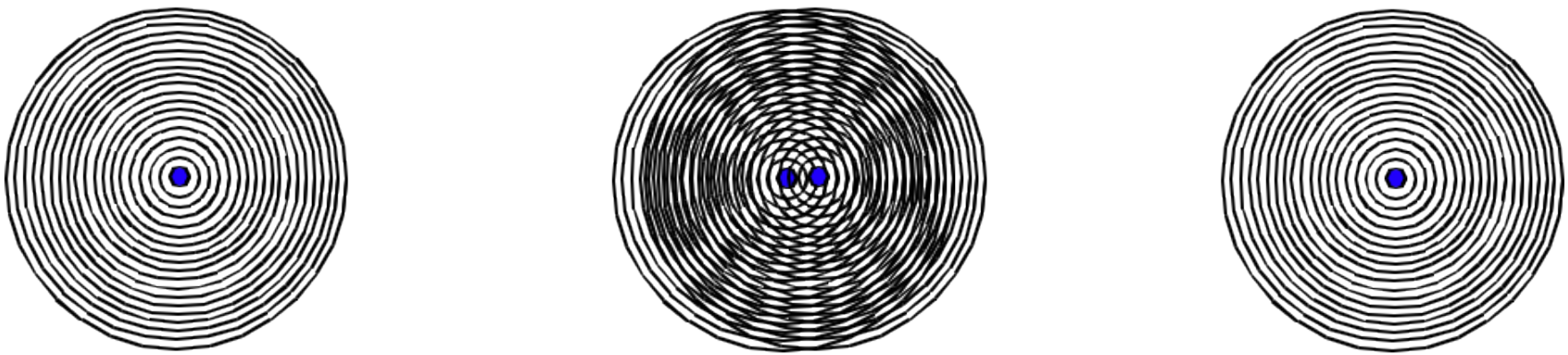

Form Factor, $F^2(q)$

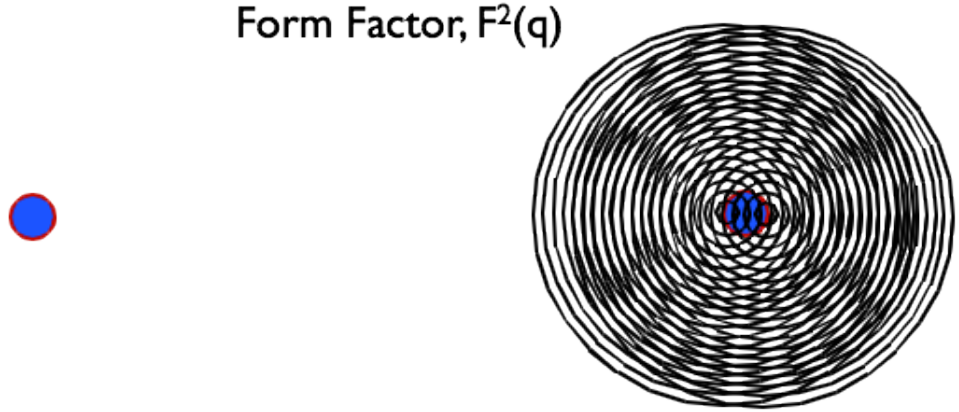

$$I(q) = A\, S(q)\, F^2(q)$$

Four Methods of SAXS Modeling

1) Calculate the amplitude for specific structures.
Viable for simple structures, spheres, rods, core/shell models
Intensity for some cases Gaussian coil.

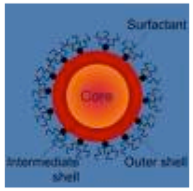

2) Develop general laws for scattering.
Viable for all structures, analysis depends on specific models. Most useful for systems with low degrees of structural regularity (unfolded states or aggregates).

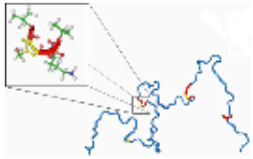

3) Calculate the pair distance distribution function PDDF from the scattered intensity. Analyze the PDDF using models and general rules.
Viable when a wide range of scattering vector, q, is available or valid extrapolations can be made to high and low q. A direct link between calculated structural features and the observed features in the data is lost.

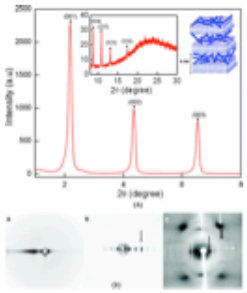

4) Calculate the PDDF using structural models (spheres).
Use an inverse Fourier transform to calculate the scattered intensity and a least-squares or other method to iterate the model parameters for a best fit.
Most useful for systems with a high degree of structural regularity (native state).

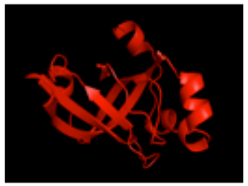

Four Methods of SAXS Modeling

1) Calculate the amplitude for specific structures.
Viable for simple structures, spheres, rods, core/shell models
Intensity for some cases Gaussian coil.

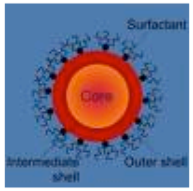

2) Develop general laws for scattering.
Viable for all structures, analysis depends on specific models. Most useful for systems with low degrees of structural regularity (unfolded states or aggregates).

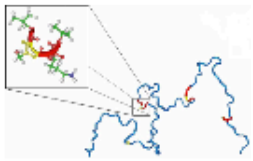

3) Calculate the pair distance distribution function PDDF from the scattered intensity. Analyze the PDDF using models and general rules.
Viable when a wide range of scattering vector, q, is available or valid extrapolations can be made to high and low q. A direct link between calculated structural features and the observed features in the data is lost.

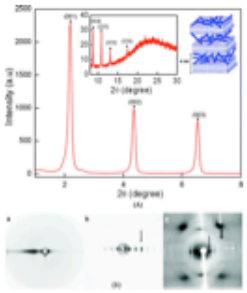

4) Calculate the PDDF using structural models (spheres).
Use an inverse Fourier transform to calculate the scattered intensity and a least-squares or other method to iterate the model parameters for a best fit.
Most useful for systems with a high degree of structural regularity (native state).

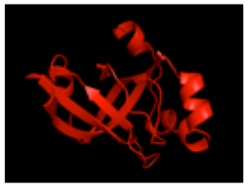

Debye Function

$$I(q) = \left\langle F^2(q) \right\rangle = V\rho_e^2 \int_0^\infty \gamma_0(r) \frac{\sin qr}{qr} 4\pi r^2 dr$$

Assumptions:

1) Centro-symmetric Particle

$$e^{-i\bar{q}\bullet OM_k} = \cos(\bar{q} \bullet OM_k)$$

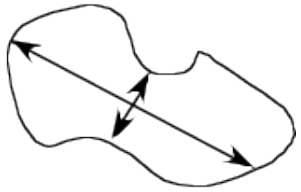

2) Random Orientation (translational & rotational symmetry)

$$\left\langle \cos(\bar{q} \bullet \bar{r}) \right\rangle = \frac{\sin qr}{qr}$$

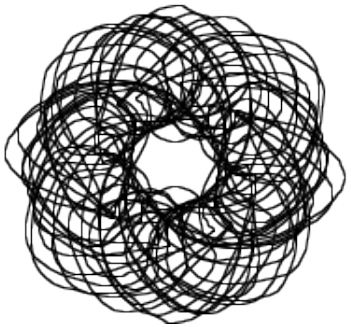

Debye Function

$$I(q) = \left\langle F^2(q) \right\rangle = V\rho_e^2 \int_0^\infty \gamma_0(r) \frac{\sin qr}{qr} 4\pi r^2 dr$$

ρ_e Electron Density

$\gamma_0(r)$ Characteristic Function, Correlation Function

Probability that at a distance "r" from a point in a particle another particle can be found

$$\gamma_0(r) = \frac{\langle V(r) \rangle}{V}$$

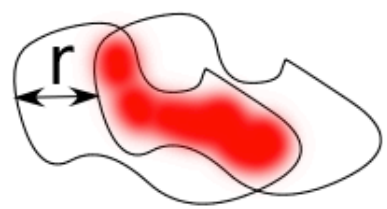

Average for translation and rotation

Debye Function

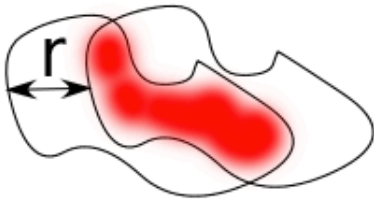

$$I(q) = \left\langle F^2(q) \right\rangle = V\rho_e^2 \int_0^\infty \gamma_0(r) \frac{\sin qr}{qr} 4\pi r^2 dr$$

$\gamma_0(r)$ Characteristic Function, Correlation Function

For simple objects such as a sphere we can calculate the characteristic function

$$\overline{V}(r) = \frac{\pi}{12}(2R - r)^2(4R + r)$$

$$\gamma_0(r) = \frac{\overline{V}(r)}{V} = 1 - \frac{3r}{4R} + \frac{1}{16}\left(\frac{r}{R}\right)^3$$

Debye Function

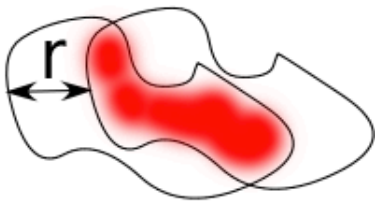

$$I(q) = \left\langle F^2(q) \right\rangle = V\rho_e^2 \int_0^\infty \gamma_0(r) \frac{\sin qr}{qr} 4\pi r^2 dr$$

$\gamma_0(r)$ Characteristic Function, Correlation Function

For simple objects such as a sphere we can calculate the characteristic function

$$\gamma_0(r) = \frac{\overline{V}(r)}{V} = 1 - \frac{3r}{4R} + \frac{1}{16}\left(\frac{r}{R}\right)^3$$

$$I(q) = Nn_e^2 \left(3\frac{\sin qR - qR\cos qR}{(qR)^3} \right)^2$$

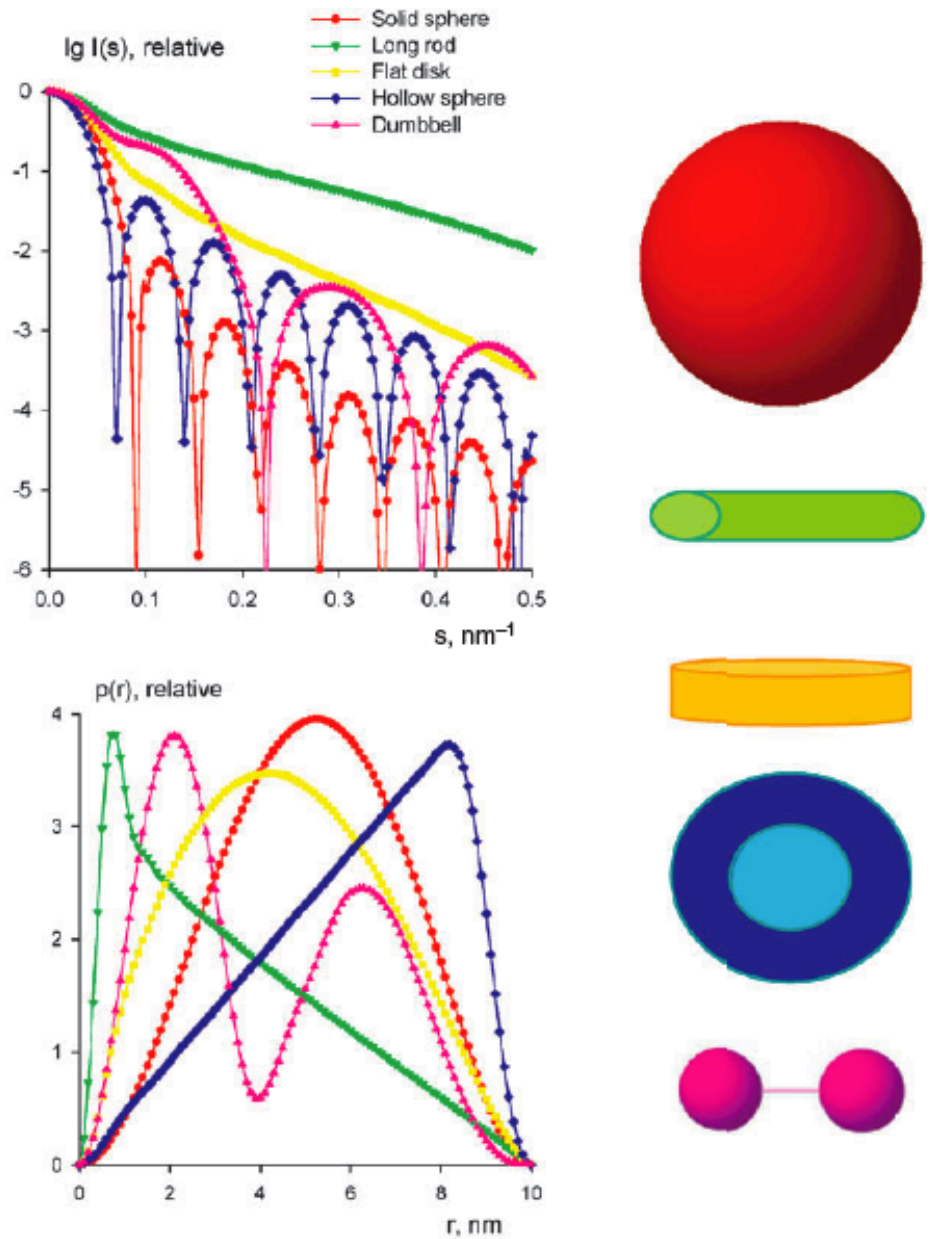

Figure 5. Scattering intensities and distance distribution functions of geometrical bodies.

Svergun DI, Koch MHJ *Rep. Prog. Phys.* **66** 1735-1782 (2003)

Other direct calculations are possible for simple objects $I(q) = Nn_e^2 F^2(q) S(q)$

Sphere

$$F_{sphere}(q) = 3\frac{\sin qR - qR\cos qR}{(qR)^3}$$

Rod

$$F^2(q) = 2\frac{Si(qL)}{qL} - 4\frac{\sin^2(qL/2)}{(qL)^2}$$

Disk

$$F^2(q) = \frac{2}{q^2R^2}\left[1 - \frac{J_1(2qR)}{qR}\right]$$

Core and Shell Sphere

$$F_{Core\&Shell}(q) = \frac{\left(V_{Shell}(\rho_{Shell} - \rho_{Solvent})F_{Sphere}(R_{Shell}) - V_{Core}(\rho_{Shell} - \rho_{Core})F_{Sphere}(R_{Core})\right)}{(V_{Core} - V_{Shell})}$$

Gaussian Polymer Chain

$$F^2(q) = 2\frac{\exp\left(-q^2R_g^2\right) + q^2R_g^2 - 1}{\left(q^2R_g^2\right)^2}$$

Core and Shell with Gaussian Chain Attached

...

Pedersen JS, *Chapter 16 in Neutrons, X-rays and Light: Scattering Methods Applied to Soft Condensed Matter,* Linder P, Zemb Th editors North Holland Press (2002).

Scattering Function for Monodisperse Spheres

Rayleigh, 1914

$$I(q) = 9G\left[\frac{\sin qR - qR\cos qR}{(qR)^3}\right]^2$$

$G = Nn_e^2$

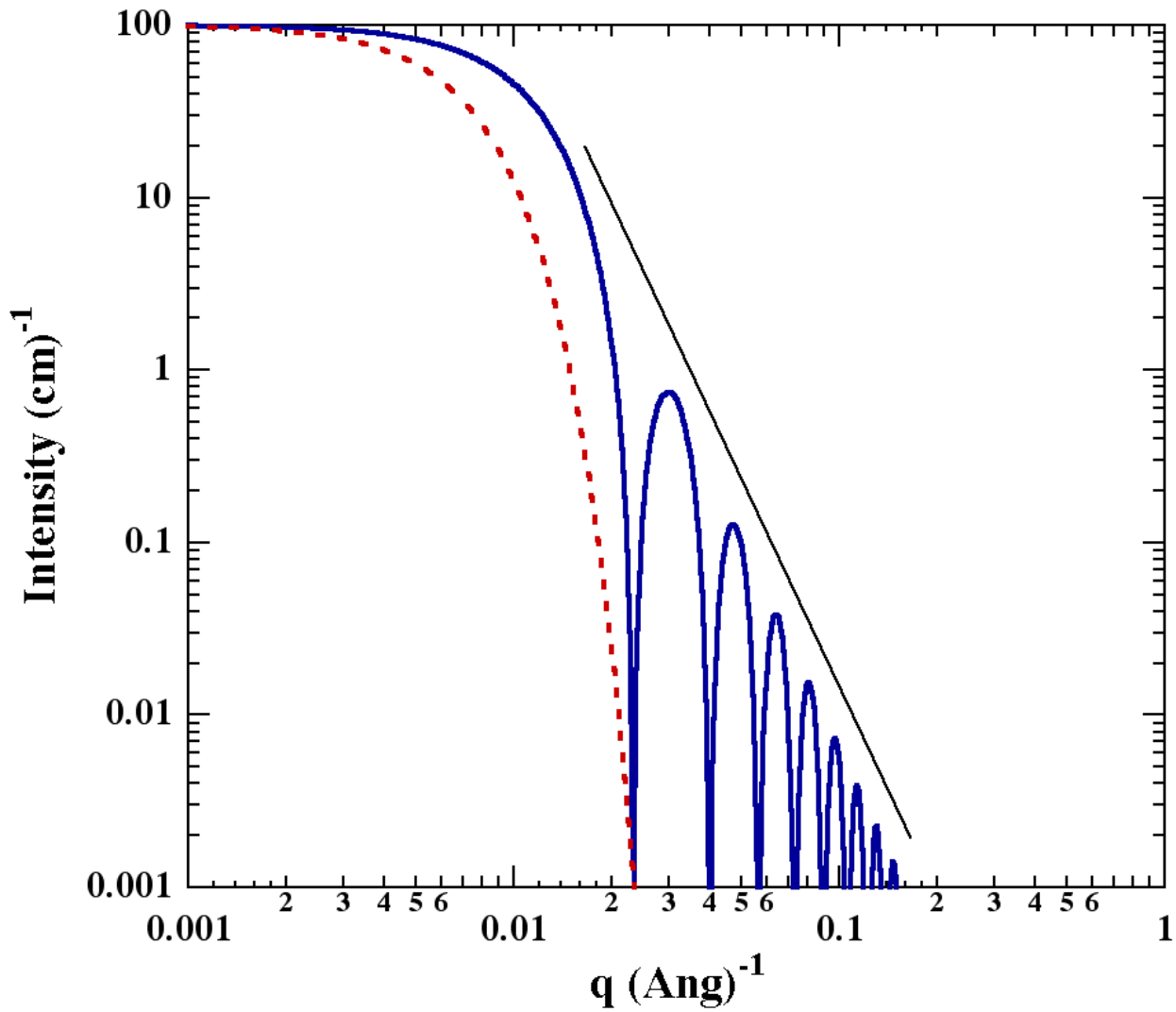

The Debye (1947) Scattering Function for a Polymer Coil

$$I(Q) = \frac{2}{Q^2}\left(Q - 1 + \exp(-Q)\right)$$

$$Q = q^2 R_g^2$$

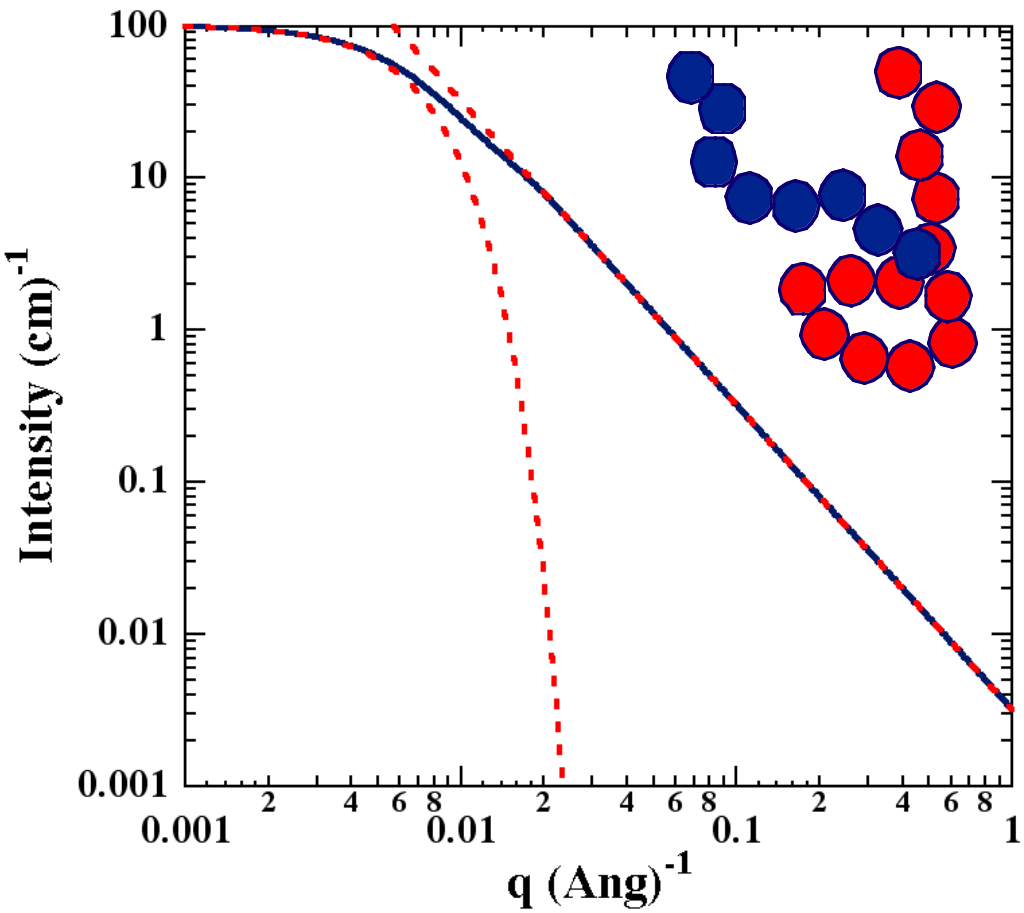

Outline:

1) Experimental Instrumentation
2) Specific Scattering Laws
3) General Scattering Laws
   Guinier's Law
   Porod's Law
   Unified Scattering Function
   Fractals
   Branching
4) Polydispersity
5) Summary

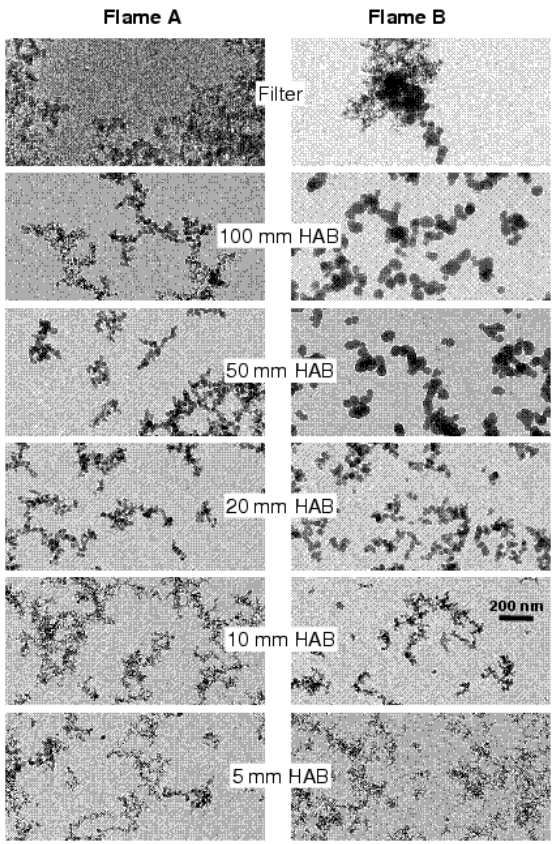

Kammler HK, Beaucage G, Kohls DJ, Agashe N. Ilavsky J
J Appl. Phys. **97**(2005) (Article 054309).

If you do not have a sphere or a Gaussian linear chain

There are some general rules for all structures

Guinier's Law
Porod's Law
Mass Fractal Scaling Laws
The Unified Function

With these tools we can build a scattering function
for any "random" structure

Binary Interference Yields Scattering Pattern.

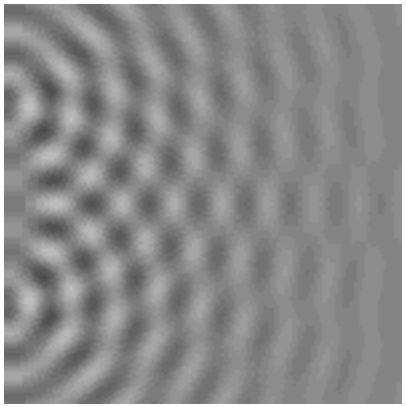

$I(q) \sim N\, n_e^2$

n_e Reflects the density of a Point generating waves

N is total number of points

$$q = \frac{4\pi}{\lambda}\sin\left(\theta/2\right) \qquad \mathrm{d} = \frac{2\pi}{\mathrm{q}} \sim r$$

General scattering laws **by which all scatters are governed**

1) "Particles" have a size and

2) "Particles" have a surface.

Binary Interference Yields Scattering Pattern.

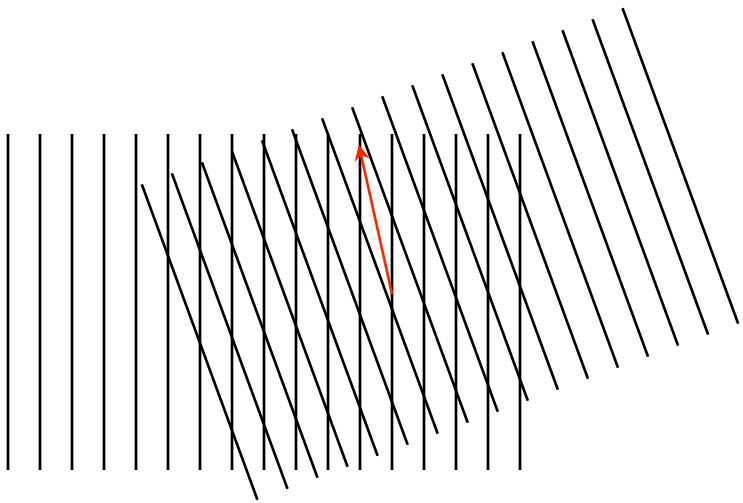

-Consider that an in-phase wave scattered at angle θ was in phase with the incident wave at the source of scattering.

-This can occur for points separated by ***r*** such that

|r| = 2π/|q|

- $$q = \frac{4\pi}{\lambda}\sin\frac{\theta}{2}$$

Binary Interference Yields Scattering Pattern.

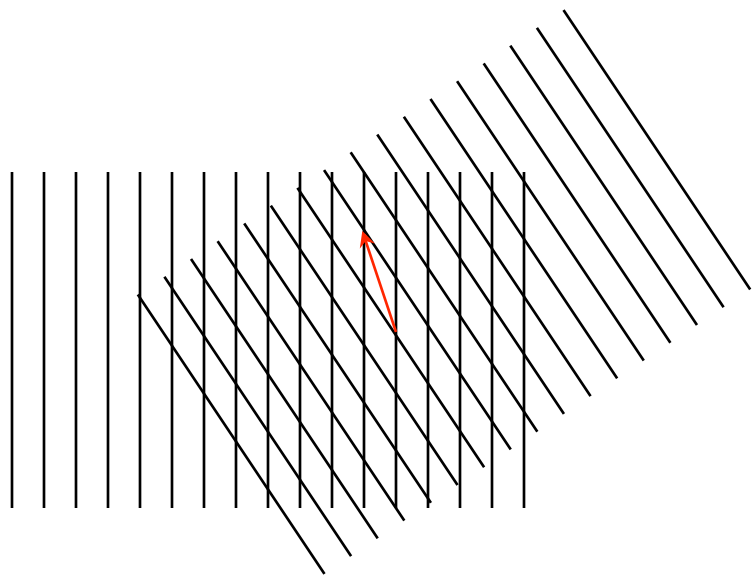

-For high θ, ***r*** is small

Binary Interference Yields Scattering Pattern.

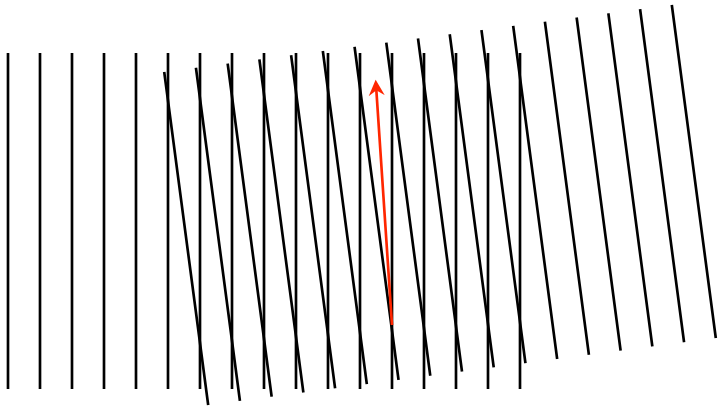

-For small θ, ***r*** is large

Binary Interference Yields Scattering Pattern.

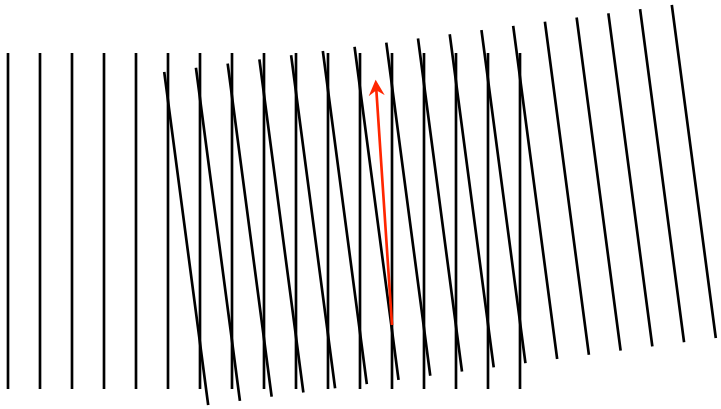

-For small θ, ***r*** is large

We can consider just the vector “r”, and for isotropic samples we do not need to consider direction.

For an isotropic sample we consider scattering as arising from the probability of the random placement of a vector ***r*** in the scattering phase.

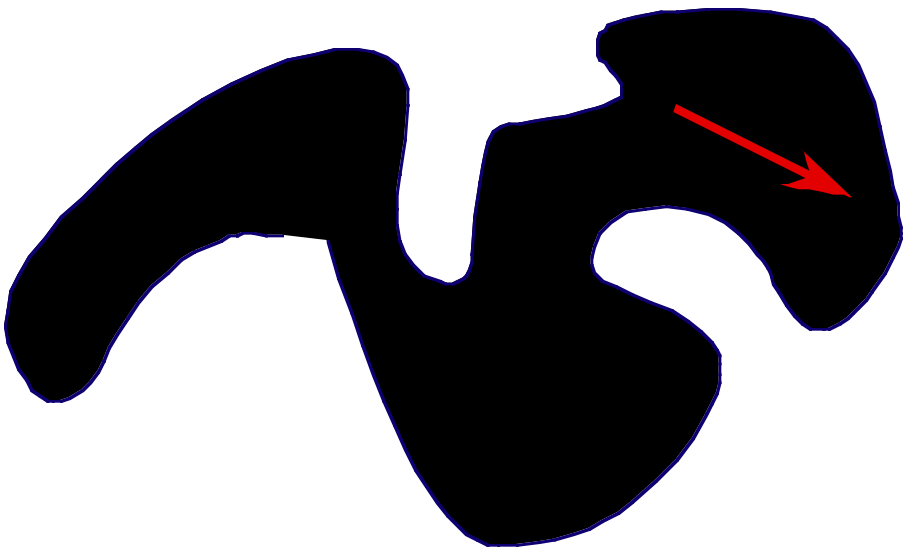

For an isotropic sample we consider scattering as arising from the probability of the random placement of a vector ***r*** in the scattering phase.

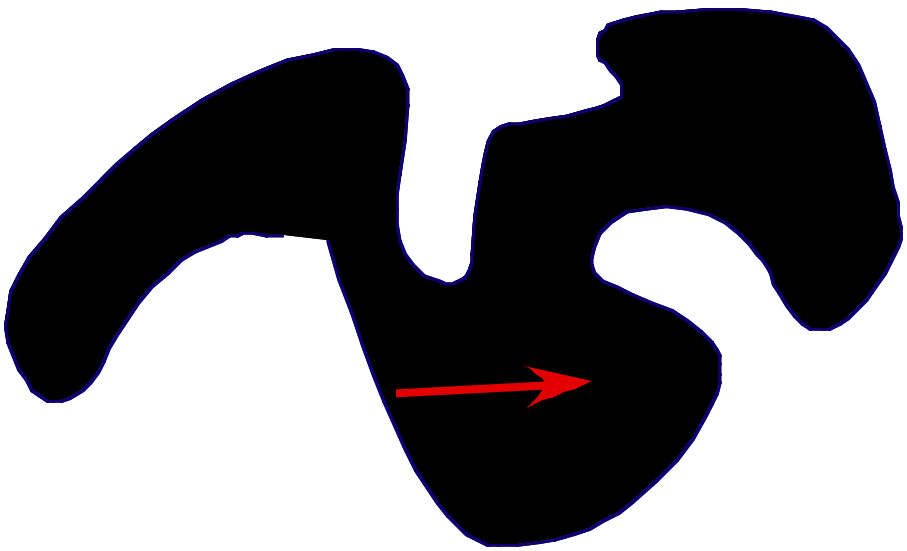

For an isotropic sample we consider scattering as arising from the probability of the random placement of a vector ***r*** in the scattering phase.

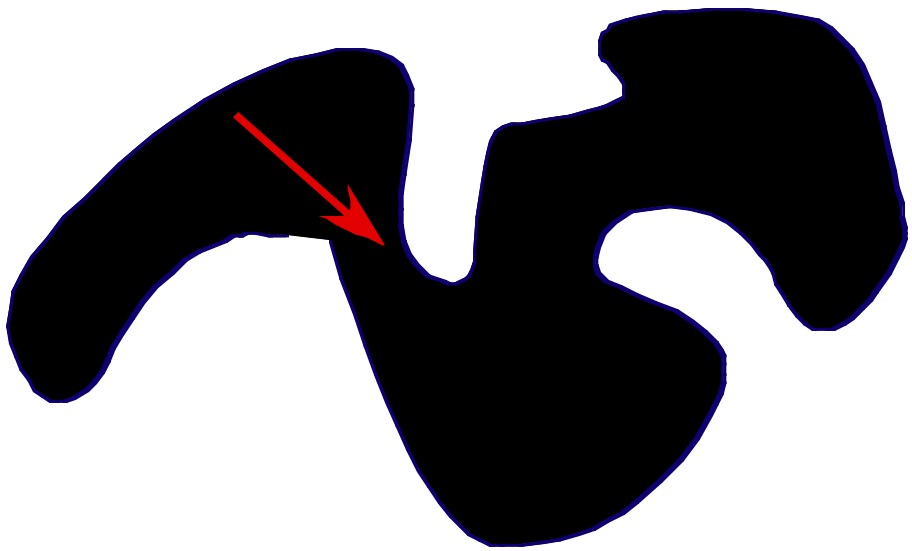

Rather than random placement of the vector we can hold The vector fixed and rotate the particle

For an isotropic sample we consider scattering as arising from the probability of the random placement of a vector ***r*** in the scattering phase.

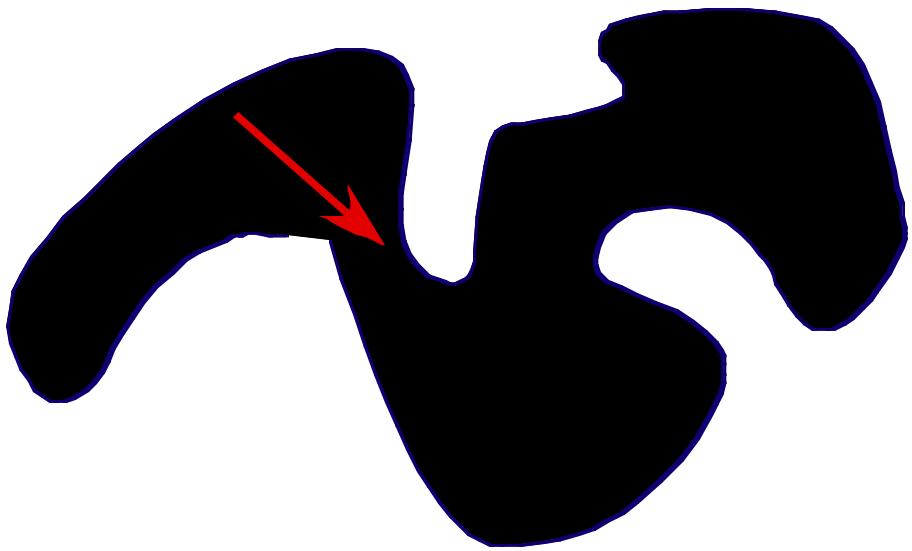

Rather than random placement of the vector we can hold The vector fixed and rotate the particle

For an isotropic sample we consider scattering as arising from the probability of the random placement of a vector ***r*** in the scattering phase.

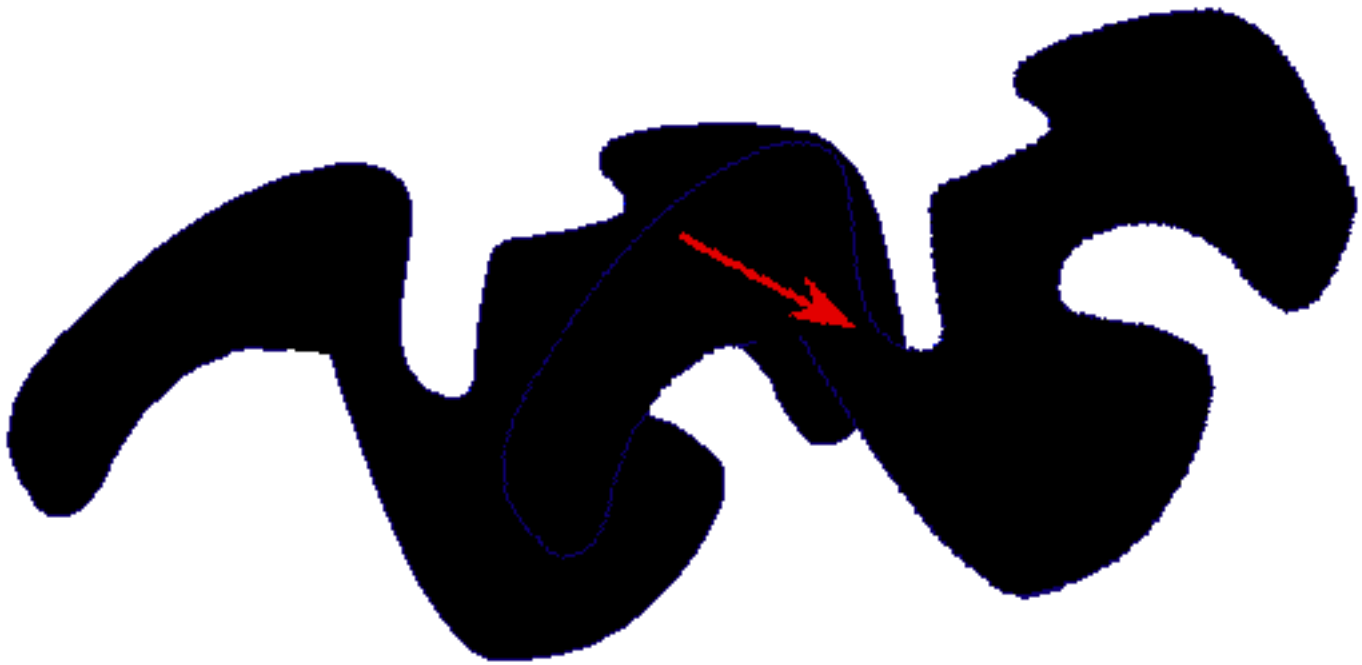

Rather than random placement of the vector we can hold The vector fixed and rotate the particle

For an isotropic sample we consider scattering as arising from the probability of the random placement of a vector ***r*** in the scattering phase.

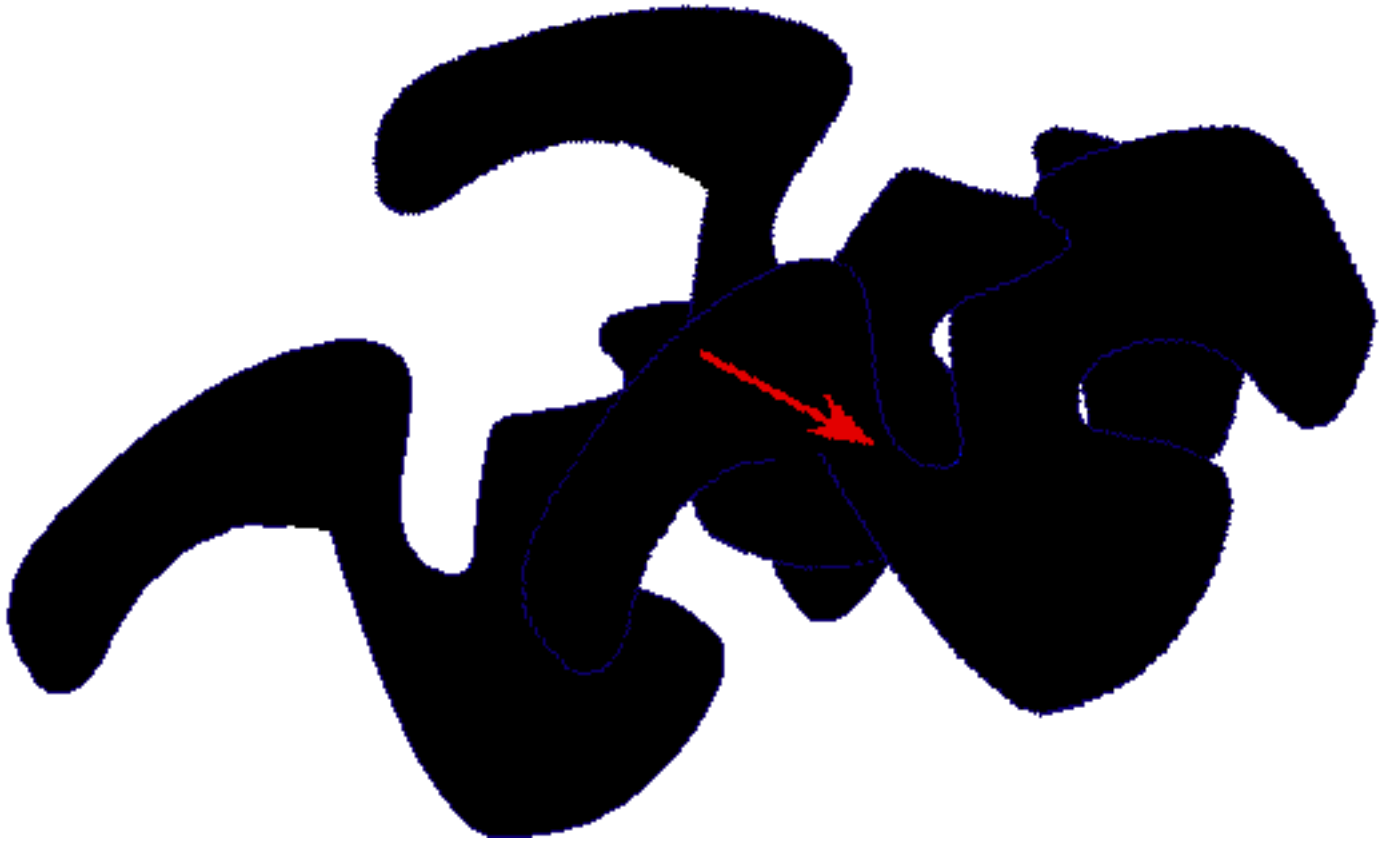

Rather than random placement of the vector we can hold The vector fixed and rotate the particle

The particle becomes a probability density function from the center of mass.

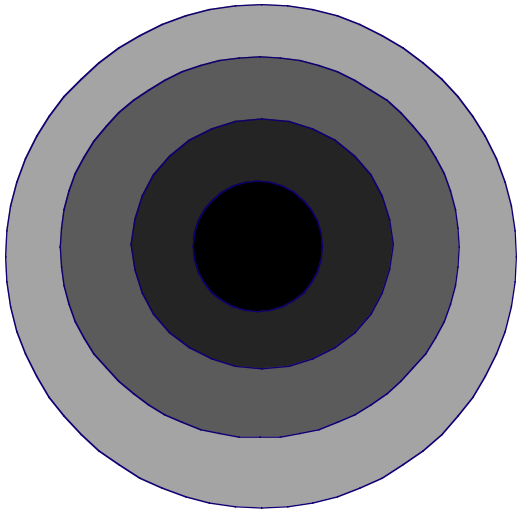

That follows a Gaussian Distribution.

$$p(r) = \exp\left(\frac{-3r^2}{4R_g^2}\right)$$

The particle becomes a probability density function from the center of mass.

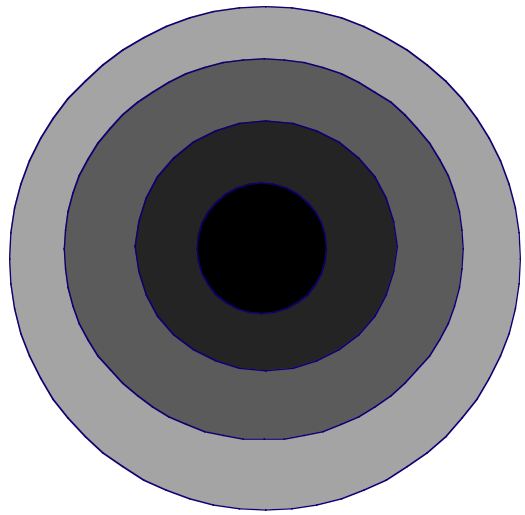

Whose Fourier Transform is Guinier's Law.

$$p(r) = \exp\left(\frac{-3r^2}{4R_g^2}\right) \quad \Rightarrow \quad \mathrm{I(q)} = G\exp\left(-\frac{q^2R_g^2}{3}\right)$$

$$\mathrm{G} = \mathrm{Nn_e^2}$$

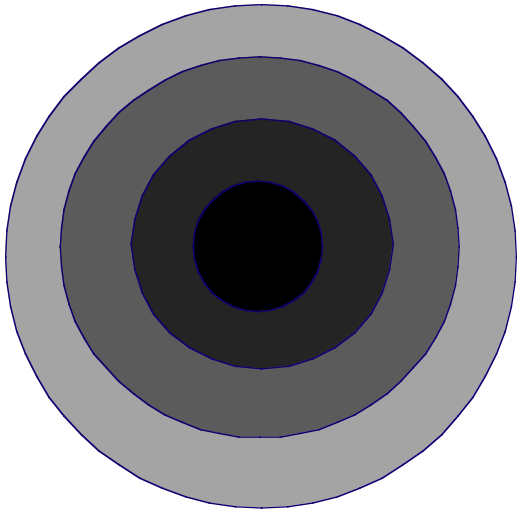

Guinier's Law Pertains to a Particle with no Surface.

$$p(r) = \exp\left(\frac{-3r^2}{4R_g^2}\right) \quad \Rightarrow \quad \mathrm{I(q)} = G\exp\left(-\frac{q^2R_g^2}{3}\right)$$

$$\mathrm{G} = \mathrm{Nn_e^2}$$

Any "Particle" can be *approximated* as a Gaussian probability distribution. (Problem: finite limit to size.)

Guinier's Law

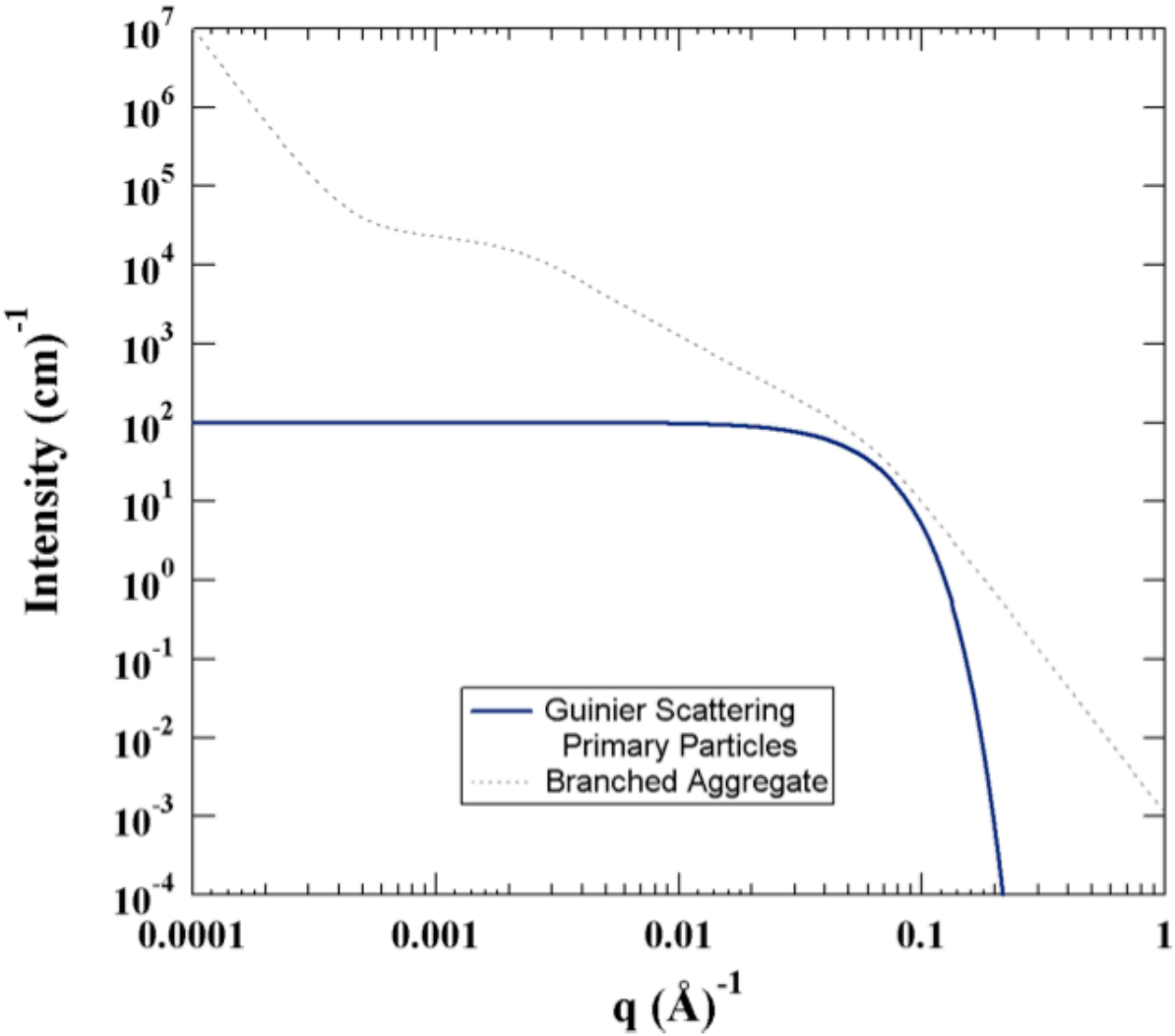

Particle with No Interface

$$I(q) = N(d)n_e^2(d)$$

$$I(q) = G_1 \exp\left(\frac{-q^2\langle R_{g,1}^2\rangle}{3}\right)$$

$$G = N\rho_e^2\langle V^2\rangle \sim \langle \mathrm{R}^6\rangle$$

$$\langle R_g^2\rangle \sim \frac{\langle \mathrm{R}^8\rangle}{\langle \mathrm{R}^6\rangle}$$

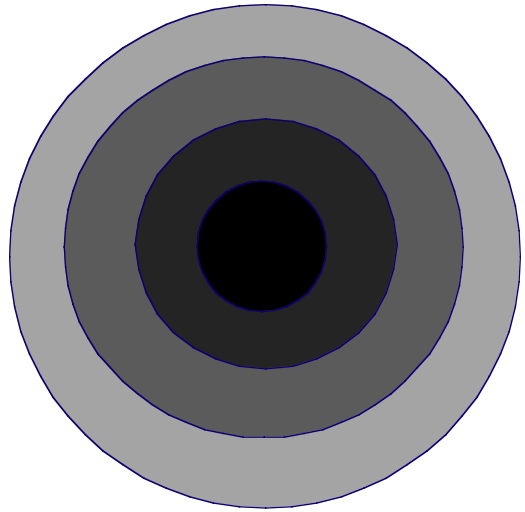

$$p(r) = \exp\left(\frac{-3r^2}{4R_g^2}\right) \quad \Rightarrow \quad \mathrm{I(q)} = G\exp\left(-\frac{q^2R_g^2}{3}\right)$$

$$\mathrm{G} = \mathrm{Nn_e^2}$$

Guinier's Law can be thought of as the
First Premise of Scattering:
All "Particles" have a finite size
reflected by the radius of gyration.

The Debye Scattering Function for a Polymer Coil

$$I(Q) = \frac{2}{Q^2}\left(Q - 1 + \exp(-Q)\right)$$

$$Q = q^2 R_g^2$$

For $qR_g << 1$

$$\exp(-Q) = 1 - Q + \frac{Q^2}{2!} - \frac{Q^3}{3!} + \frac{Q^4}{4!} - \ldots$$

$$I(q) = 1 - \frac{Q}{3} + \ldots \approx \exp\left(-\frac{q^2 R_g^2}{3}\right)$$

Guinier's Law!

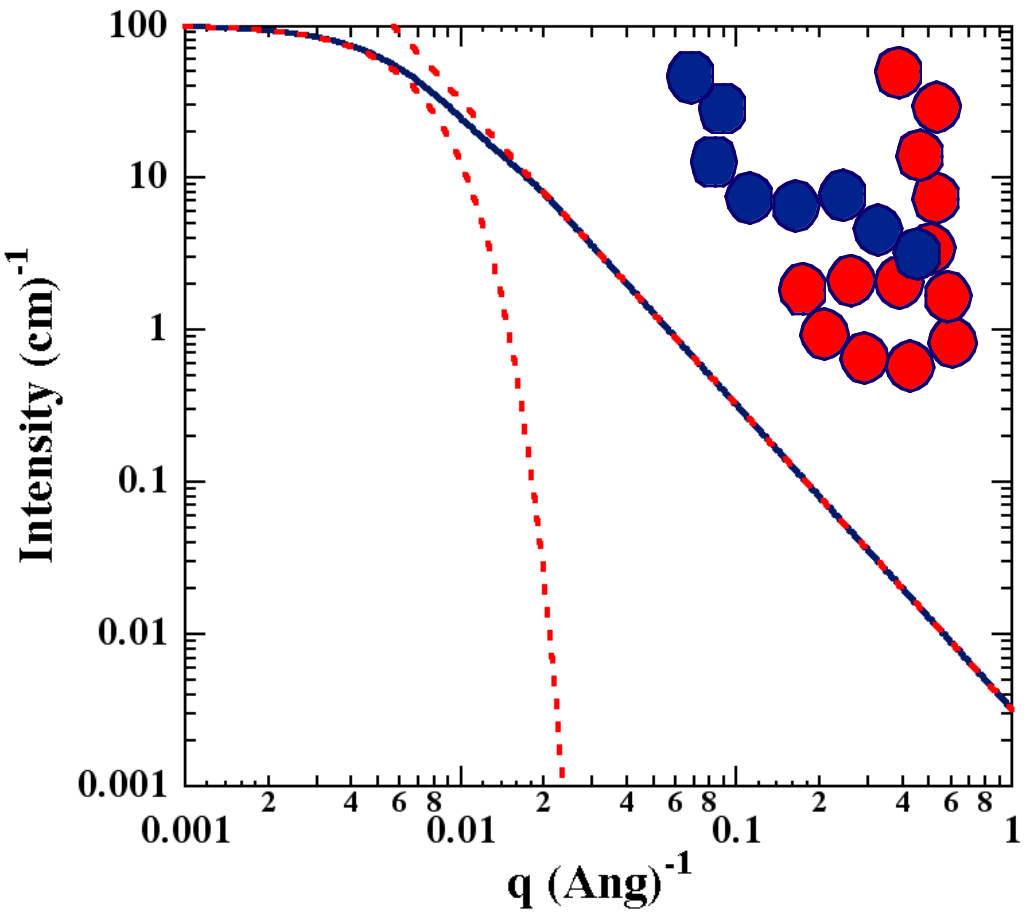

At the other extreme consider a surface.

$$I(q) \sim N\, n_e^2$$

n_e Reflects the density of a Point generating waves

N is total number of points

$I(q) \sim N\, n_e^2$

n_e Reflects the density of a Point generating waves

N is total number of points

At the other extreme we consider a surface.

The only location for contrast between phases is at the interface (for every vector r there is a vector r/2)

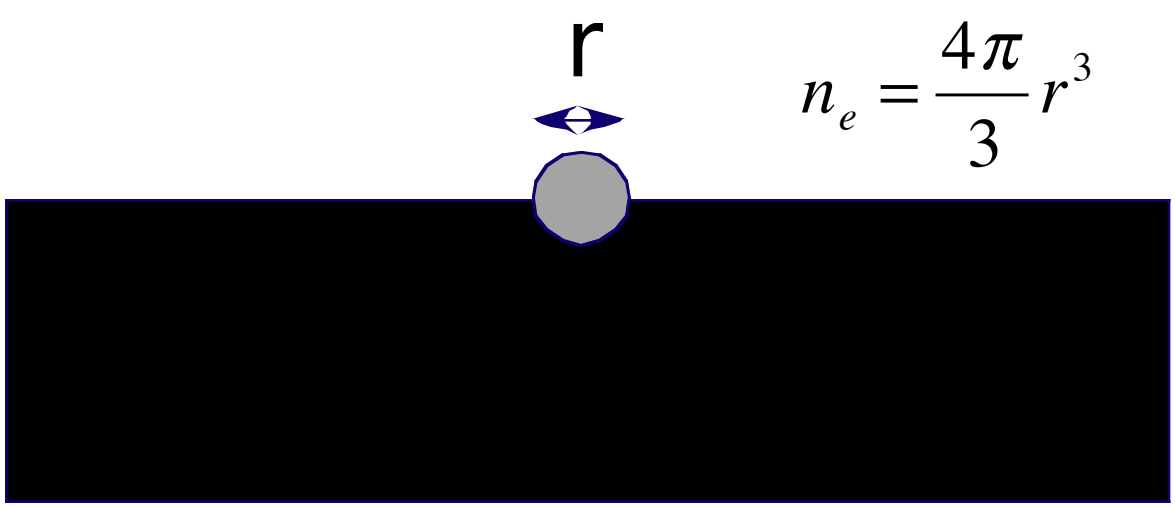

$$n_e = \frac{4\pi}{3} r^3$$

$I(q) \sim N\, n_e^2$

n_e Reflects the density of a Point generating waves

N is total number of points

At the other extreme we consider a surface.

We can fill the interface with spheres of size ***r***

r

$N = S/(\pi r^2)$

$$n_e = \frac{4\pi}{3} r^3$$

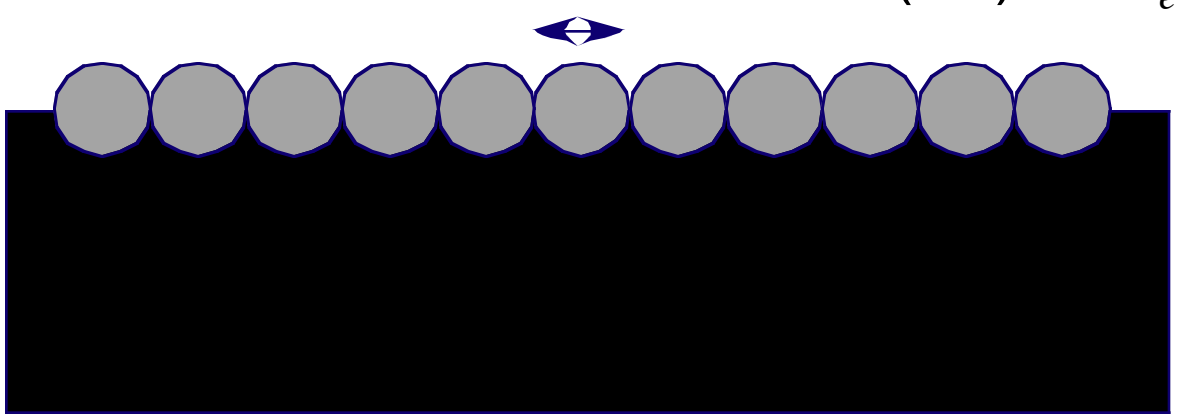

Porod's Law can be thought of as the

Second Premise of Scattering:

All "Particles" have a surface reflected by S/V.

($d_p = (S/V)^{-1}$)

$$I(q) \sim N n_e^2 \sim \left(\frac{S}{\pi r^2}\right)\left(\frac{4\pi r^3}{3}\right)^2 \sim \frac{16 S \pi r^4}{9} \quad \Rightarrow \quad \frac{2\pi n_e^2 \left(\frac{S}{V}\right)}{V q^4}$$

$N = S/(\pi r^2)$

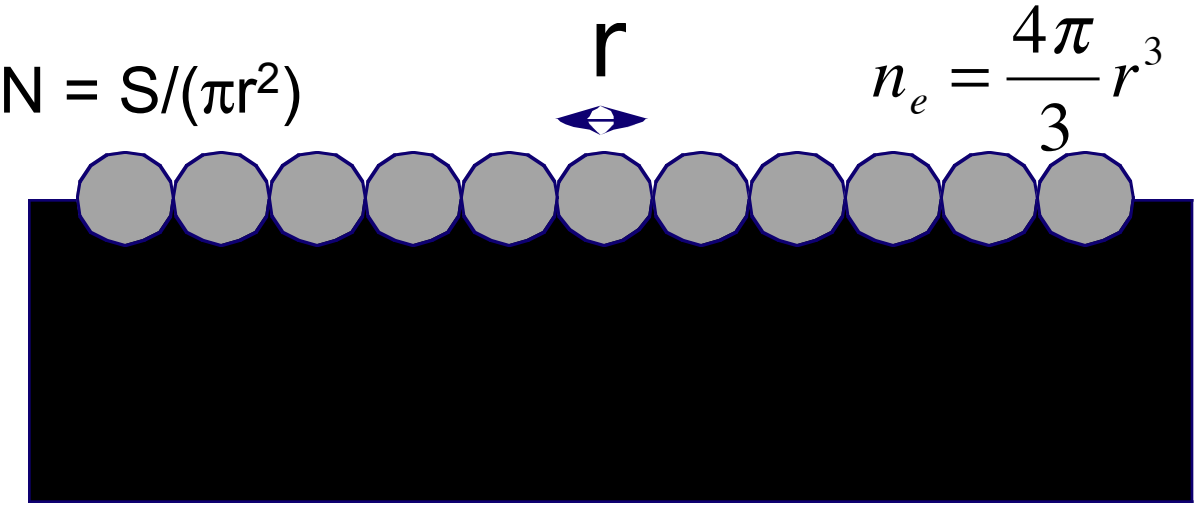

$$n_e = \frac{4\pi}{3} r^3$$

For a Rough Surface: $2 \leq d_s < 3$

(This Function decays to Porod's Law at small sizes)

$$I(q) \sim N n_e^2 \sim \left(\frac{S}{r^{d_s}}\right)\left(\frac{4\pi r^3}{3}\right)^2 \sim S r^{6-d_s} \quad \Rightarrow \quad \frac{S}{q^{6-d_s}}$$

$$N \sim \frac{S}{r^{d_s}} \qquad n_e = \frac{4\pi}{3} r^3$$

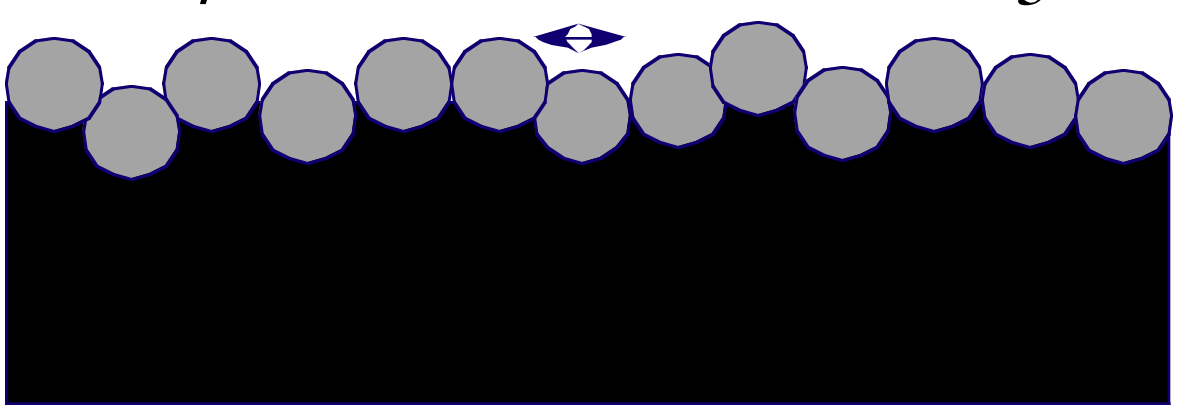

Sphere Function

$$I(q) = 9G\left[\frac{\sin qR - qR\cos qR}{(qR)^3}\right]^2$$

For qR >> 1

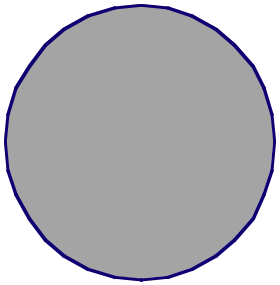

<sinqR> => 0
<cos^{2}qR> => 1/3

$$I(q) \approx \frac{G}{q^4 R^4}$$

Porod's Law for a Sphere!

General Laws for Scattering

Mass Fractal Power-Law

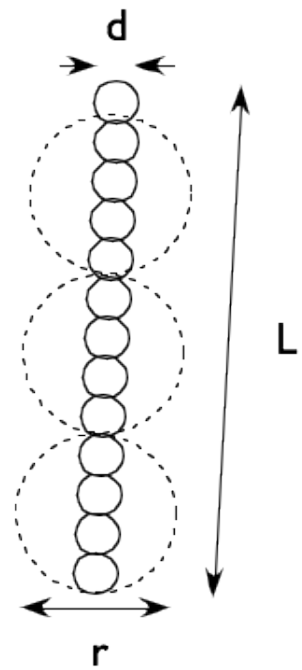

A) Rod

$$I(1/r) \sim N(r)n(r)^2 \qquad N(r) \sim \left(L/r\right) \qquad n(r) \sim \left(r/d\right)$$

$$I(1/r) \sim \left(L/d\right)r \Rightarrow \left(L/d\right)q^{-1} = Nq^{-1}$$

General Laws for Scattering

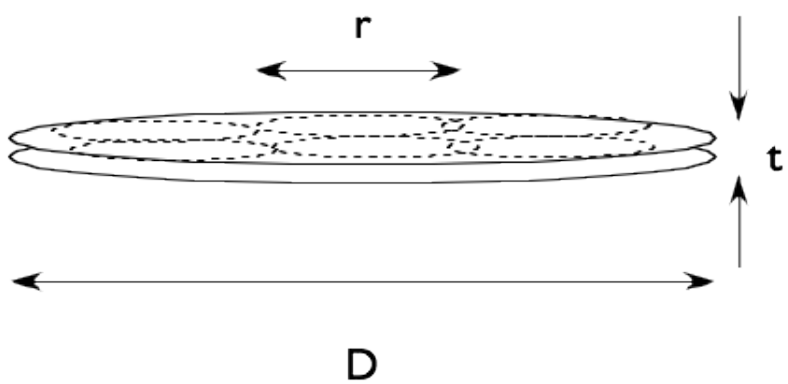

B) Disk

$$I(1/r) \sim N(r)n(r)^2 \qquad N(r) \sim \left(D/r\right)^2 \qquad n(r) \sim \left(r/t\right)^2$$

$$I(1/r) \sim \left(D/t\right)^2 r^2 \Rightarrow \left(D/t\right)^2 q^{-2} = Nq^{-2}$$

General Laws for Scattering

Mass Fractal Power-Law

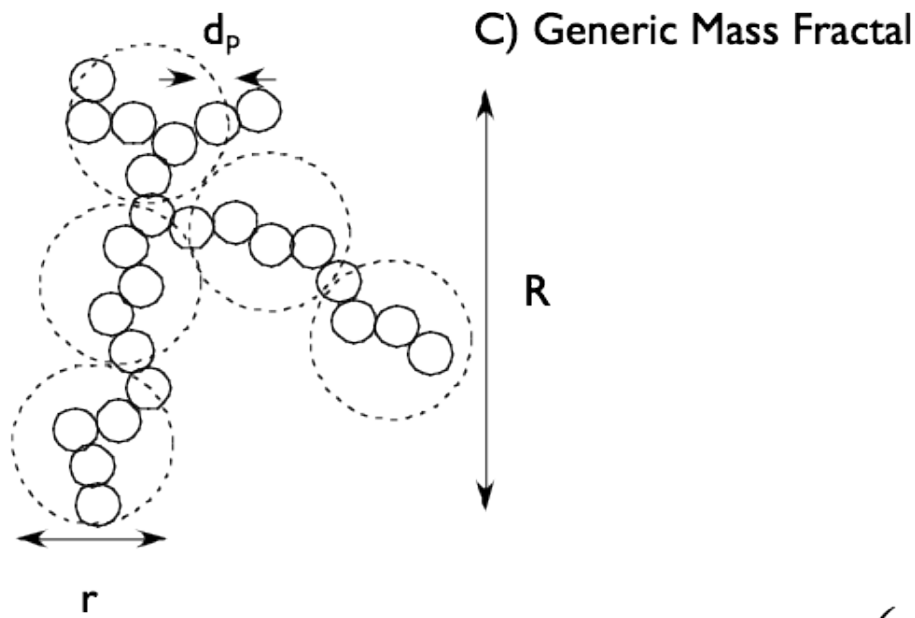

$$I(1/r) \sim N(r)n(r)^2 \qquad N(r) \sim \left(R/r\right)^{d_f} \qquad n(r) \sim \left(r/d_p\right)^{d_f}$$

$$I(1/r) \sim \left(R/d_p\right)^{d_f} r^{d_f} \Rightarrow \left(R/d_p\right)^{d_f} q^{-d_f} = Nq^{-d_f}$$

First and Second Premise of Scattering Incorporated in the Unified Function

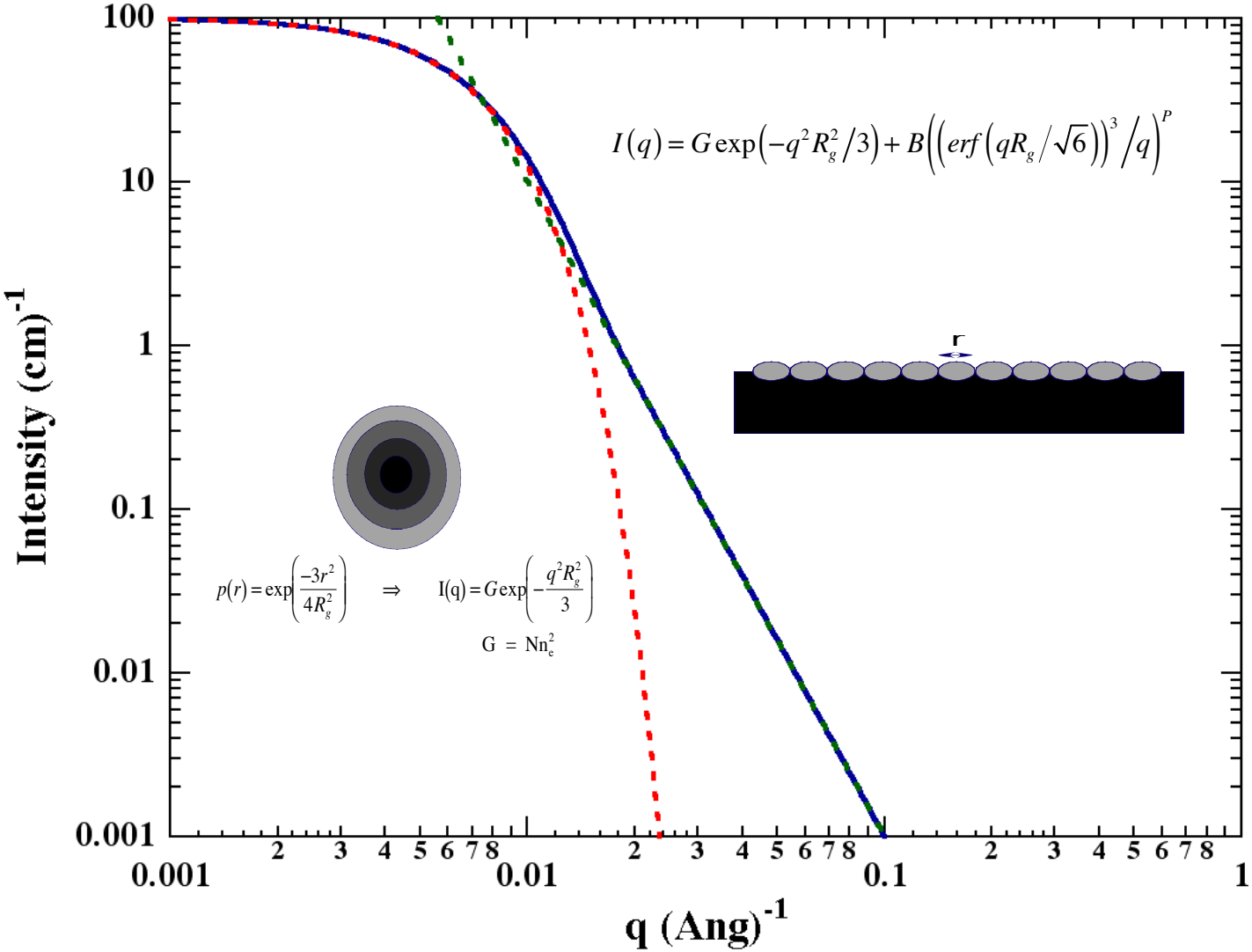

Approximations Leading to a Unified Exponential/Power-Law Approach to Small-Angle Scattering, Beaucage, G, *J. Appl. Cryst.* **29** 7171-728 (1995)

General Laws for Scattering

Unified Function

$$I(q) = G\exp(-q^2R_g^2/3) + B\{[\mathrm{erf}\,(qR_g/6^{1/2})]^3/q\}^P$$

One Structural Level

$$\begin{aligned} I(q) \simeq\ & G\exp(-q^2R_g^2/3) \\ & + B\exp(-q^2R_{\mathrm{sub}}^2/3)\{[\mathrm{erf}\,(qR_g/6^{1/2})]^3/q\}^P \\ & + G_s\exp(-q^2R_s^2/3) + B_s\{[\mathrm{erf}\,(qR_g/6^{1/2})]^3/q\}^{P_s} \end{aligned}$$

Two Structural Levels

$$\begin{aligned} I(q) \simeq \sum_{i=1}^{n}\Big(& G_i\exp(-q^2R_{g_i}^2/3) + B_i\exp(-q^2R_{g_{(i+1)}}^2/3) \\ & \times\{[\mathrm{erf}\,(qkR_{g_i}/6^{1/2})]^3/q\}^{P_i}\Big). \end{aligned}$$

"n" Structural Levels

Beaucage G *J. Appl. Cryst.* **28** 717-728 (1995).

General Laws for Scattering

Unified Function

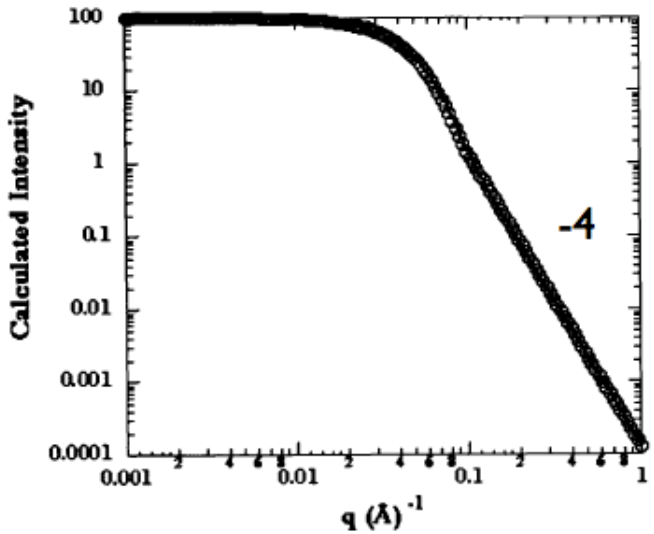

Fig. 11. Calculated scattering (○) from polydisperse spheres with Porod surfaces (power law −4). The solid line follows equation (24) with $R_g = 39.495$ Å as calculated and $P = 4$, $G = 100$ cm^{-1} (fixed in the sphere calculation) and $B = 0.000\,127\,52$ from Porod's law.

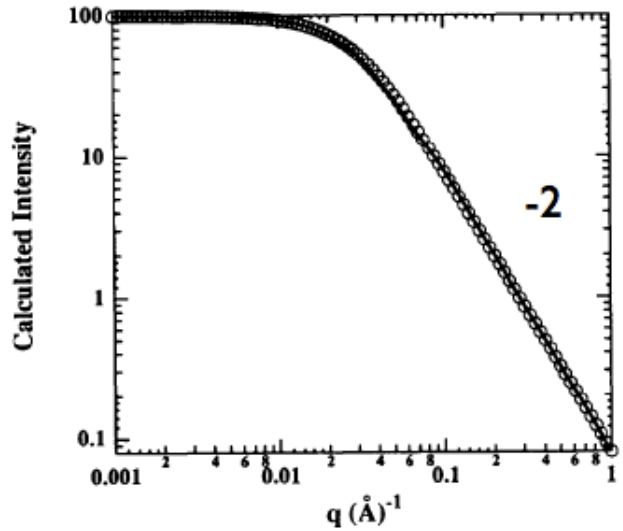

Fig. 10. Log–log plot of Debye equation (○) and equation (24) (solid line). For the Debye equation, $R_g = 50$ Å and $A = 100$ cm^{-1}. For the unified equation, (24), all parameters are fixed. $R_g = 50$ Å, $G = 100$ cm^{-1}, $P = 2$ (the Debye equation represents a mass fractal with $d_f = 2$) and $B = 0.08 = 2G/R_g^2$ from equation (30).

Beaucage G *J. Appl. Cryst.* **28** 717-728 (1995).

General Laws for Scattering

Unified Function

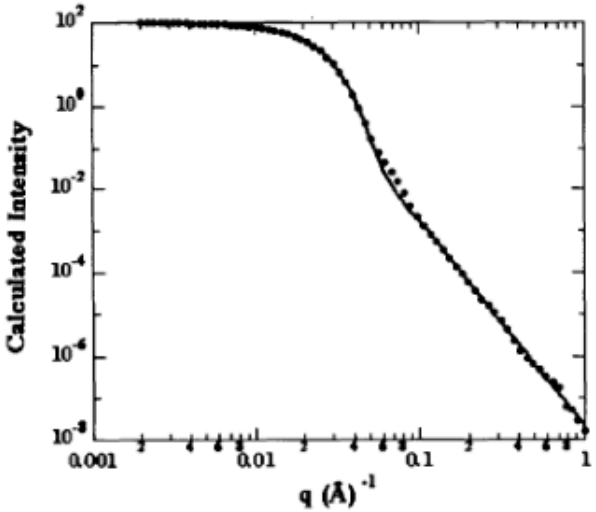

Fig. 12. Calculated scattering curve for an ellipsoid of revolution with a spherical shell of lower electron density, 0.36 of core, with major : minor axis ratio of 4 : 1 and minor axis of $R = 50$ Å and 60 Å for the core and shell, respectively. Equation (24) is calculated using $R_g = 87.9$, $G = 100$ cm^{-1}, $P = 4.91$ and $B = 1.99 \times 10^{-8}$. The mismatch at $q = 0.07$ Å^{-1} is due to a residual Fourier peak that has not been averaged out and that would normally not appear in experimental data for a diffuse interface.

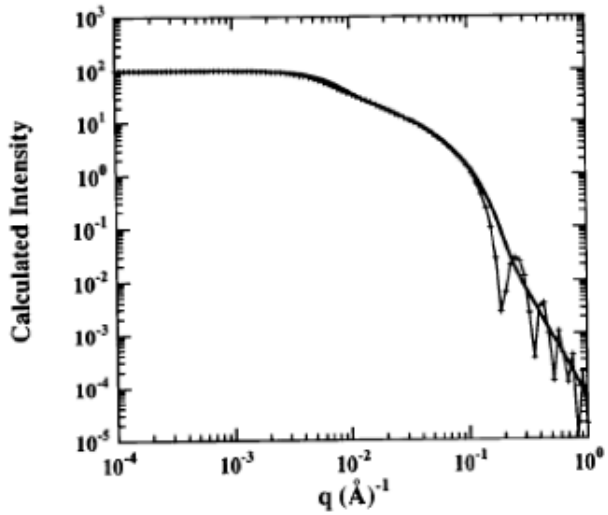

Fig. 13. Calculated scattering curve [Guinier & Fournet, 1955, p. 19, equation (33)] from randomly oriented rods of diameter 40 Å and length 800 Å (+). $I(0)$ is fixed at 100. The calculated scattering curve using equation (28) is shown by the bold line, and $G = 100$, $R_g = 231.4$ Å, $P = 1$, $B = 0.393$, $R_{sub} = R_s = 17.3$ Å, $G_s = 0.111$, $B_s = 6.25 \times 10^{-5}$ and $P_s = 4$ as discussed in the text. High-q oscillations in the + curve are due to poor averaging in the calculation.

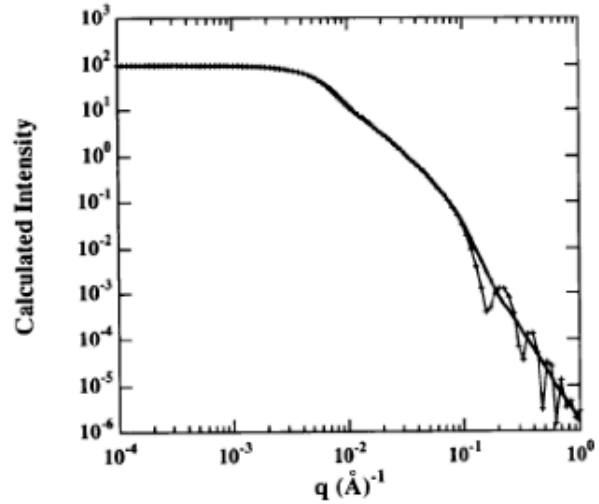

Fig. 14. Calculated scattering curve [Guinier & Fournet, 1955, p. 19, equation (33)] from randomly oriented disc-like lamellae of thickness 40 Å and diameter 800 Å (+). $I(0)$ is fixed at 100. The calculated scattering curve using equation (28) is shown by the bold line, and $G = 100$, $R_g = 283.1$ Å, $P = 2$, $B = 1.25 \times 10^{-3}$, $R_{sub} = R_s = 20$ Å, $G_s = 2.78 \times 10^{-4}$, $B_s = 1.56 \times 10^{-6}$ and $P_s = 4$ as discussed in the text. High-q oscillations in the + curve are due to poor averaging in the calculation.

Beaucage G *J. Appl. Cryst.* **28** 717-728 (1995).

General Laws for Scattering

Unified Function

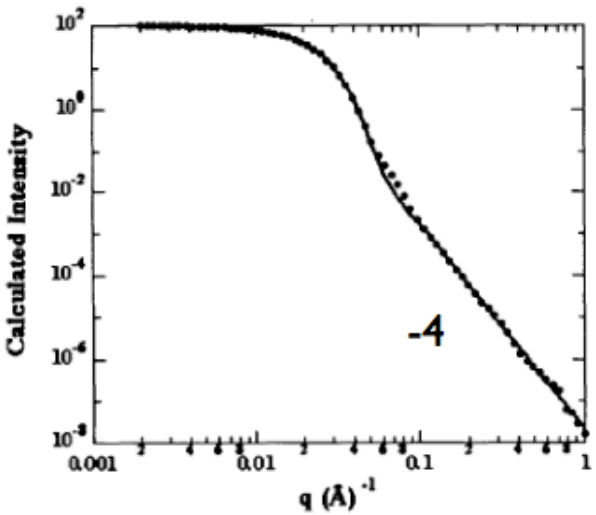

Fig. 12. Calculated scattering curve for an ellipsoid of revolution with a spherical shell of lower electron density, 0.36 of core, with major : minor axis ratio of 4 : 1 and minor axis of $R = 50$ Å and 60 Å for the core and shell, respectively. Equation (24) is calculated using $R_g = 87.9$, $G = 100$ cm^{-1}, $P = 4.91$ and $B = 1.99 \times 10^{-8}$. The mismatch at $q = 0.07$ Å^{-1} is due to a residual Fourier peak that has not been averaged out and that would normally not appear in experimental data for a diffuse interface.

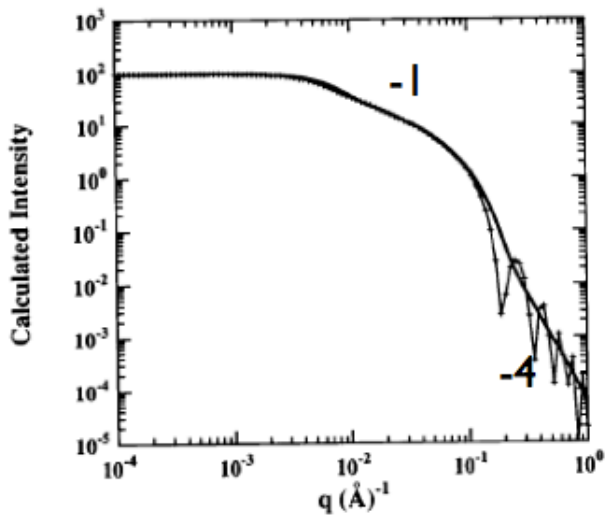

Fig. 13. Calculated scattering curve [Guinier & Fournet, 1955, p. 19, equation (33)] from randomly oriented rods of diameter 40 Å and length 800 Å (+). $I(0)$ is fixed at 100. The calculated scattering curve using equation (28) is shown by the bold line, and $G = 100$, $R_g = 231.4$ Å, $P = 1$, $B = 0.393$, $R_{sub} = R_s = 17.3$ Å, $G_s = 0.111$, $B_s = 6.25 \times 10^{-5}$ and $P_s = 4$ as discussed in the text. High-q oscillations in the + curve are due to poor averaging in the calculation.

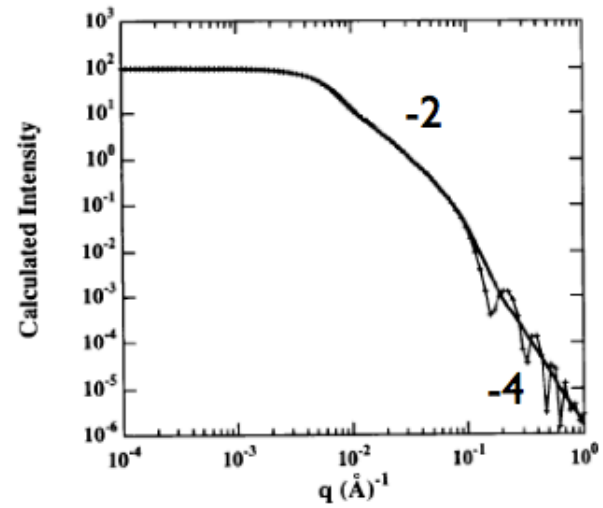

Fig. 14. Calculated scattering curve [Guinier & Fournet, 1955, p. 19, equation (33)] from randomly oriented disc-like lamellae of thickness 40 Å and diameter 800 Å (+). $I(0)$ is fixed at 100. The calculated scattering curve using equation (28) is shown by the bold line, and $G = 100$, $R_g = 283.1$ Å, $P = 2$, $B = 1.25 \times 10^{-3}$, $R_{sub} = R_s = 20$ Å, $G_s = 2.78 \times 10^{-4}$, $B_s = 1.56 \times 10^{-6}$ and $P_s = 4$ as discussed in the text. High-q oscillations in the + curve are due to poor averaging in the calculation.

Beaucage G *J. Appl. Cryst.* **28** 717-728 (1995).

Construction of
A Scattering Curve

Complex Scattering Pattern (Unified Calculation)

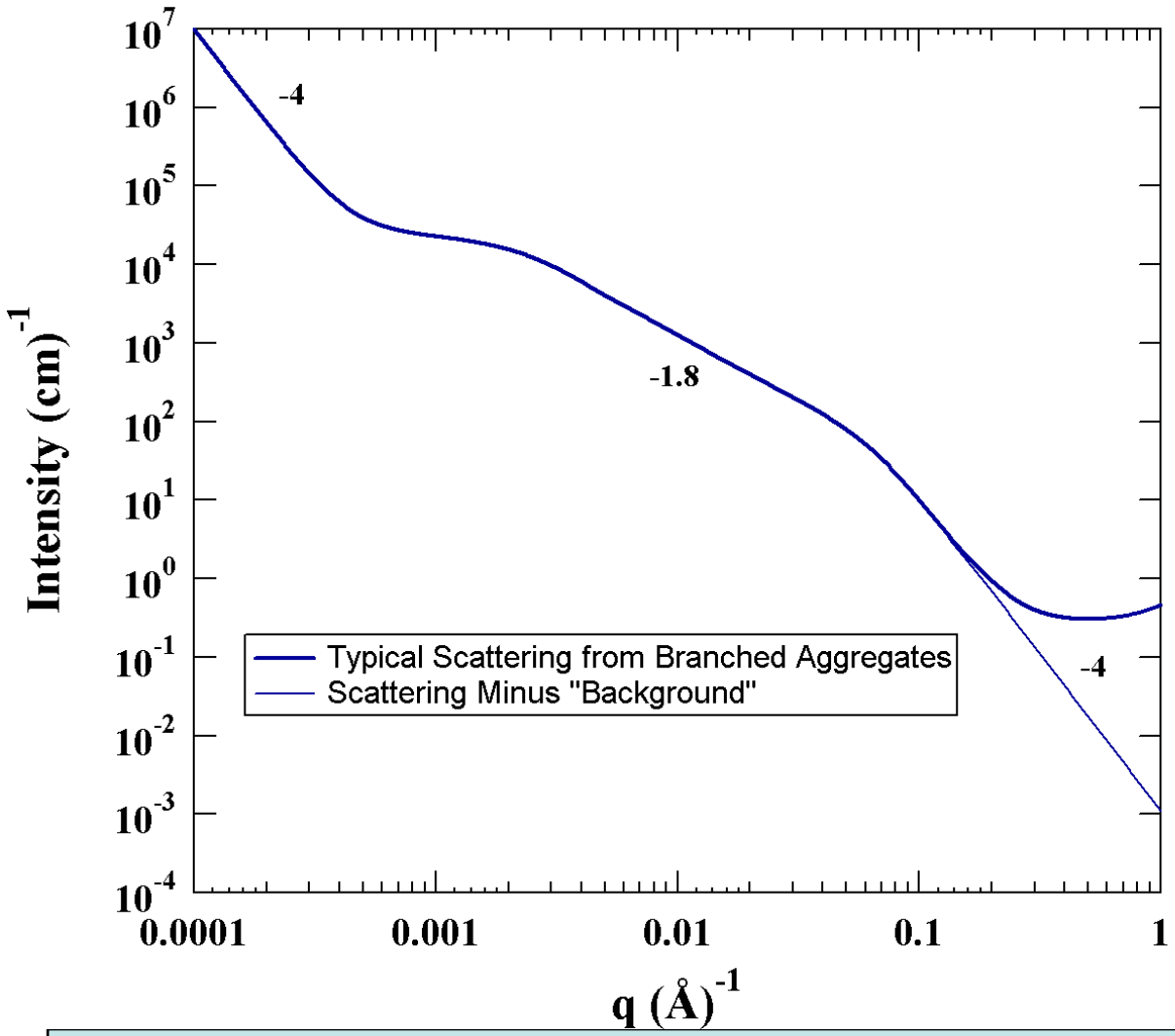

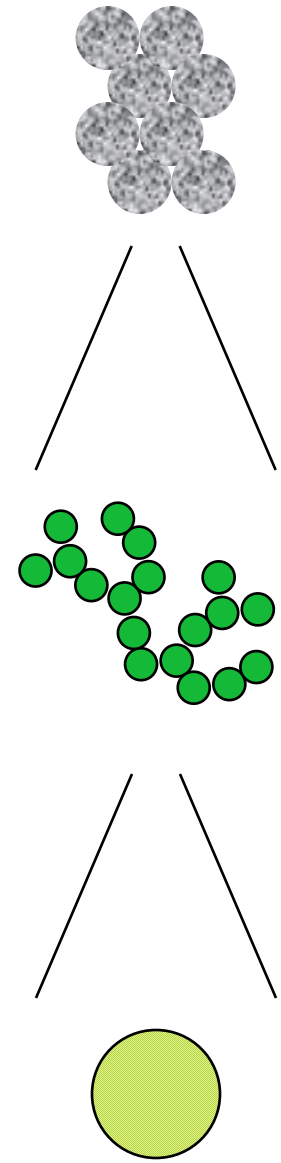

$$q = \frac{2\pi}{d} \qquad I(q) = N(d)n_e^2(d)$$

N = Number Density at Size "d"

n_e = Number of Electrons in "d" Particles

Guinier's Law

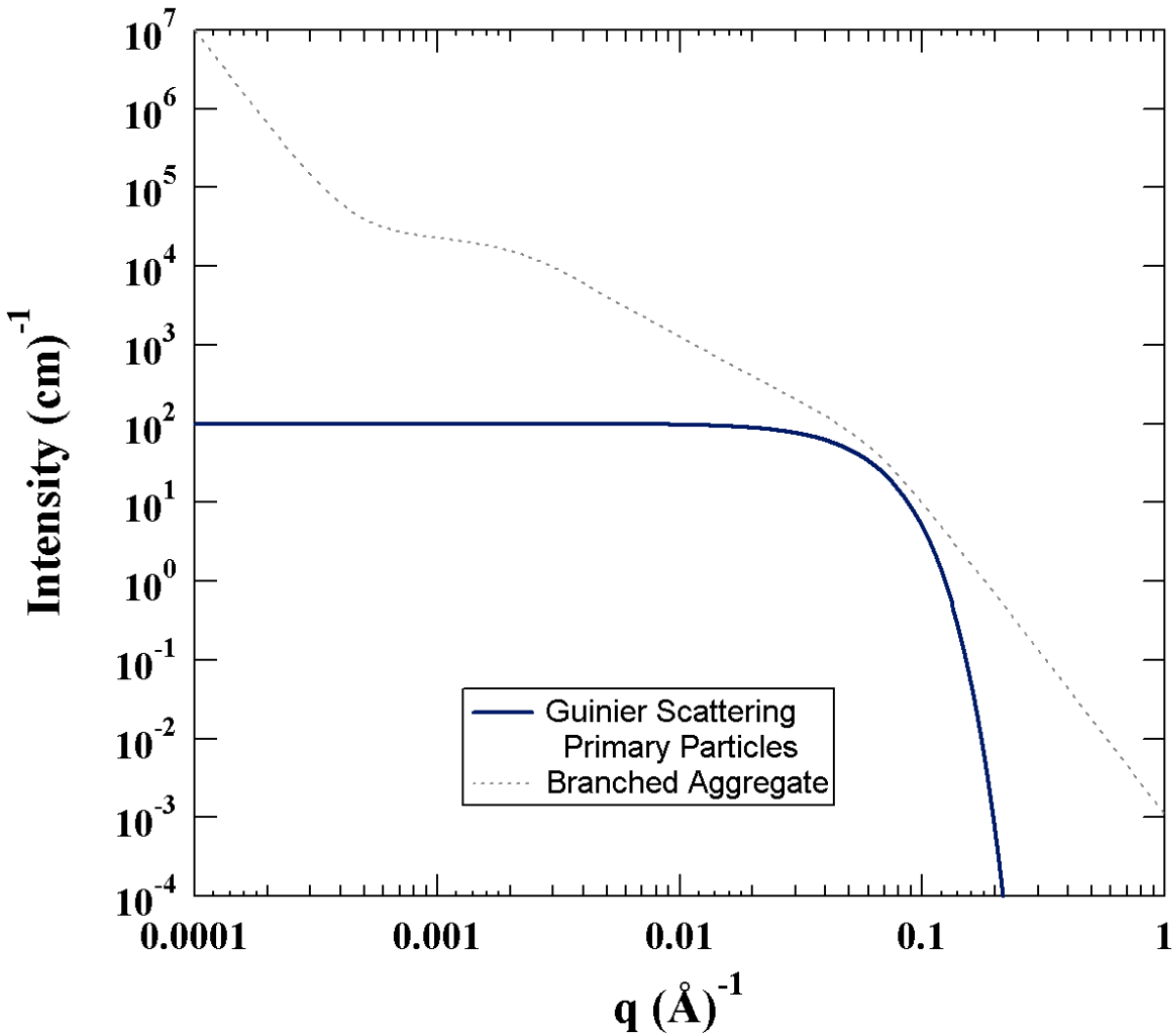

Particle with No Interface

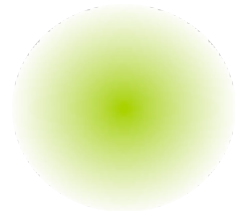

$$I(q) = N(d) n_e^2(d)$$

$$I(q) = G_1 \exp\left(\frac{-q^2 \langle R_{g,1}^2 \rangle}{3} \right)$$

$$G = N \rho_e^2 \langle V^2 \rangle \sim \langle \mathrm{R}^6 \rangle$$

$$\langle R_g^2 \rangle \sim \frac{\langle \mathrm{R}^8 \rangle}{\langle \mathrm{R}^6 \rangle}$$

Guinier and Porod Scattering

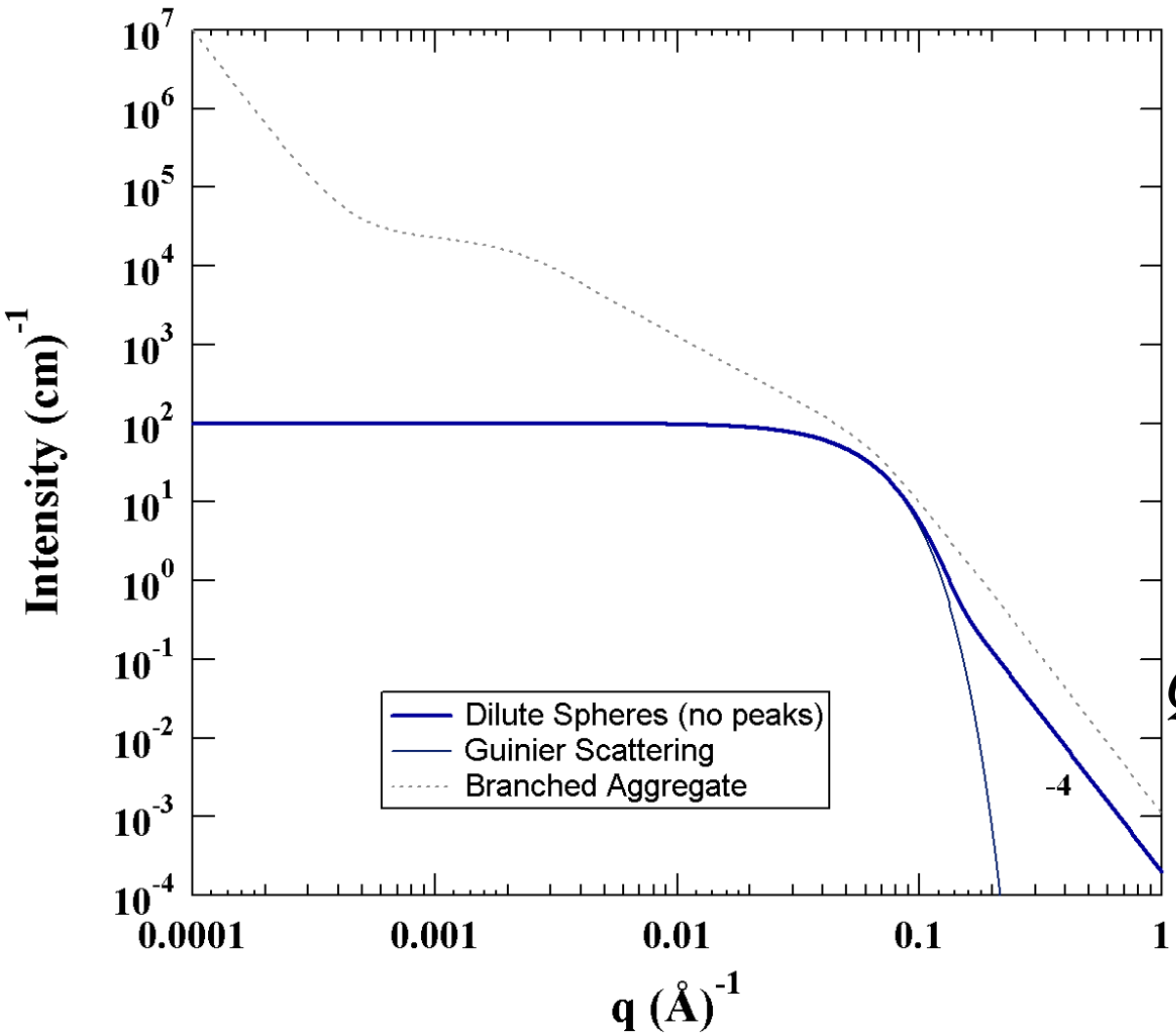

Spherical Particle
With Interface (Porod)

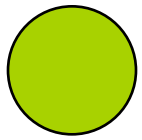

$$I(q) = B_P q^{-4}$$

$$B_P = 2\pi N \rho_e^2 \langle S \rangle$$

$$\langle S \rangle \sim \langle R^2 \rangle$$

$$Q = \int q^2 I(q) dq = N \rho_e^2 \langle R^3 \rangle$$

$$d_p = \frac{Q}{2\pi B_P} = \frac{\langle R^3 \rangle}{\langle R^2 \rangle}$$

Structure of Flame Made Silica Nanoparticles
By Ultra-Small-Angle X-ray Scattering
Kammler/Beaucage Langmuir 2004 20 1915-1921

Polydispersity Index, PDI

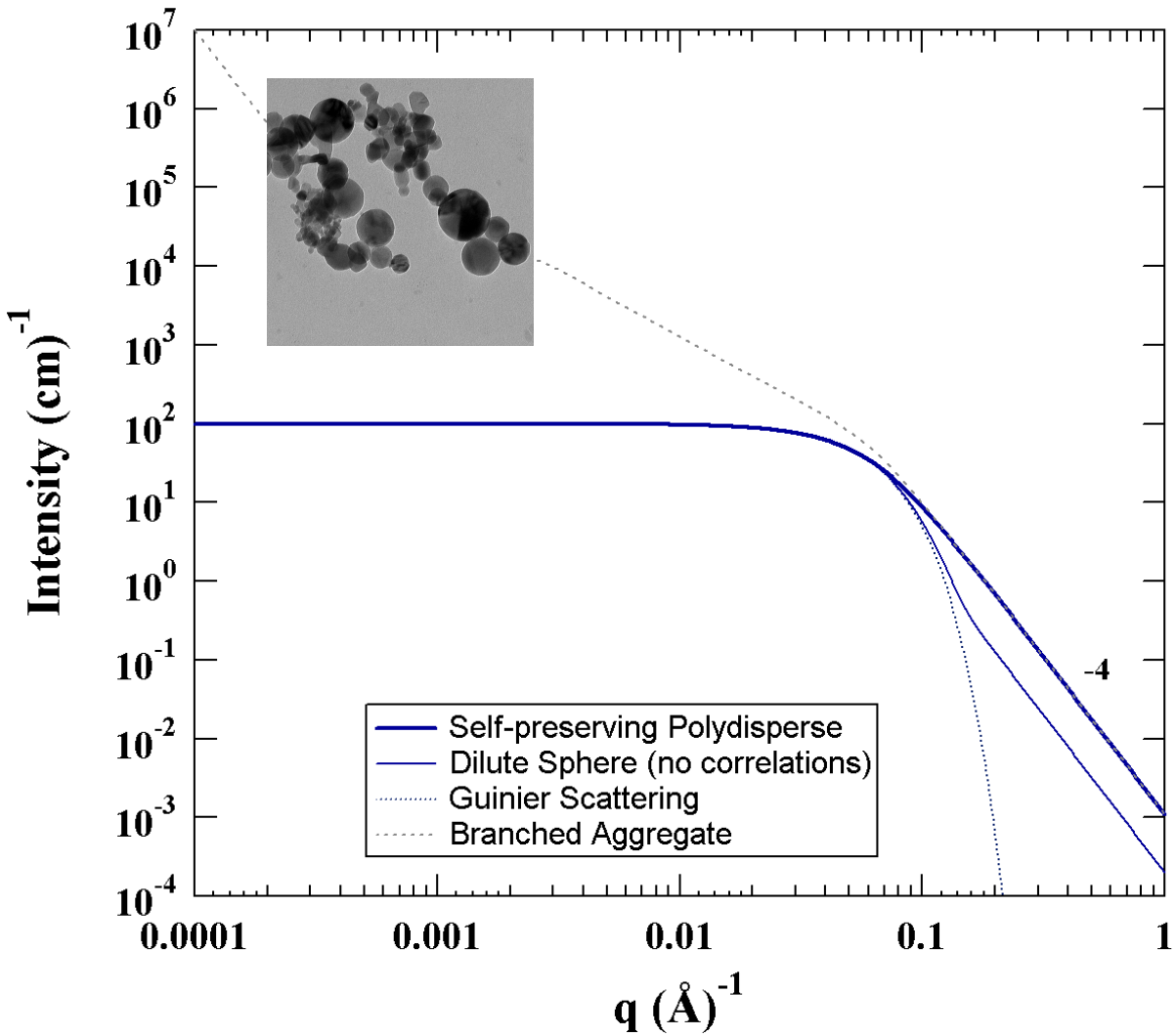

Particle size distributions from small-angle scattering using global scattering functions, Beaucage, Kammler, Pratsinis J. Appl. Cryst. 37 523-535 (2004).

Polydisperse Particles

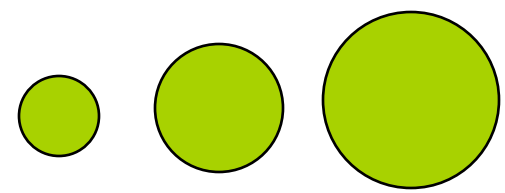

$$PDI = \frac{B_P R_g^4}{1.62G}$$

$$\sigma = \ln(\sigma_g) = \left[\frac{\ln(PDI)}{12}\right]^{1/2}$$

$$m = \left[\frac{5R_g^2}{3e^{14\sigma^2}}\right]^{1/2}$$

Linear Aggregates

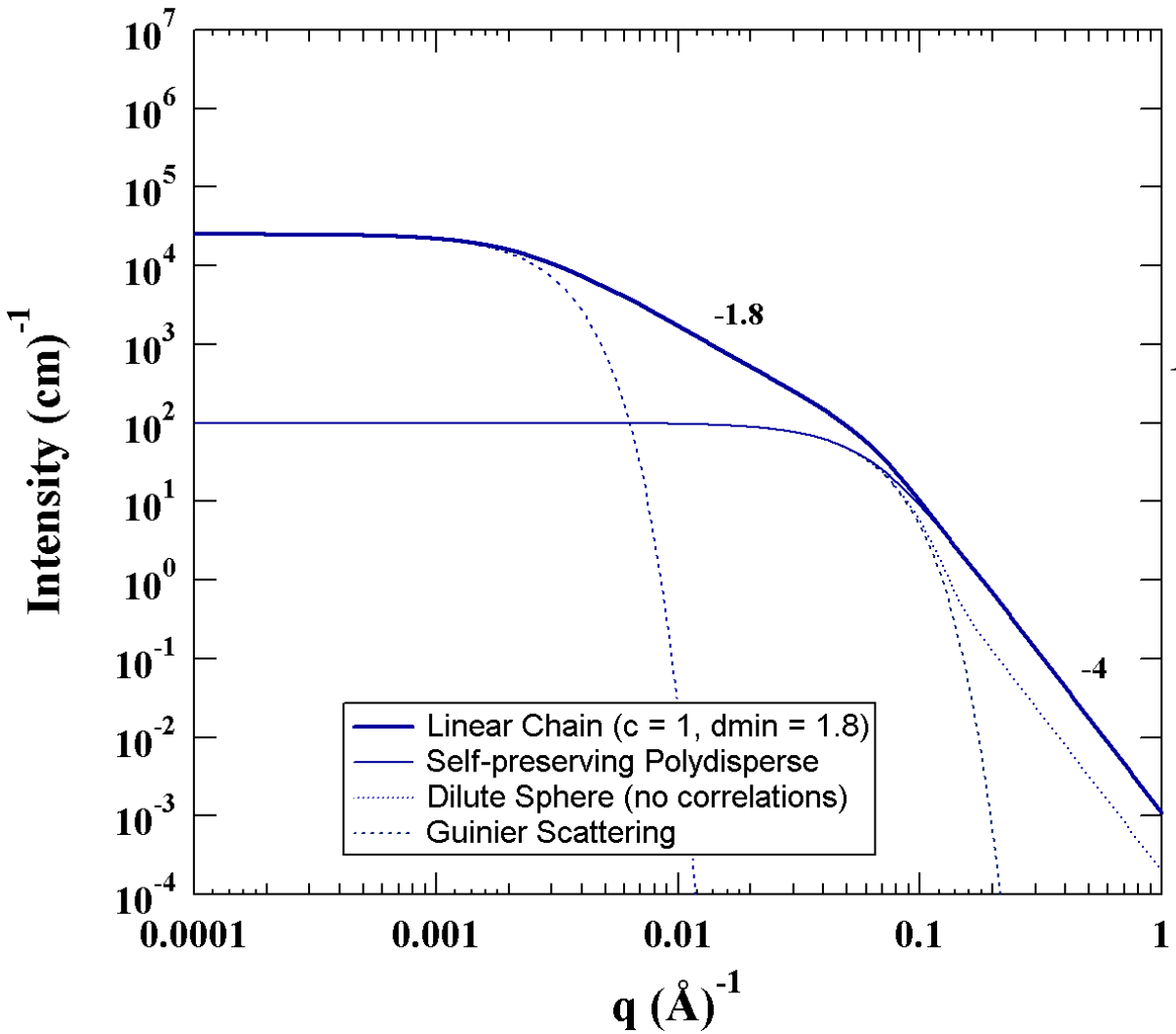

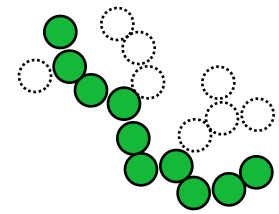

$$I(q) = G_2 \exp\left(\frac{-q^2 \left\langle R_{g,2}^2 \right\rangle}{3}\right)$$

$$z = \frac{G_2}{G_1} = \left(\frac{R_2}{R_1}\right)^{d_f}$$

$$I(q) = B_f q^{-d_f}$$

$$B_f = \frac{G_2 d_f}{R_{g,2}^{d_f}} \Gamma\left(d_f/2\right)$$

Beaucage G, Small-angle Scattering from Polymeric Mass Fractals of Arbitrary Mass-Fractal Dimension, J. Appl. Cryst. 29 134-146 (1996).

Branched Aggregates

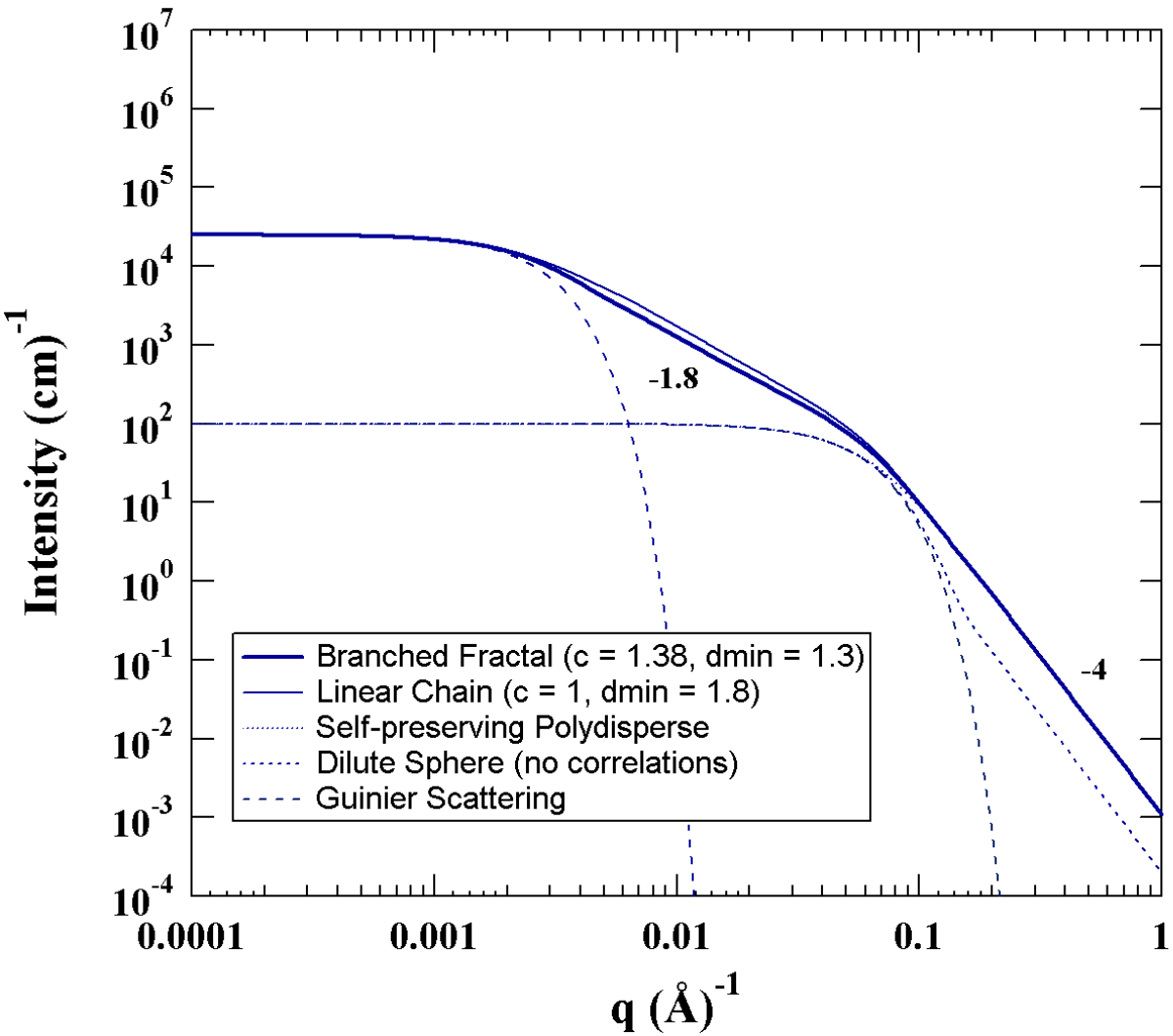

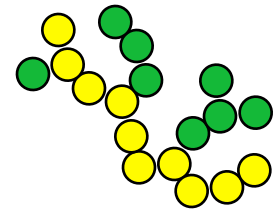

$$p = \left(\frac{R_2}{R_1}\right)^{d_{\min}} = z^{1/c}$$

$$c = \frac{d_f}{d_{\min}}$$

$$\phi_{Br} = 1 - \left(\frac{R_2}{R_1}\right)^{d_{\min} - d_f}$$

$$B_f = \frac{G_2 d_{\min}}{R_{g,2}^{d_f}} \Gamma\left(d_f/2\right)$$

Beaucage G, Determination of branch fraction and minimum dimension of fractal aggregates Phys. Rev. E 70 031401 (2004).

Large Scale (low-q) Agglomerates

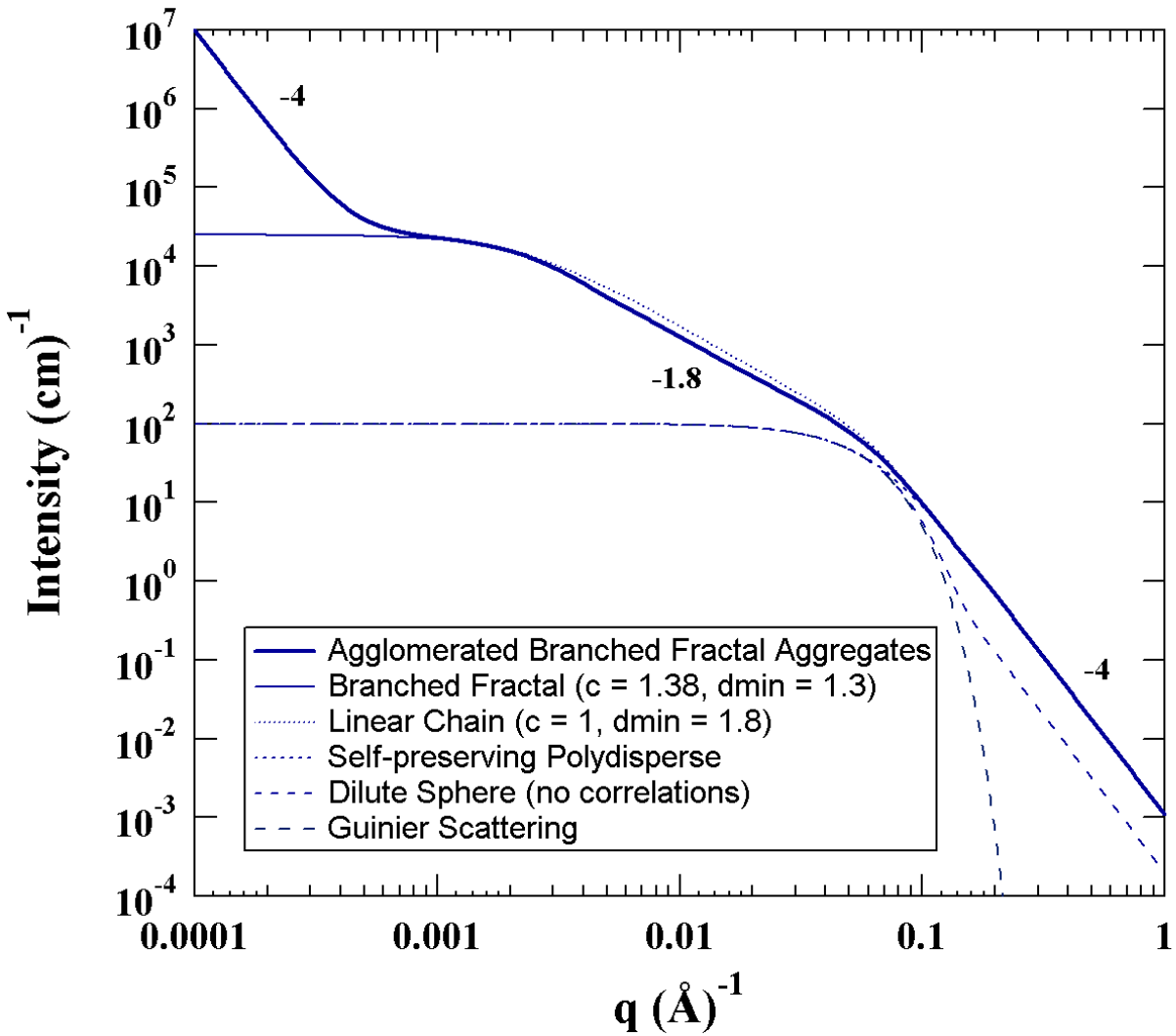

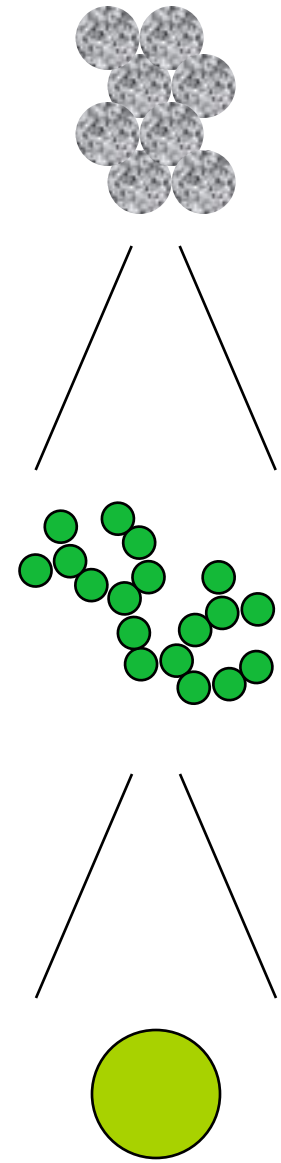

$$I(q) = B_P q^{-4}$$

Small-scale Crystallographic Structure

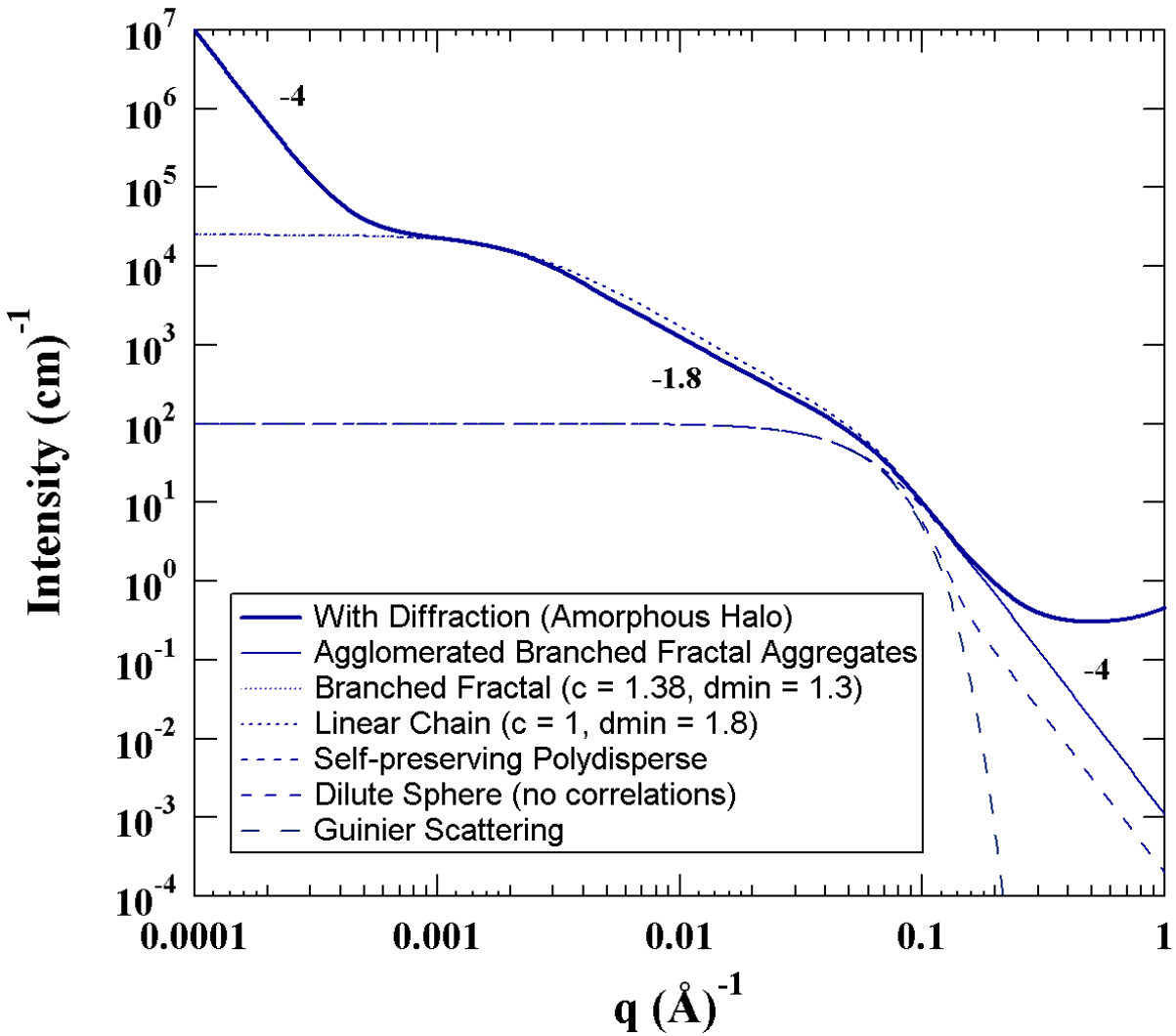

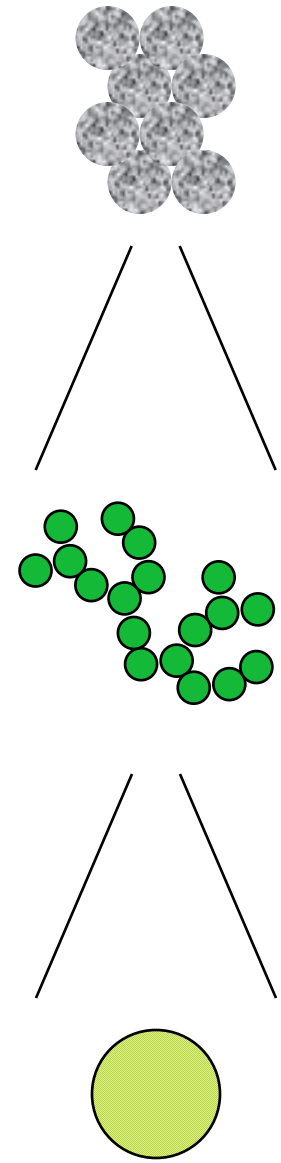

Branched Aggregates

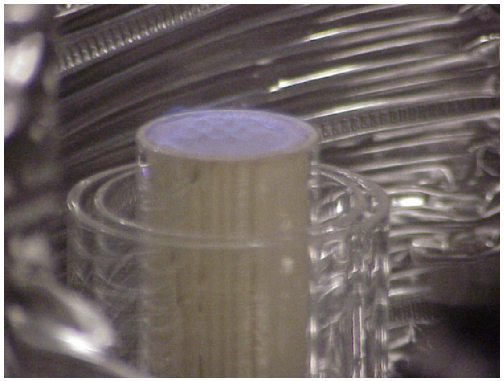

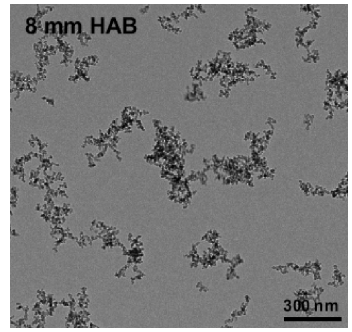

APS UNICAT
Silica Premixed Flames
J. Appl. Phys 97 054309
Feb 2005

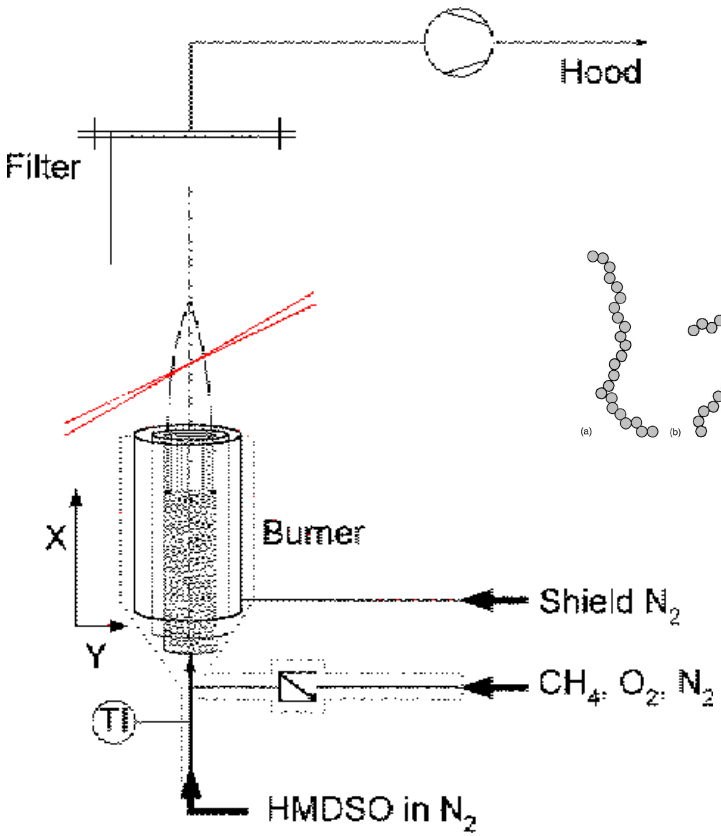

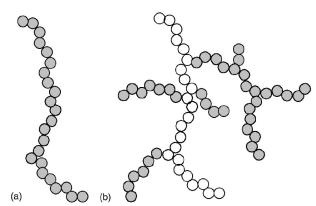

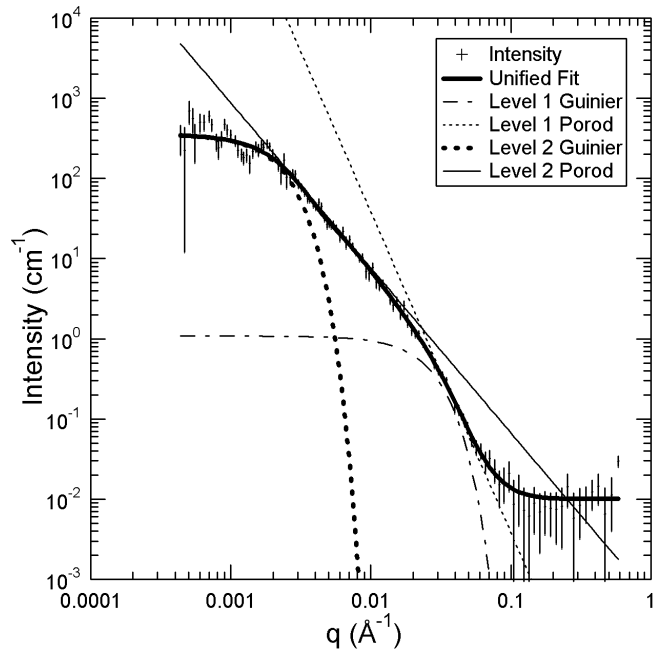

5mm LAT 16mm HAB
Typical Branched Aggregate
$d_p = 5.7$ nm
$z = 350$
$c = 1.5$, $d_{min} = 1.4$, $d_f = 2.1$
$\phi_{br} = 0.8$

Beaucage G, *Determination of branch fraction and minimum dimension of fractal aggregates* Phys. Rev. E 70 031401 (2004).

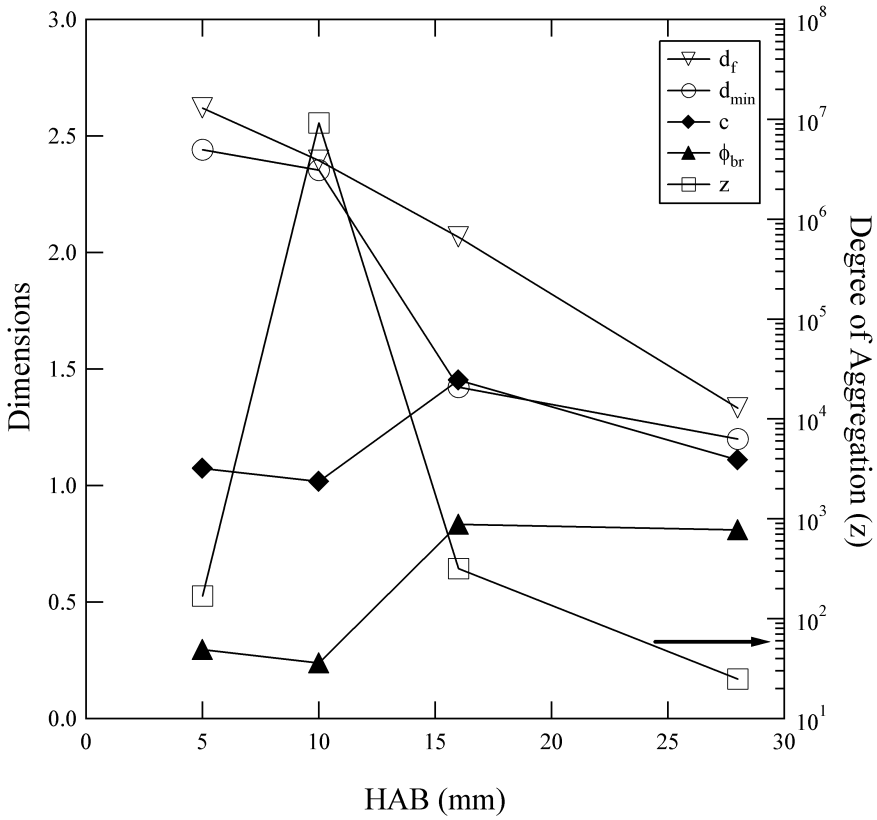

5 mm LAT

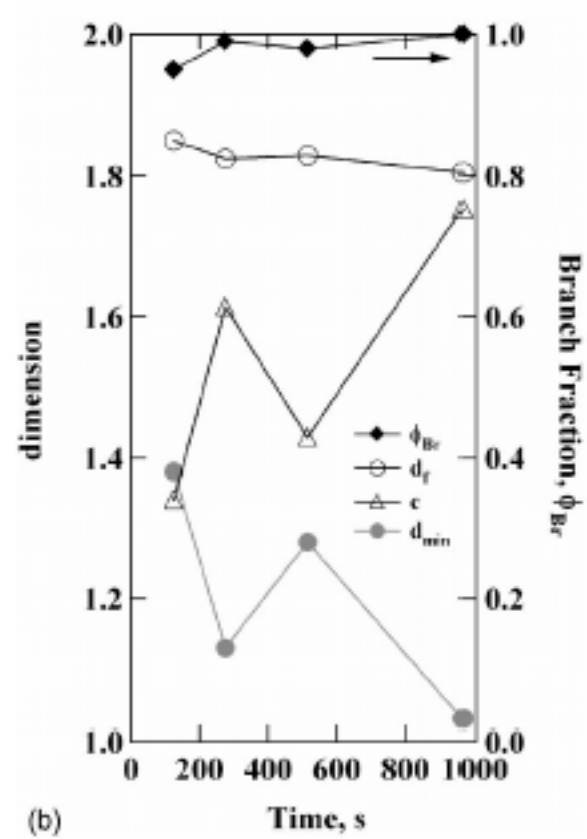

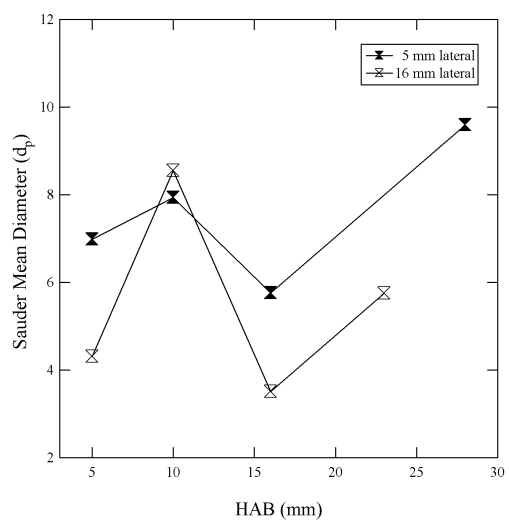

-Behavior is Similar to Simulation
d_f drops due to branching

-Aggregate Collapse

-Entrainment High in the Flame

Particle Size, d_p

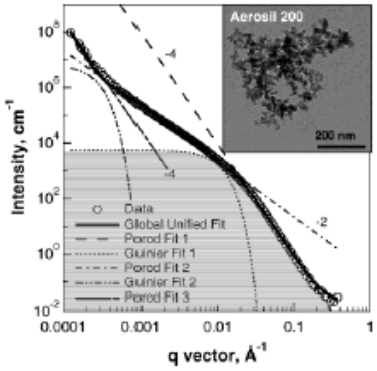

Figure 1. An USAXS pattern of agglomerated fumed silica (Aerosil 200, Degussa AG). The scattering data (circles) are well described by the global unified fit equation (solid line). Furthermore, three Porod regimes (dashed line, dashed–dotted line, and long–short-dashed line) are shown together with the Guinier regimes (dotted line and dashed–double-dotted line). The appearance of the second Porod (weak power-law) regime (0.0005 Å^{-1} < q < 0.01 Å^{-1}) proves that these particles are agglomerated and mass fractal as shown by the TEM insert. The gray shaded area indicates the integral part for determination of d_{VS}.

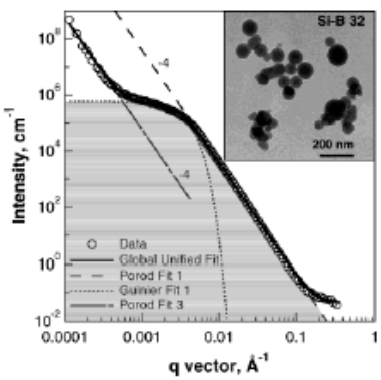

Figure 2. A USAXS plot of a nonagglomerated fumed silica (Si-B 32) made in a 17 g/h sustained premixed flame reactor (ref 18). The scattering data (circles) are well described by the global unified fit equation (solid line). Furthermore, Porod regimes (dashed line and long–short-dashed line) are shown together with the Guinier regime (dotted line). The lack of the Porod (weak power-law) regime at 0.0005 Å^{-1} < q < 0.005 Å^{-1} indicates that the particles are nonagglomerated as shown by the TEM insert. The gray shaded area indicates the integral part for determination of d_{VS}.

Porod's Law

$$\gamma_0(r) = 1 - \frac{S}{4V} r + \ldots$$

$$I(q) = \frac{2\pi\rho^2 S}{q^4}$$

$$d_p = V/S = \langle R^3 \rangle / \langle R^2 \rangle$$

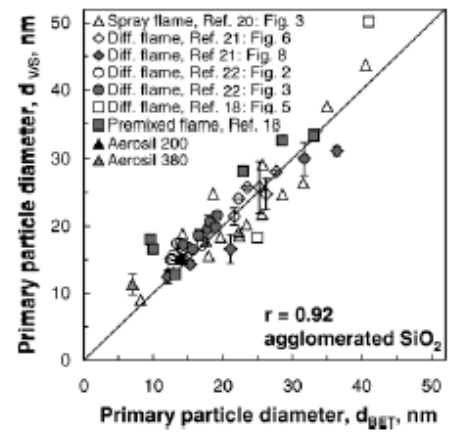

Figure 3. Comparison of d_{VS} and d_{BET} for agglomerated silica powders made in our vapor- or liquid-fed flame aerosol reactors (refs 18 and 20–22) and those of commercially available powders (Aerosil 200 and Aerosil 380, Degussa AG).

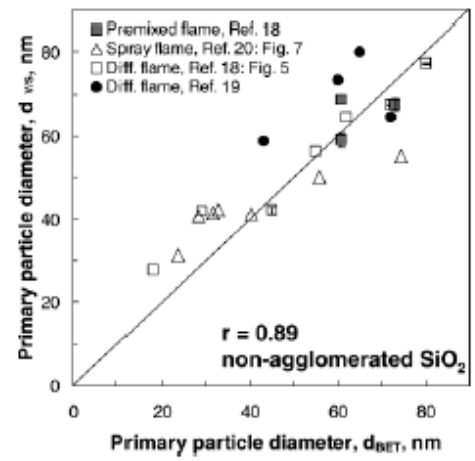

Figure 4. Comparison of d_{VS} and d_{BET} for various nonagglomerated silica powders made in our vapor-fed (refs 18 and 19) and liquid-fed (ref 20) flame aerosol reactors.

Structure of flame made silica nanoparticles by ultra-snall-angle x-ray scattering. Kammmler HK, Beaucage G, Mueller R, Pratsinis SE *Langmuir* **20** 1915-1921 (2004).

For Particles with Correlations (Concentrated non-fractal)

$$I(q) = I_{dilute}(q)S(q) = I_{dilute}(q)\frac{1}{1+pA(q,\xi)}$$

$$p = packing\ factor,\ \mathrm{A}(\mathrm{q},\xi) = \frac{3(\sin q\xi - q\xi\cos q\xi)}{(q\xi)^3}$$

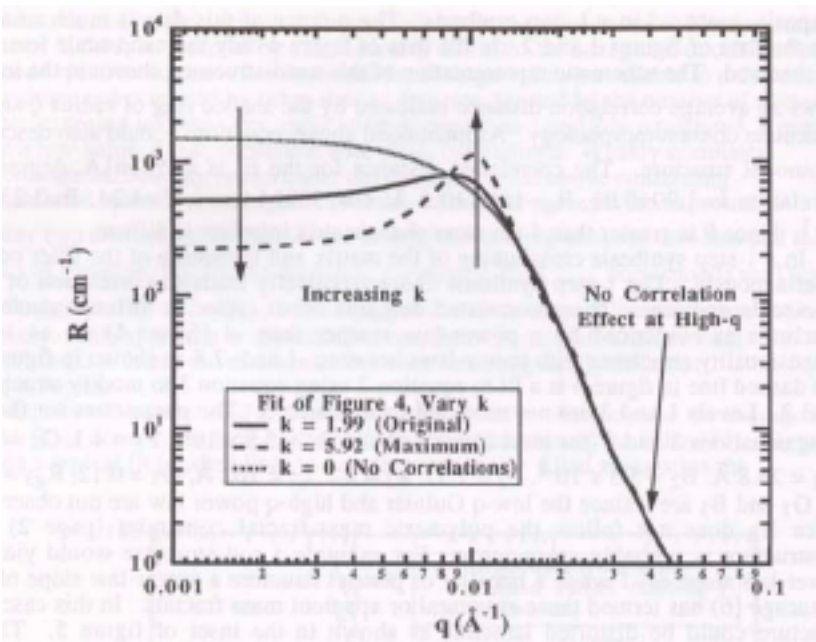

Figure 6. Demonstration of the effect of varying the packing factor "k" on the scattering pattern for the data of figure 4. Packing of the domains does not affect the power-law scaling regime at high-q.

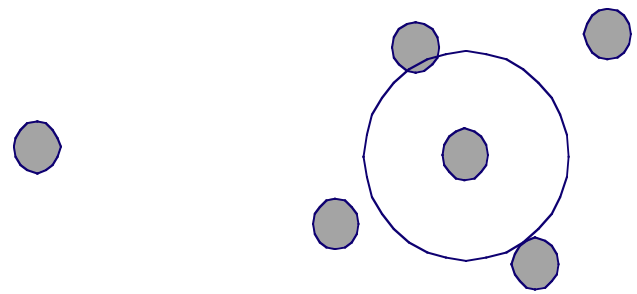

Branching in different systems

- Long Chain and Short Chain

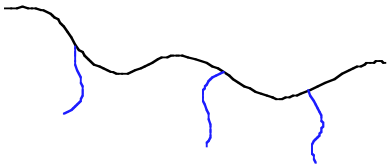

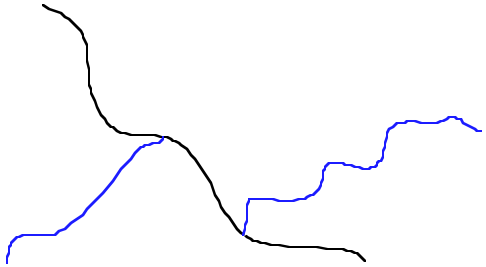

- Model Branched Polymers (Stars, Hyperbranched, Dendrimers)

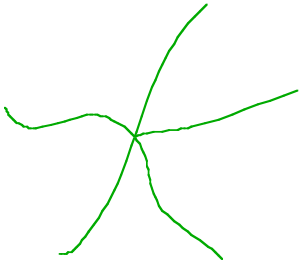

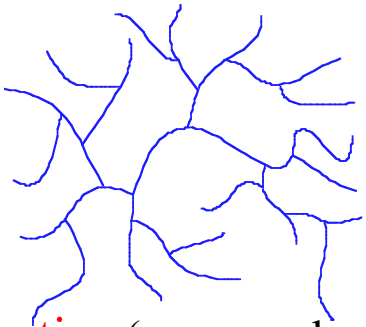

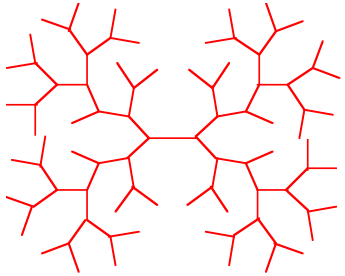

- Branching governed by kinetics (nano-scale aggregates)

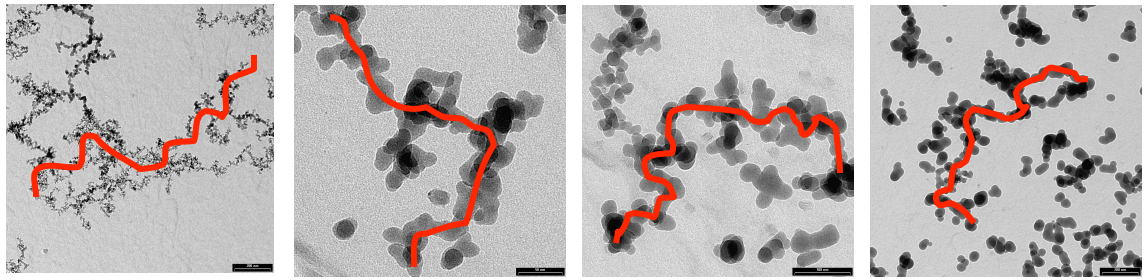

Fractal dimensions (d_f, d_{min}, c) and degree of aggregation (z)

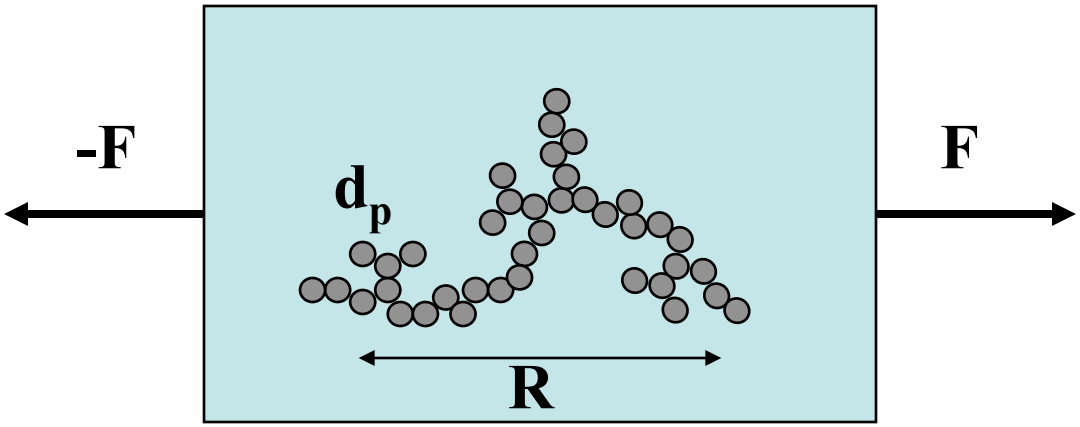

$$z \sim \left(\frac{R}{d_p}\right)^{d_f}$$

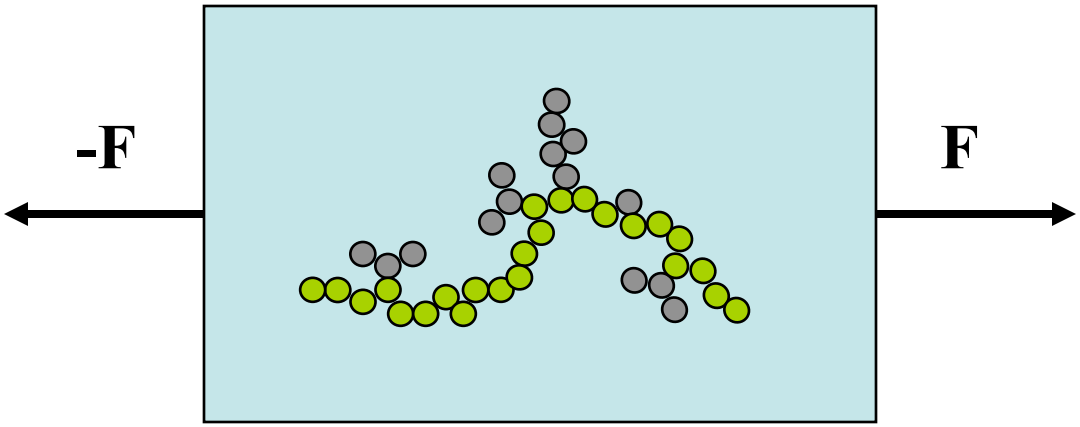

$$p = z_{\min} \sim \left(\frac{R}{d_p}\right)^{d_{\min}}$$

$$z \sim p^c = p^{d_f/d_{\min}}$$

d_{min} should effect perturbations & dynamics, transport electrical conductivity & a variety of important features.

Beaucage G, *Determination of branch fraction and minimum dimension of frac. agg.* Phys. Rev. E **70** 031401 (2004).
Kulkarni, AS, Beaucage G, *Quant. of Branching in Disor. Mats.* J. Polym. Sci. Polym. Phys. **44** 1395-1405 (2006).

Linear/Branched Polyethylene

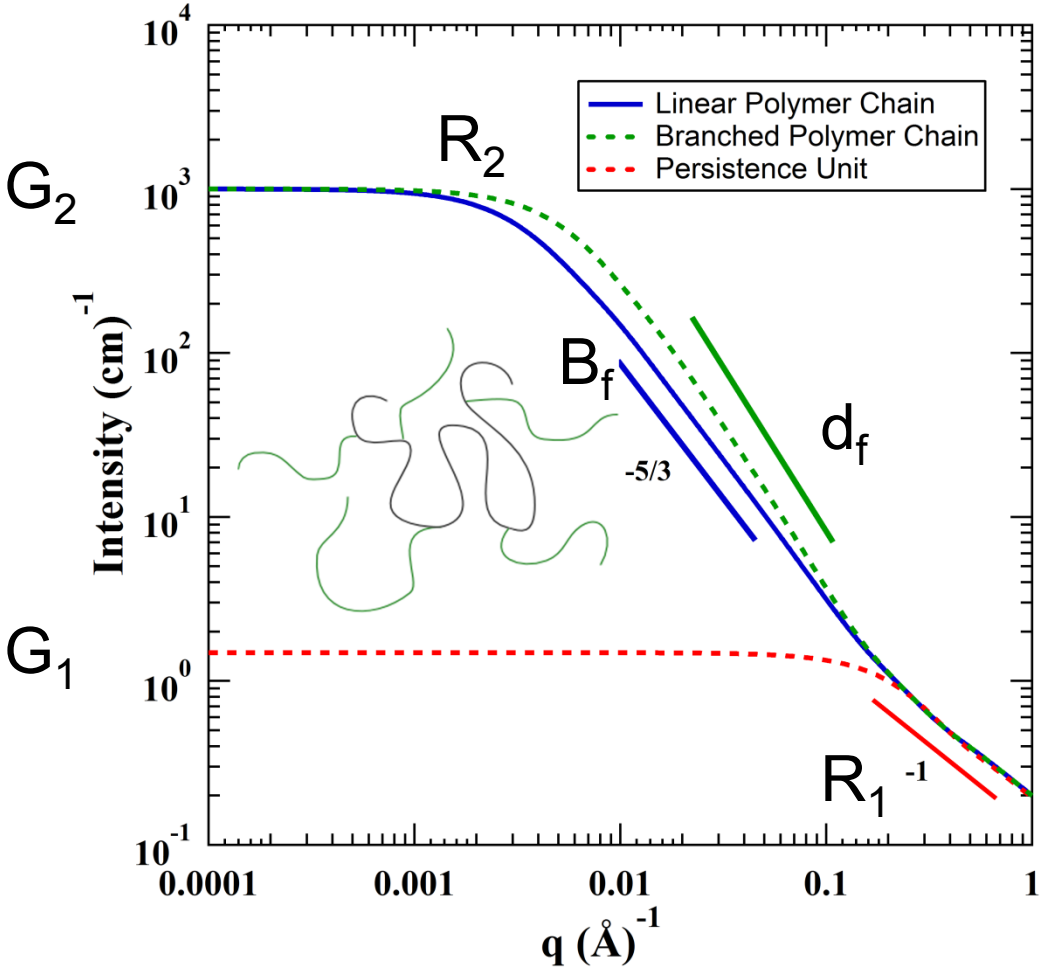

$$d_{\min} = \frac{B_f R_{g,2}^{d_f}}{G_2 \Gamma\left(d_f/2\right)}$$

Beaucage, G., Determination of branch fraction and minimum dimension of mass-fractal aggregates. *Physical Review E* **2004,** *70* (3).

Branching dimensions are obtained by combining local scattering laws

Printed Electronics Solar Cells

Silicon cluster	Extracted Parameters	
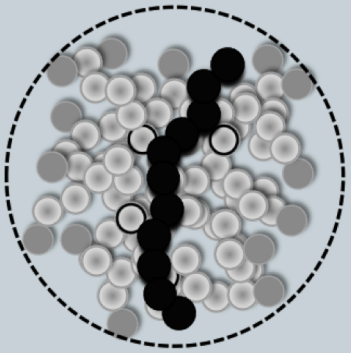	Fractal Dimension	2.64
	Degree of Aggregation	47,600
	Primary Particle Diameter	43 Å
	Aggregate Diameter	368 Å
	Minimum Dimension	1.14
	Connectivity dimension	2.32
	Number of branches	13,200
	Branch fraction	0.998
	Meandering fraction	0.733
	Branches in minimum path	27
	Number per branch	3.6

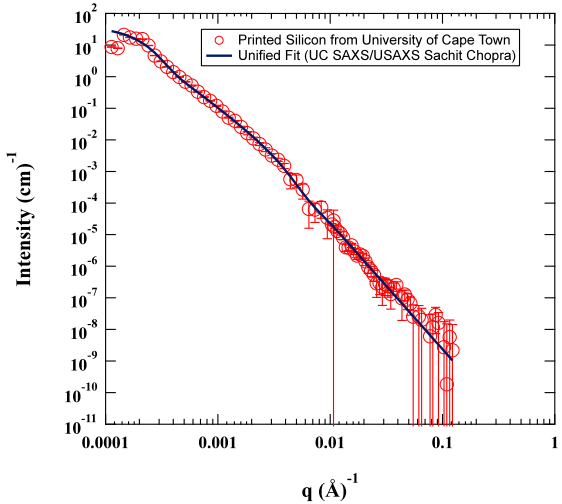

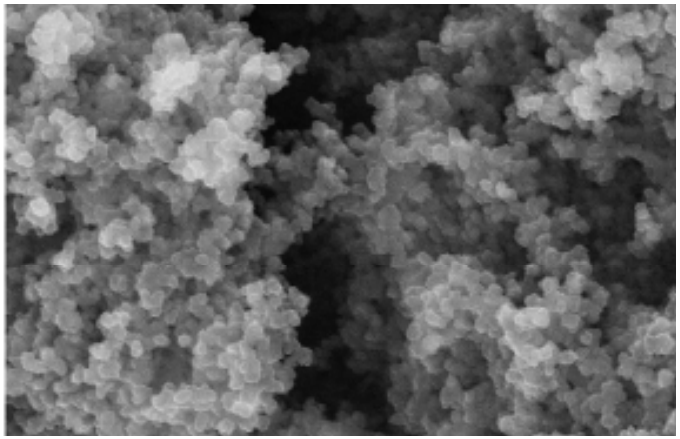

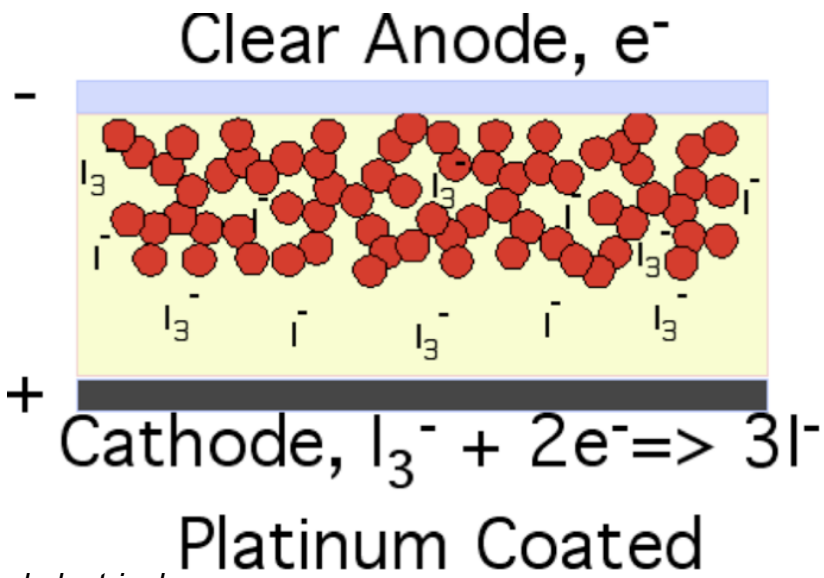

Beaucage G, Jonah E, Britton DA, Härting M, *Aggregate structure and electrical performance of printed silicon layers*, in preparation (2010).

Summary:

1) Experimental Instrumentation
2) Specific Scattering Laws
3) General Scattering Laws
   Guinier's Law
   Porod's Law
   Unified Scattering Function
   Fractals
   Branching
4) Polydispersity
5) Summary

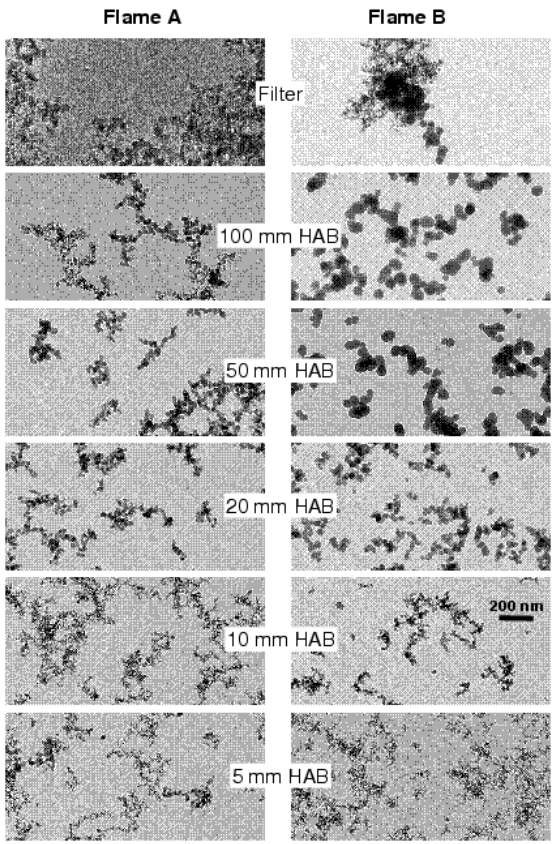

Kammler HK, Beaucage G, Kohls DJ, Agashe N. Ilavsky J
J Appl. Phys. **97**(2005) (Article 054309).

Particle Size Distributions
From SAXS

Particle Size Distribution Curves From SAXS

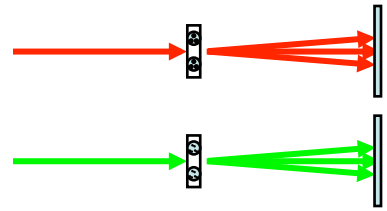

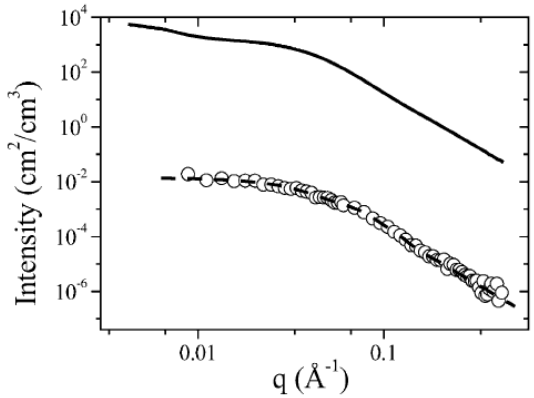

Fig. 7. ASAXS scattering curve measured at 8308 eV on the fresh catalyst (full line). The circles represent the separated scattering curve ($KI(q)$) obtained by subtracting the normalized scattering curves measured at 8308 and 8326 eV. The dashed line represent the best fit to the data using the approach described in the text.

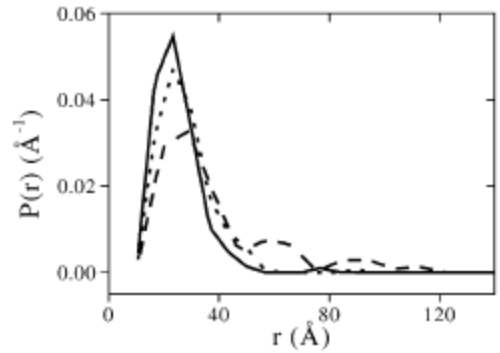

Fig. 8. Normalized nickel number particle size distributions of catalysts sintered at 650 °C obtained by ASAXS as described in the text. The nickel particles are assumed to be spherical with radius r, but otherwise no assumption on the shape of the distribution is made. The full line is the distribution of the fresh catalyst. The short dash (long dash) is the distribution after sintering for 5 h (100 h).

Assumption Method

i) Assume a distribution function.

ii) Assume a scattering function (sphere)

iii) Minimize calculation

$$I(q) = 9G\left[\frac{\sin qR - qR\cos qR}{(qR)^3}\right]^2$$

Particle Size Distribution Curves From SAXS

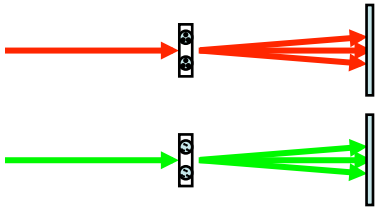

Assumption Method.

- **i) Assume a distribution function.**
- **ii) Assume a scattering function (sphere)**
- **iii) Minimize calculation**

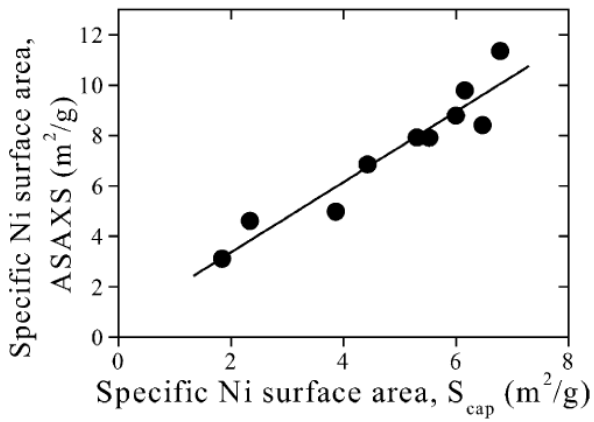

Fig. 11. Comparison of specific nickel surface areas derived from the sulfur chemisorption capacity (S_{cap}) and ASAXS (Tables 3 and 4). The line is the result of a linear regression ($S_{ASAXS} = 1.4(0.2)S_{S_{cap}} + 0.6(0.8)$), where the number in parentheses is the standard deviation of the fit.

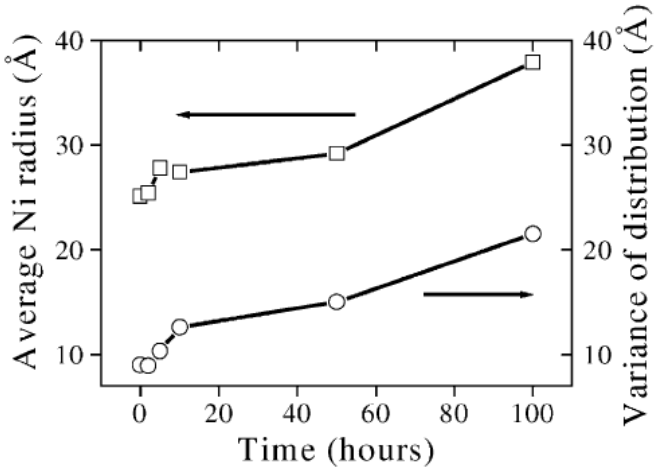

Fig. 10. Average nickel particle radius (squares) and variance (circles) of distribution determined by ASAXS after sintering at 650 °C.

Sintering of Ni/Al$_2$O$_3$ catalysts studied by anomalous small angle x-ray scattering.
Rasmussen RB, Sehested J, Teunissen HT, Molenbroek AM, Clausen BS
***Applied Catalysis A.* 267, 165-173 (2004).**

Not unique &
Based on assumptions
But widely used & easy to understand

Particle Size Distribution Curves From SAXS

$$PDI = \frac{B_P R_g^4}{1.62G}$$

Unified Method

i) Global fit for B_P and G.

ii) Calculate PDI (no assumptions & unique "solution")

iii) Assume log-normal distribution for σ_g and distribution curve (or other models)

iv) Data to unique solution
Solution to distribution

$$\sigma = \ln(\sigma_g) = \left[\frac{\ln(PDI)}{12}\right]^{1/2}$$

$$m = \left[\frac{5R_g^2}{3e^{14\sigma^2}}\right]^{1/2}$$

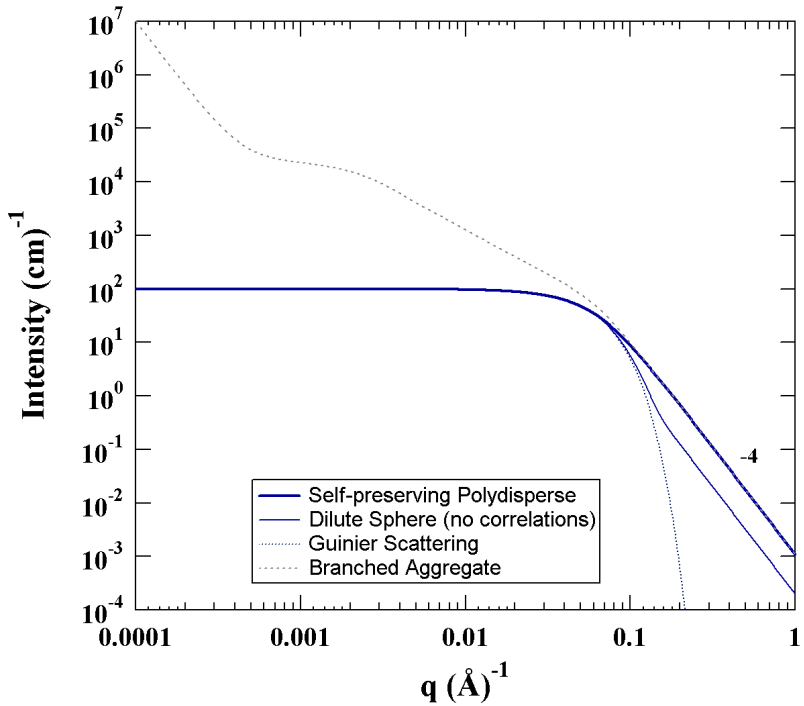

Advantages

- Generic PDI (asymmetry also)
- Global fit (mass fractal etc.)
- Direct link (data => dispersion)
- Use only available terms
- Simple to implement

Particle Size Distribution Curves from SAXS

PDI/Maximum Entropy/TEM Counting

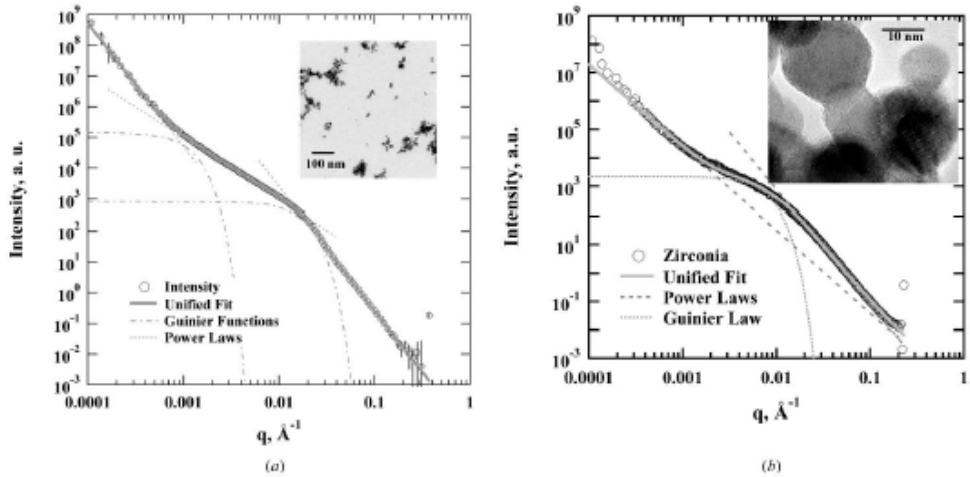

Figure 2
USAXS data from aggregated nanoparticles (circles) showing unified fits (bold grey lines), primary particle Guinier and Porod functions at high q, the intermediate mass fractal scaling regime and the aggregate Guinier regime (dashed lines). (*a*) Fumed titania sample with multi-grain particles and low-q excess scattering due to soft agglomerates. $d_{VIS} = 16.7$ nm (corrected to 18.0 nm), PDI = 3.01 ($\sigma_g = 1.35$), $R_g = 11.2$ nm, $d_f = 1.99$, $z_{\pm 1} = 175$, $z_{R_g} = 226$, $R_{g2} = 171$ nm. From gas adsorption, $d_p = 16.2$ nm. (*b*) Fumed zirconia sample (Mueller *et al.*, 2004) with single-grain particles, as shown in the inset. The primary particles for this sample have high polydispersity leading to the observed hump near the primary particle scattering regime. $d_{VIS} = 20.3$ nm, PDI = 10.8 ($\sigma_g = 1.56$), $R_g = 26.5$ nm, $d_f = 2.90$. From gas adsorption, $d_p = 19.7$ nm.

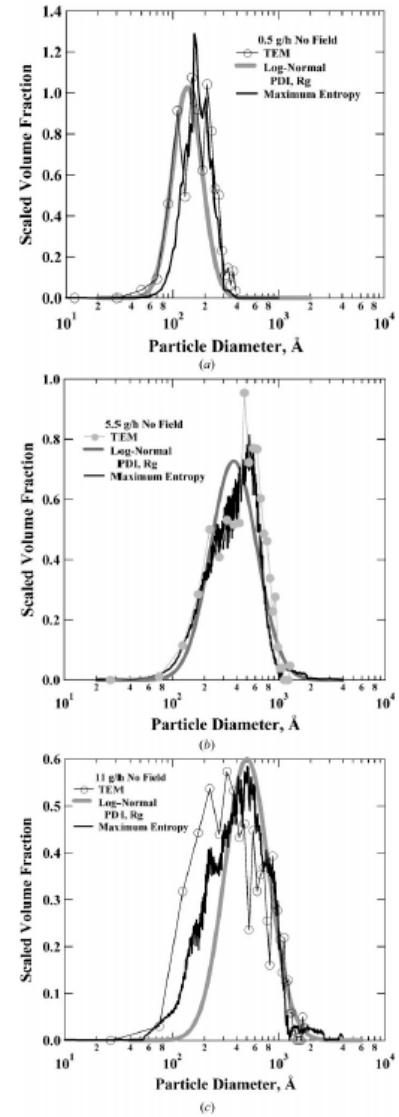

Figure 6
Comparison of particle volume distributions for titania made without an electric field using TEM (circles; Kammler *et al.*, 2003), PDI (grey line) and maximum entropy (black line). (*a*) 0.5 g h^{-1} [fractal $d_{VIS} = 12.1$ nm, PDI = 3.52 ($\sigma_g = 1.38$), $R_g = 8.9$ nm, $d_f = 1.59$, $z_{\pm 1} = 1160$, $z_{R_g} = 1343$]. (*b*) 5.5 g h^{-1} [$d_{VIS} = 37.2$ nm, PDI = 20.0 ($\sigma_g = 1.65$), $R_g = 50.8$ nm]. (*c*) 11 g h^{-1} [$d_{VIS} = 46.8$ nm, PDI = 15.5 ($\sigma_g = 1.61$), $R_g = 60.8$ nm]. (3 g h^{-1} is shown in Fig. 5.)

Particle size distributions from small-angle scattering using global scattering functions, Beaucage, Kammler, Pratsinis J. Appl. Cryst. 37 523-535 (2004).

Particle Size Distribution Curves From SAXS

Maximum Entropy Method

i) Assume sphere or other scattering function
ii) Assume most random solution
iii) Use algorithm to guess/compare/calculate
iv) Iterate till maximum "entropy"

Advantages

- No assumption concerning distribution function
- No assumption for number of modes
- Matches detail PSD's well

Related Alternatives

- Regularization

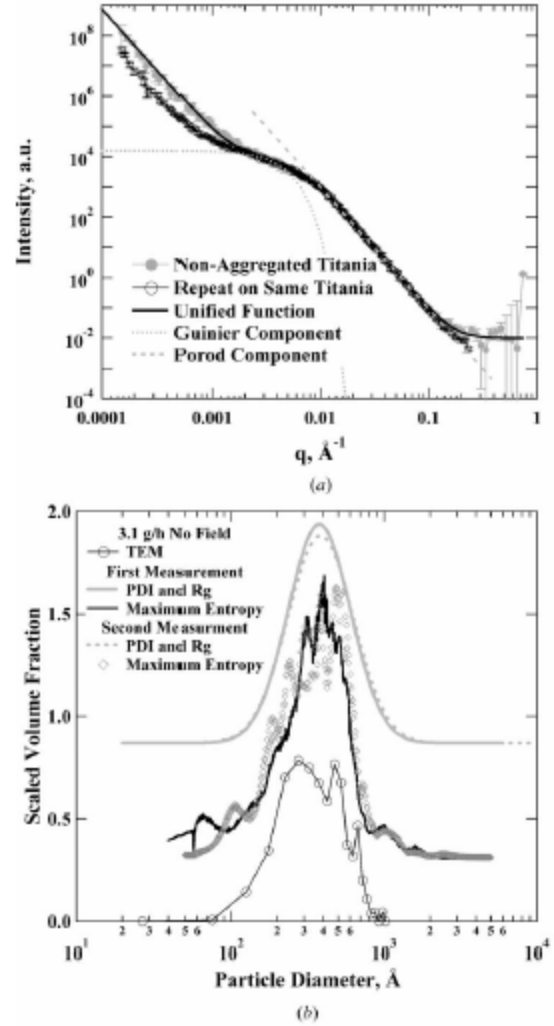

Figure 5
3.1 g h^{-1} titania. (*a*) Repeat USAXS runs on a non-aggregated titania powder (Fig. 1). (*b*) Particle size distributions from TEM (circles; Kammler *et al.*, 2003), equations (1), (2), (17) and (18) using PDI and R_g, and using the maximum-entropy program of Jemian (Jemian *et al.*, 1991). Distribution curves are shifted vertically for clarity. d_{VIS} = 34.9 nm, PDI = 14.4 (σ_g = 1.60), R_g = 44.2 nm.

Particle size distributions from small-angle scattering using global scattering functions, Beaucage, Kammler, Pratsinis J. Appl. Cryst. 37 523-535 (2004).

Software for My Collaborators/Students

Particle Size Distribution Curves From SAXS

All Methods are available in Jan Ilavsky's Igor Code

http://www.uni.aps.anl.gov/usaxs/

Anomalous Scattering

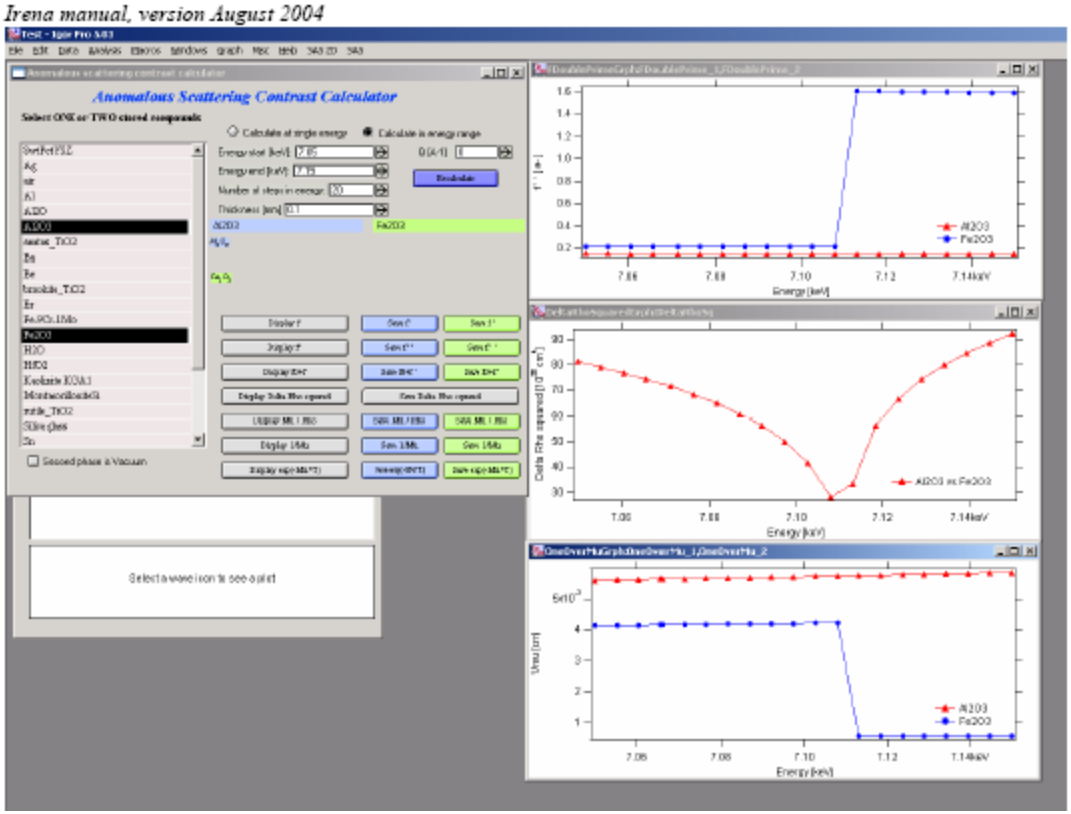

Particle Size Distribution Curves From SAXS

All Methods are available in Jan Ilavsky's Igor Code

http://www.uni.aps.anl.gov/usaxs/

Unified Fit

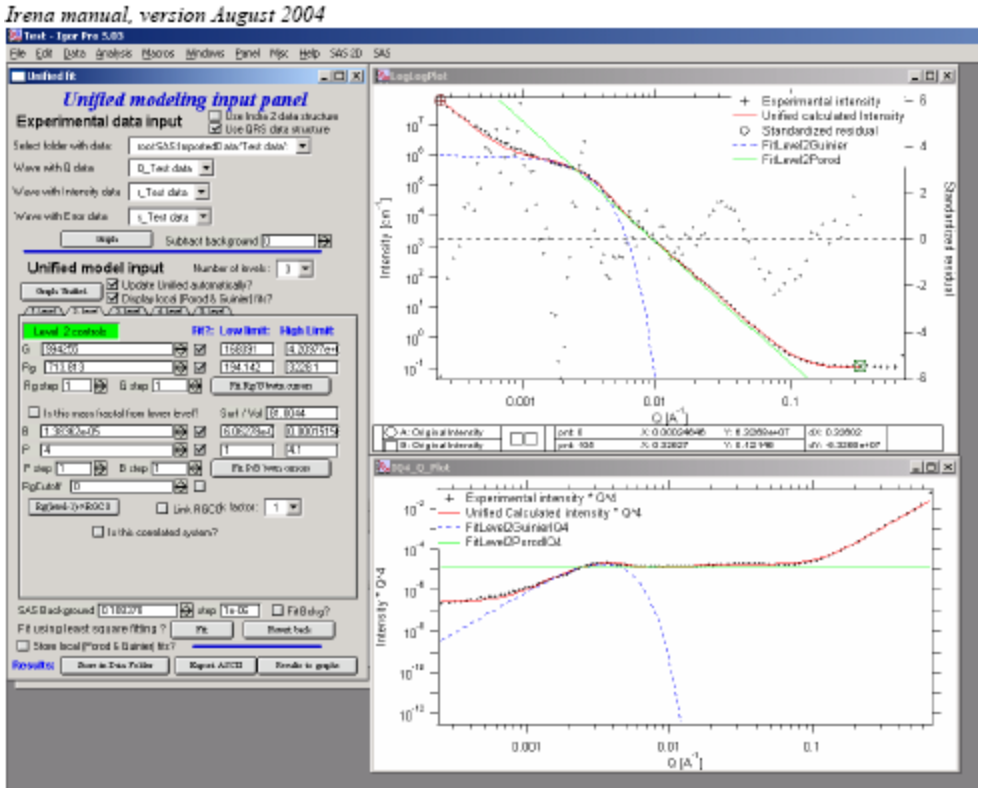

Particle Size Distribution Curves From SAXS

All Methods are available in Jan Ilavsky's Igor Code

http://www.uni.aps.anl.gov/usaxs/

Sphere (or any thing you could imagine) Distributions

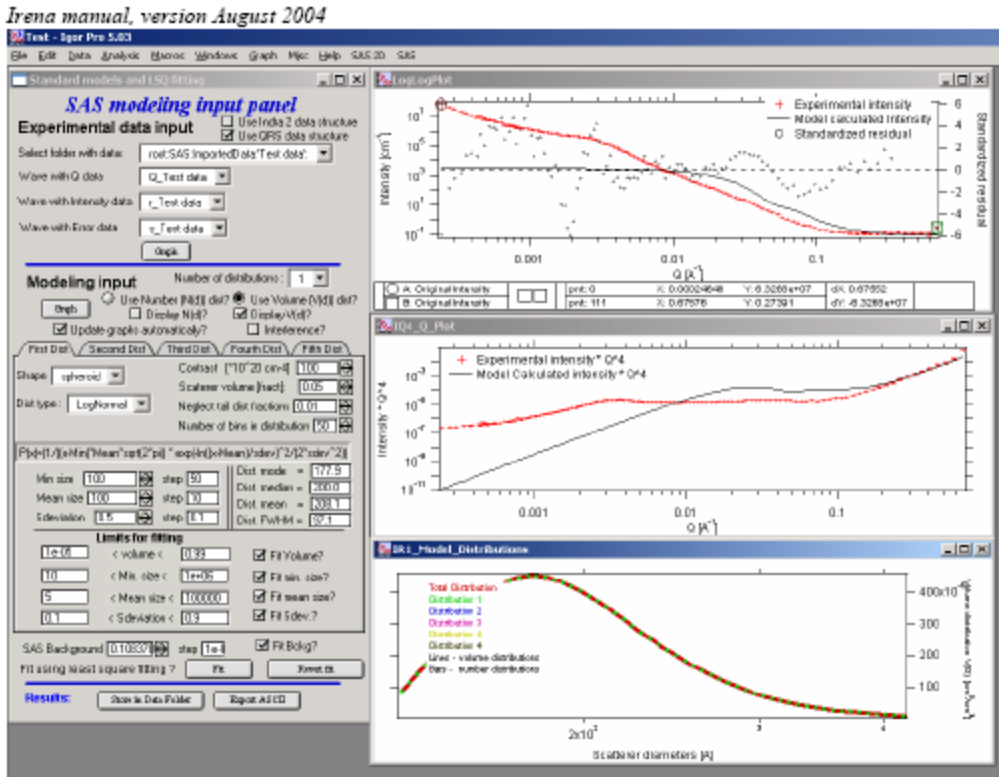

Particle Size Distribution Curves From SAXS

All Methods are available in Jan Ilavsky's Igor Code

http://www.uni.aps.anl.gov/usaxs/

Maximum Entropy/Regularization Code (Jemian)